

UNIVERSIDAD AUTÓNOMA DE MADRID



**FACULTAD DE CIENCIAS
DEPARTAMENTO DE QUÍMICA INORGÁNICA**

Tesis Doctoral

**Novel Nanostructures based on Modified
Oligonucleotides**

Romina A. Lorca Contreras

Madrid, Diciembre 2015

UNIVERSIDAD AUTÓNOMA DE MADRID



**FACULTAD DE CIENCIAS
DEPARTAMENTO DE QUÍMICA INORGÁNICA**

**Memoria presentada por Romina A. Lorca Contreras para
optar al grado de Doctor en Química Inorgánica Molecular
por la Universidad Autónoma de Madrid.**

TUTOR DE TESIS

DIRECTOR DE TESIS

Dr. Félix Zamora Abanades Dr. Álvaro Somoza Calatrava

Madrid, Diciembre 2015

AGRADECIMIENTOS.

Se agradece el apoyo financiero de:

Ministerio Chileno de educación, a través de CONICYT. Por la Beca Doctoral (Beca de Doctorado en el Extranjero, Beca Chile.

Ministerio Español de Ciencia e Innovación Grants: SAF2010-15440, ACI2009-0969, MAT2011-15219-E y MAT2010-20843-C02-01).

A la Asociación española contra el Cáncer.

Imdea Nanociencia.

AGRADECIMIENTOS.

Parece que fue ayer, cuando tome una de las decisiones más importantes de mi vida. Dejando atrás todo lo seguro y conocido, para embarcarme en esta gran aventura. Que ha sido muy intensa y gratificante, con la cual he logrado aprender una infinidad de cosas que me han llevado a un gran crecimiento científico y que sin duda me ha aportado un enriquecimiento personal incalculable. Ya han pasado cuatro años y a aventura ha llegado a su fin. Pero todo esto, no habría sido posible, sin la ayuda de toda la gente que de una u otra manera ha contribuido, para que esta aventura llegara a buen puerto.

Es por esto, que quiero expresar mi más sincero agradecimiento e intentaré no olvidarme de nadie pero si es así, espero me perdone.

En primer lugar quiero agradecer a mi director de tesis, el Dr. Álvaro Somoza por la confianza y apoyo entregado, por su dedicación y preocupación más allá de lo científico. Por motivarme siempre a mejorar. Álvaro has sido mucho más que un director.

A mi tutor, el Dr. Félix Zamora. Por darme la oportunidad de hacer la tesis en la UAM y haberme llevado hasta Álvaro.

Al Dr. Alfonso Latorre, quien ha tenido un papel fundamental en el desarrollo de esta tesis. ¡Alfon! muchas gracias por toda tu ayuda, motivación y cariño desde el primer momento que llegue al laboratorio.

A mis compañeros del grupo de investigación Ana Latorre, Siamak Javani, Christian Duarte y en especial, al Dr. Antonio Aires y el Dr. Pierre Couleaud, por ser más que compañeros de grupo, sin su amistad y ayuda este trabajo no hubiese sido tan gratificante.

Al Dr. Carlos González y el Dr. Miguel Garavis, por su ayuda en los experimentos de RMN.

A Miguel Angel Fernández y Pablo Ares, quienes me han enseñado la técnica de AFM.

A los compañeros de la facultad de ciencias Cristina Hermosa, Khaled, Diego y David Por hacer más gratas las largas jornadas de AFM.

A los amigos, que si bien no han participado directamente en la realización de este trabajo. Han sido un apoyo fundamental. Antonio, Alfredo, Chory, Isaac, Félix, Javi, Jorge, Lucio, Macaco, Nacho, Piti, Sergio, Rubén a las “Gacitas” Mary, Gema y Raquel, Lidia, Patri, Cristina y en especial a Javier Troyano por abrirme las puertas de su mundo. A Merino por todos esos lindos momentos que además llegaron cuando más los necesitaba. ¡Chicos! Muchas gracias por todos esos lindos momentos, que hicieron que este tiempo en Madrid, fuera mucho más enriquecedora y amena.

A los amigos de Chile, Esteban, Judith, Profe Juan, La Madre y Luis Lemus que a pesar de la distancia siempre han estado presentes dándome su apoyo.

Finalmente agradezco a mi familia, en especial a mis padres, por su infinito amor y comprensión, por motivarme siempre a tratar de conseguir los sueños y por enseñarme que con perseverancia y dedicación se consiguen los objetivos.

Resumen

Los oligonucleótidos han mostrado una gran versatilidad en nanotecnología, debido principalmente a sus propiedades únicas de reconocimiento y auto-ensamblaje, su tamaño nanométrico y su gran estabilidad. Estas características hacen de ellos unos elementos singulares para la construcción en la nanoescala. En este sentido los oligonucleótidos se han utilizado para generar estructuras muy definidas en 2 y 3 dimensiones compuestas exclusivamente de DNA.

Por otro lado la incorporación de moléculas orgánicas en los oligonucleótidos proporciona un mayor control en el diseño, arquitectura y funcionalidad de las nanoestructuras formadas. Lo que ha generado grandes avances en campos como la nanomedicina y la ciencia de los materiales. En concreto, este tipo de derivados se ha aplicado exitosamente en la preparación de complejos nanodispositivos, motores nanomecánicos, así como en la síntesis orgánica dirigida.

Basados en estos antecedentes, el trabajo de esta tesis doctoral se ha centrado en la síntesis de oligonucleótidos modificados para la preparación de diferentes nanoestructuras.

Los grupos funcionales utilizados preferentemente han sido alquinos y tioles, los cuales se han introducido en los extremos de los oligonucleótidos. Con estos derivados se han preparado estructuras complejas mediante la reacción de click con derivados de benceno modificados con azidas. Estos sistemas se han empleado en la preparación de nuevos materiales fluorescentes basados en nanoclústeres de plata

(ADN-AgNCs), lo cuales resultaron ser hasta 60 veces más fluorescentes que estructuras de cadena simple. Además de evaluar sus propiedades fluorescentes, se realizó una caracterización estructural mediante técnicas espectroscópicas de Dicroísmo Circular (CD) y Resonancia magnética nuclear de protón (^1H -RMN). Por otra parte mediante la funcionalización de nanopartículas de oro con secuencias de ADN (ADN-AuNPs) hemos desarrollado un nuevo ligando para la reacción *Click*, que ha resultado ser mucho más eficiente que los ligandos comerciales empleados normalmente. Este nuevo ligando ha sido empleado en la preparación de nuevas nanoestructuras bidimensionales mediante dos aproximaciones. La primera consiste en la formación de dos trímeros con secuencias complementarias, cuyo ensamblaje da lugar a estructuras 2D. La segunda aproximación consiste en la formación de estas nanoestructuras híbridas 2D mediante la formación de enlaces covalentes.

Table of Contents

General Introduction.....	1
Deoxyribonucleic acid (DNA).....	3
DNA structures	6
DNA in Nanotechnology	15
Nanostructures Based on Chemically Modified Oligonucleotides	21
 Chapter 1. DNA-AgNCs.	 27
Introduction.	29
Silver Nanocluster	31
Silver nanocluster stabilized by Oligonucleotides.....	32
Objectives.....	35
Results and discussion.....	36
Synthesis of DNA trimers	40
Synthesis of benzene derivatives.....	42
Synthesis of modified solid support.....	43
Click reaction between modified oligonucleotides and benzene derivatives.....	45
DNA Silver Nanoclusters (DNA-AgNCs).....	45

Characterization of DNA-AgNCs.....	47
Conclusions.....	58

Chapter 2. Structural Characterization of DNA-AgNCs 59

Introduction.....	61
Objectives.....	64
Results and Discussion.	65
Characterization by ¹ H-NMR.....	65
Characterization by CD Spectroscopy.....	71
Conclusions.....	79

Chapter 3. Novel Catalyst for Click Reaction.

Introduction.....	83
Objective.....	89
Result and discussions	90
Synthesis of modified solid support.....	91
Modification of AuNPs with oligonucleotides.....	96
Comparison of the catalytic effect of different catalysts.....	92
Optimization of Gold NPs Catalyst.....	94
2D Hybrid Nanostructures by Self-Assembly of complementary sequences.....	99
2D Hybrid Nanostructures by covalent bonds.....	104

Conclusions.....	106
------------------	-----

Experimental procedures

General methods.....	111
Synthesis of azides.....	113
Synthesis of modified solid support.....	116
Oligonucleotide Synthesis.....	122
Click reaction between modified DNA and benzene derivatives	123
Synthesis of gold nanoparticles.....	125
Functionalization of Gold nanoparticles with oligonucleotides...	125
Click reaction with Fluoreogenic reagent.....	126

Annexed 1 Oligonucleotides Synthesis	127
---	-----

Annexed 2 Publications	136
-------------------------------------	-----

GENERAL INTRODUCTION

Deoxyribonucleic acid (DNA)

Deoxyribonucleic acid (DNA) is a nucleic acid that contains the genetic instructions used in the development and functioning of all known living organisms and some viruses, and is responsible for their hereditary transmission of these instructions.¹ Regarding its structure and chemical composition, DNA is an anionic polymer, which monomers are known as nucleotides. Each nucleotide has three components: a sugar, a nucleobase and a phosphate group. The sugar is deoxyribose, which is connected through position 1 to the nucleobase. The standard nucleobases are aromatic and heterocyclic nitrogenous compounds with two or more nitrogen atoms, which are classified into two groups: purines or purine bases, adenine (**A**) and guanine (**G**), and pyrimidines or pyrimidine bases, cytosine (**C**) and thymine (**T**). The combination of the sugar and the nucleobases yields their corresponding nucleosides: deoxyadenosine (**dA**), deoxyguanosine (**dG**), deoxycytidine (**dC**) and thymidine (**dT**) (Figure 1A). The last component of the DNA, the phosphate group, is used to connect each monomer along the polymer. In a standard DNA strand, one end contains a phosphate group on the 5' carbon of the sugar ring (defined as the 5' end) and at the other end a hydroxyl group on the 3' carbon of the sugar ring (defined as the 3' end) (Figure 1B).

¹ A. D. Hershey, M. Chase, *J. Gen. Physiol.* **1952**, 36, 39-56.

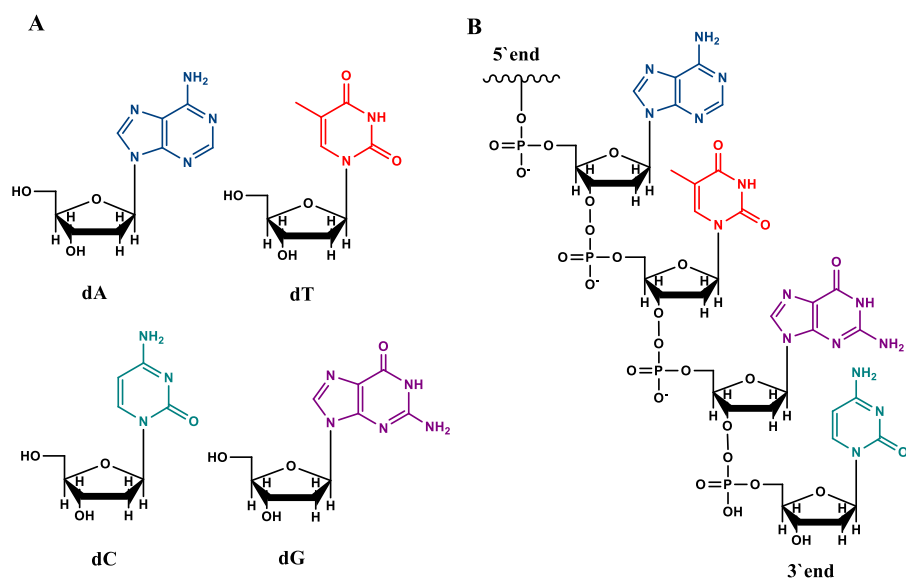


Figure 1. A) Structure of nucleosides. B) Oligonucleotide strand.

The DNA structure was elucidated through a multidisciplinary collaboration between Rosalind Franklin (chemist and X-ray crystallographer), Maurice Wilkins (physicist and molecular biologist), James Watson (molecular biologist, geneticist and zoologist) and Francis Crick (molecular biologist, biophysicist, and neuroscientist). Watson and Crick reported the structure of DNA in 1953^{2,3} and were awarded jointly with Maurice Wilkins in 1962 the Nobel Prize for Physiology or Medicine

² J. D. Watson and F. H. Crick, *Nature* **1953**, 171, 737-738.

³ J. D. Watson and F. H. Crick, *Nature* **1953**, 171, 964-967.

"for their discoveries concerning the molecular structure of nucleic acids and its significance for information transfer in living material"

Particularly, they reported that DNA was present as a double stranded structure (dsDNA), where two complementary single-strands of DNA (ssDNA) hybridize into a double helix structure in anti-parallel direction, (one strand from 5' to 3' and the other one from 3' to 5'). The DNA double helix is stable due to the formation of hydrogen bonds between complementary nucleobases of the two strands (Figure 2). This interaction takes place with high selectivity between purine and pyrimidine nucleobases, particularly, adenine pairs with thymine and guanine with cytosine. In addition, the double helix is stabilized further through hydrophobic and π - π interactions. Particularly, the hydrophobic groups of the DNA (the nucleobases) are located inside the double helix and hydrophilic components (the phosphate groups) outside making duplex structure soluble and stable in water. On the other hand the nucleobases stack partially along the DNA structure increasing its thermal stability due to the π - π interaction between aromatic rings.⁴ Despite the different stabilisation effects, the duplex can be opened easily, as a zipper, by mechanical forces or high temperatures.⁵

⁴ P. Ponnuswamy, M. Gromiha, *J. Theor. Biol.* **1994**, *169*, 419-432.

⁵ H. Clawsen-Shaumann, M. Rief, C. Tolksdorf and H. E. Gaub, *Biophys. J.* **2000**, *78*, 1997-2007.

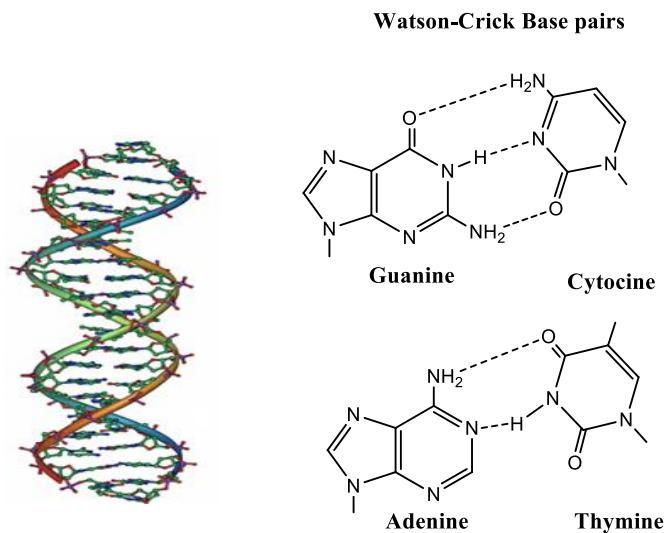


Figure 2. Formation of double helix by The Watson-Crick base-pairing rule.

DNA structures

The secondary structure obtained by the interaction of two complementary DNA strands is a double helix, which can be arranged in a dextrorotatory or laevorotatory structure. DNA is mainly found as dextrorotatory duplex in a conformation known as B-DNA. However, it can also adopt other conformations known as A-DNA (dextrorotatory) and Z-DNA (laevorotatory).

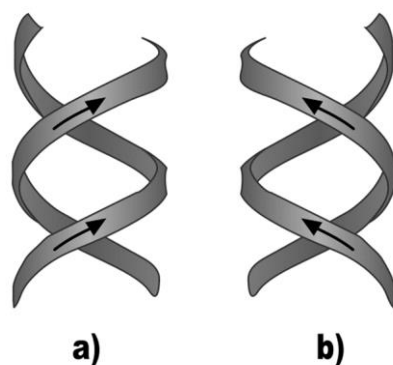


Figure 3. a) Dextrorotatory and b) laevorotatory structures.

When two DNA strands are wound round each another, grooves appear between the strands exposing some functional groups of the nucleobases. The grooves appear as a result of the angles formed between the sugars of the basepairs, which can generate two types of slits around the surface of the double helix: the major groove (2.2 nm wide), and the minor groove (1.2 nm wide)⁶ (figure 4). These grooves allow the DNA structure to interact with different molecules with high selectivity, such as proteins (transcription factors),⁷ small molecules⁸ and also with inorganic complexes,⁹ among others.

⁶ R. Wing, H. Drew, T. Takano, C. Broka, S. Tanaka, K. Itakura, R. Dickerson, *Nature*, **1980**, 287, 755-758.

⁷ C. Pabo, R. Sauer, *Ann. Rev. Biochem.*, **1984**, 53, 293-321.

⁸ H. Song, J. T. Kaiser, J. K. Barton, *Nature Chemistry*, **2012**, 4, 616-620.

⁹ *Metal Complex-DNA Interactions* Edited by Nick Hadjiladis and Einar Sletten **2009** Blackwell Publishing Ltd. ISBN: 978-1-405-17629-3.

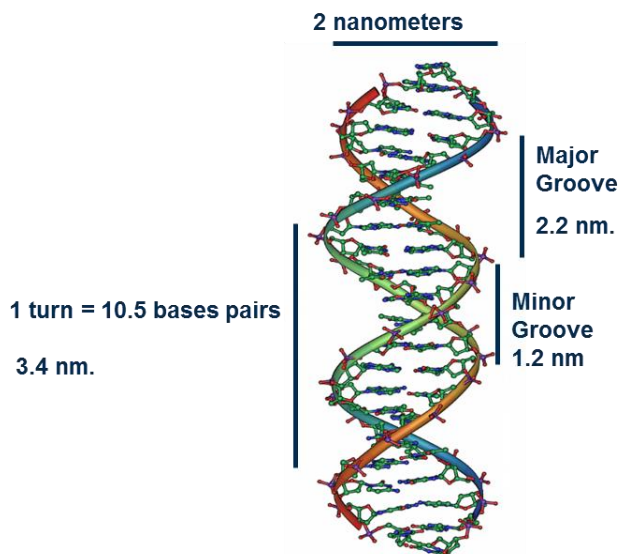


Figure 4. Structure of B-DNA duplex.

As mentioned before, the double helix of DNA can exist in different conformations.¹⁰ However, only B-DNA has been found in living organisms. The conformation adopted by the DNA (Figure 5), depends on the direction of supercoiling, the presence of chemical modifications on the bases and environmental conditions, such as concentration of metal ions and polyamines.¹¹

B-DNA is the most common conformation in the conditions prevailing in cells. This structure is the dextrorotatory double helix described by Watson and Crick, which requires about 10 to 10.5 base pairs to make a complete turn.

¹⁰ A. Ghosh, M. Bonsal, *Acta Crystallographica D Biological Crystallography*, **2003**, 59, 620-626.

¹¹ H. S. Basu, B. G. Feuerstein, D. A. Zarling, R. H. Shafer, L. J. Marton, *J. Biomol. Struct. Dyn.* **1988**, 6, 299-309

A-DNA is also a dextrorotatory structure but broader and shorter than the B-DNA. In this case each turn contains 11 bp, which results in a slightly smaller angle of torsion. Furthermore, the major groove is deeper and narrower, while the minor groove is wider and shallower than in B-DNA. A-DNA occurs in non-physiological conditions, such as in dehydrated forms of DNA, whereas in the cell might be found in hybrid DNA-RNA structures as well as in DNA-protein complexes.¹²

Z-DNA is a levorotatory conformer of DNA, which can be found in DNA segments where nucleobases have been modified, allowing major conformational changes.¹³

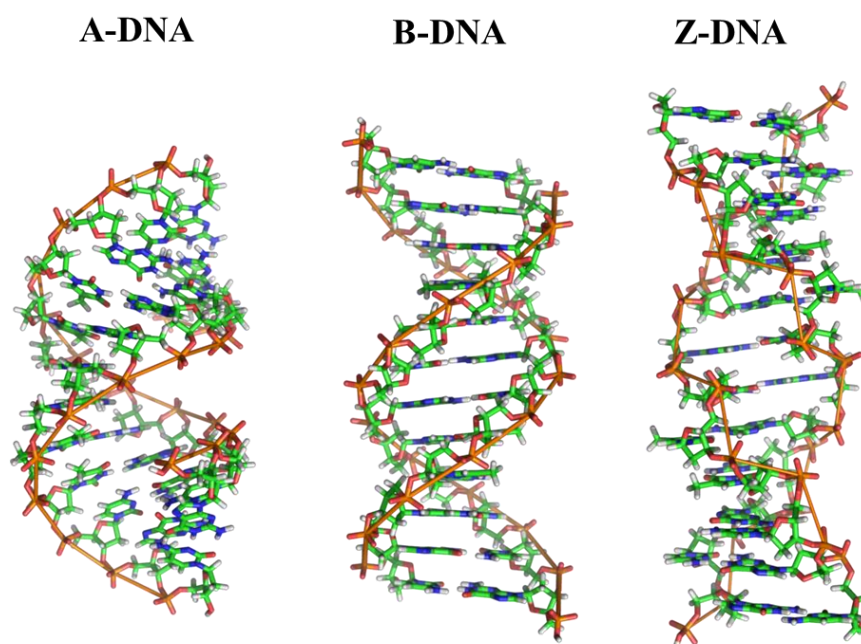


Figure 5. Double helix of DNA in different conformations.¹⁴

¹² X. J. Lu, Z. Shakked, W. K. Olsen, *J. Mol. Biol.* **2000**, 300, 819-840.

¹³ S. Rothenburg, F. Koch-Nolte, F. Haag, *Immunological Reviews*, **2001**, 184, 286–298.

In addition, DNA may also adopt other conformations around dG or dC rich regions. For example, G-rich sequences are capable of folding into structures where four guanine bases interact to form stable structures known as G-quadruplexes.¹⁵ These structures are stabilized through hydrogen bonds between the guanines and the chelation of a metal ion in the center of each unit of four guanines¹⁶ (Figure 6).

In a G-quadruplex structure it might be involved one, two, or four DNA molecules, which can be arranged in different orientations such as parallel, antiparallel, or hybrid parallel–antiparallel.¹³

¹⁴ https://en.wikipedia.org/wiki/Z-DNA#/media/File:A-DNA,_B-DNA_and_Z-DNA.png

¹⁵ S. Burge, G. Parkinson, P. Haxel, A. Todd, S. Neidle, *Nucleic Acids Research*, **2006**, 34, 19, 5402-5415.

¹⁶ G. Parkinson, M. Lee, S. Neidle, *Nature*, **2002**, 417, 876-80

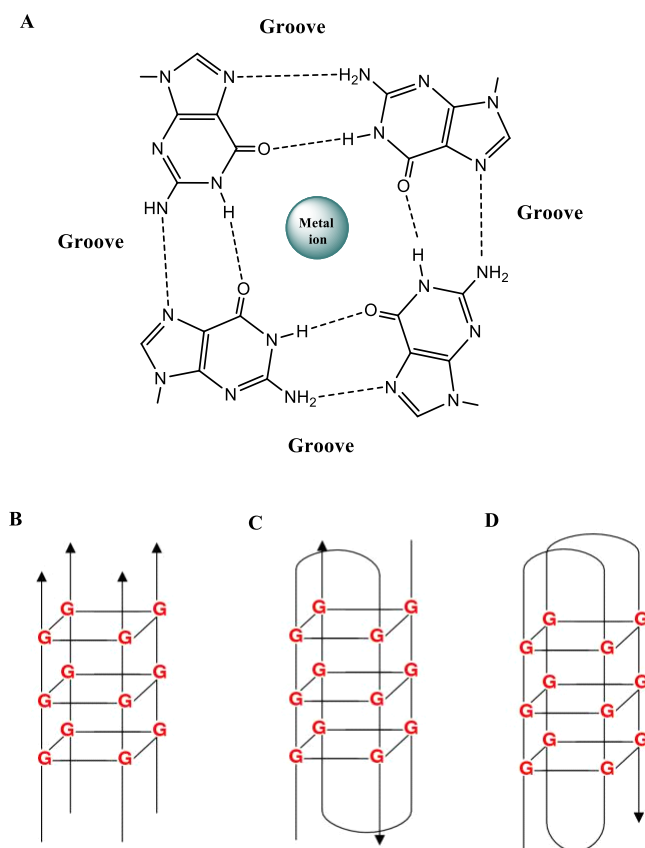


Figure 6. A) The arrangement of guanine bases in the G-quartet, shown together with a centrally placed metal ion. Hydrogen bonds are shown as dotted lines, and the positions of the grooves are indicated, B) Intermolecular parallel G-quadruplex, C) Intermolecular antiparallel G-quadruplex and D) Intermolecular antiparallel G-quadruplex.

On the other hand, C-rich regions have also the ability to form folded structures known as i-motifs.^{17,18} These structures are formed in acidic

¹⁷ a) K. Gehring, J. L. Leroy, M. Gueron, *Nature*, 1993, 363, 561–565; b) C. Kang, I. Berger, C. Lockshin, R. Ratliff, R. Moyzis, A. Rich, *Proc. Natl. Acad. Sci. U. S. A.*, 1994, 91, 11636–11640.

pHs and involve the formation of cytosine-cytosine base pairs. In this case three hydrogen bonds stabilize the structure, where one N3 of the base pair is protonated (Figure 7).

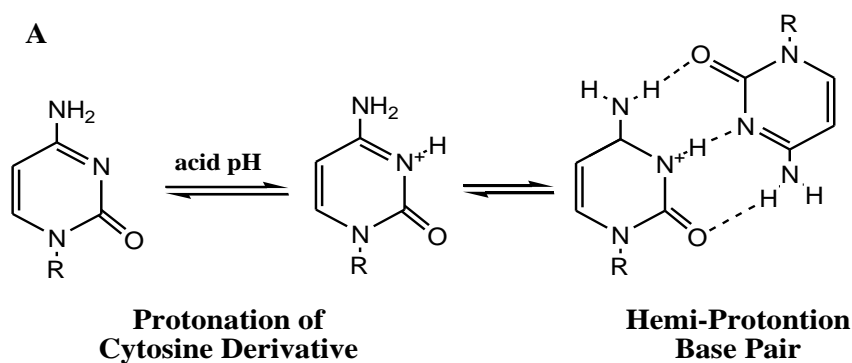


Figure 7. Formation of cytosine-cytosine base pair

This interaction can lead to unimolecular structures through intramolecular interactions, however, when intermolecular interactions are involved, structures with multiple molecularity (bi, tetra) can be obtained as well^{15b, 15c} (Figure 8).

¹⁸ (a) J. L. Leroy, M. Gueron, J. L. Mergny, C. Helene, *Nucleic Acids Res.* **1994**, 22, 1600. (b) S. Nonin, A. T. Phan, J. L. Leroy, *Structure* **1997**, 5, 1231-1247. (c) S. Nonin, J. L. Leroy, *J. Mol. Biol.* **1996**, 261, 399-414.

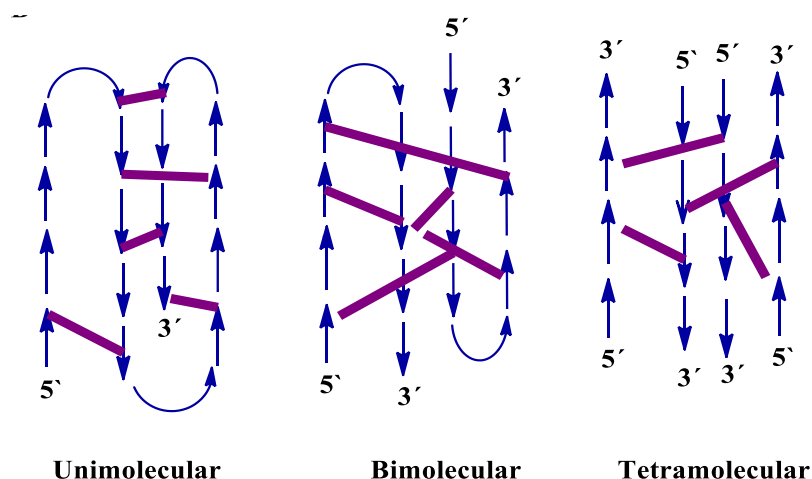


Figure 8. Representation of possible i-motif.

One of the most common technique employed in the characterisation of the secondary structure of biomolecules, including DNA, is circular dichroism spectroscopy (CD). This technique arises from differential absorption of right-handed and left-handed circularly polarized light by chiral molecules.¹⁹ In nucleic acids there are three possible sources of chirality. The first one comes from the sugar moiety (especially from position C1); this chirality causes monomeric nucleosides to exhibit CD. The second source of chirality is the helicity of the secondary structures adopted by nucleic acids. The third source of CD signals results from long-range tertiary ordering of DNA. CD of monomeric constituents of

¹⁹ J. Kypr, I. Kejnovská, K. Bednářová, M. Vorlíčková, *Circular Dichroism Spectroscopy of Nucleic Acids*, *Comprehensive Chiroptical Spectroscopy, Volume 2: Applications in Stereochemical Analysis of Synthetic Compounds, Natural Products, and Biomolecules*, First Edition. Edited by N. Berova, P. L. Polavarapu, K. Nakanishi, and R. W. Woody. Published **2012** by John Wiley & Sons, Inc. chapter pp, 575-586.

nucleic acids and short single-stranded fragments has been described previously.²⁰ A summary of the signals present in the representative structures is detailed below.

The **B-form** provides a rather weak CD spectrum containing a positive band around 275 nm and a negative band at around 245 nm.

The **A-form** of DNA provides a much stronger CD spectrum than the B-form. The A-form spectrum is dominated by a strong positive band at 260 nm and a strong negative band at 210 nm.

The **Z-form** presents a CD that is more or less a mirror image of the B-form.

G-quadruplexes present different topologies that can be distinguished by CD spectroscopy. Particularly, the spectrum of parallel quadruplexes contains a dominating positive band at 260 nm; antiparallel quadruplexes present a positive band at 295 nm and a negative one around 260 nm. The bands at 260 and 295 nm probably reflect populations of *anti* and *syn* glycosidic angles of the dG residues in the particular quadruplex arrangements. The 260-nm band is similar in shape to that of the A-form, which indicates similar base stacking.²¹ G-quadruplexes, however, have a positive band at 210 nm where the A-form has a negative band.

²⁰ W. C. Johnson, *CD of nucleic acids, in Circular Dichroism, Principles and Applications*, 2nd ed., N. Berova, K. Nakanishi, and R. Woody, eds., Wiley-VCH, New York, **2000**, pp. 703–718.

²¹ J. Kypr, M. Fialova, J. Chladkova, M. Tumova, M. Vorlickova, *Eur. Biophys. J.* **2001**, *30*, 555–558.

The CD of **i-motif** structures present positive band at 290 nm and negative band at 260 nm.

DNA in Nanotechnology

The nanometric size of DNA, its stability and its ability to generate stable duplexes between complementary sequences have stimulated the development of multiple applications of DNA in nanotechnology in the last years. This area of research was initiated by Prof. Nadrian C. Seeman in the 90's, who demonstrated the potential of DNA in the preparation of a variety of nanostructures through self-assembly processes. It is particularly relevant the preparation of 2D structures for the functionalisation of surfaces. His approach is based on the preparation of units (tiles) composed of DNA whose ends are composed of single stranded DNA molecules that can anneal with the complementary strands present in other tile.²² (Figure 9).

²² N. C Seeman, *Annu. Rev. Biochem.* **2010**, 79, 65–87.

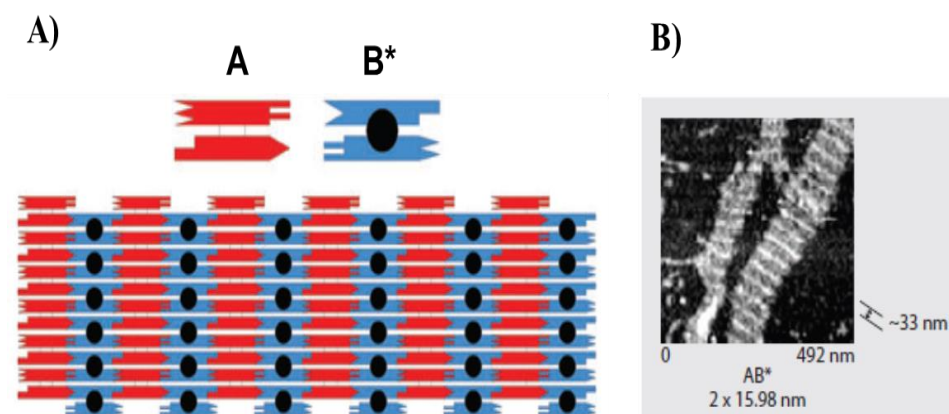


Figure 9. Two-dimensional DNA arrays developed by Seeman where A and B* represent units “Tiles”. A) An alternating array of A and B* molecules. B) The atomic force microscope (AFM) image at right shows stripes separated by ~33 nm, near the predicted distance of 32 nm.²²

The main problem of this approach is that the formation of the structures is very sensitive to multiple variables such as, purity, concentration and ratio of oligonucleotides, buffer employed, annealing procedure, etc.

In 2006, Rothmund described a very robust approach to prepare nanometric structures based on DNA. It is known as DNA origami, and it requires the use of a long circular single stranded DNA and hundreds of small oligonucleotide strands, known as staples. In this case there is no need to control precisely the parameters mentioned in the previous method, and the structures are obtained easily by mixing the DNA strands (Figure 10).²³

²³ P. W. K Rothmund, *Nature*. **2006**, 440, 297–302.

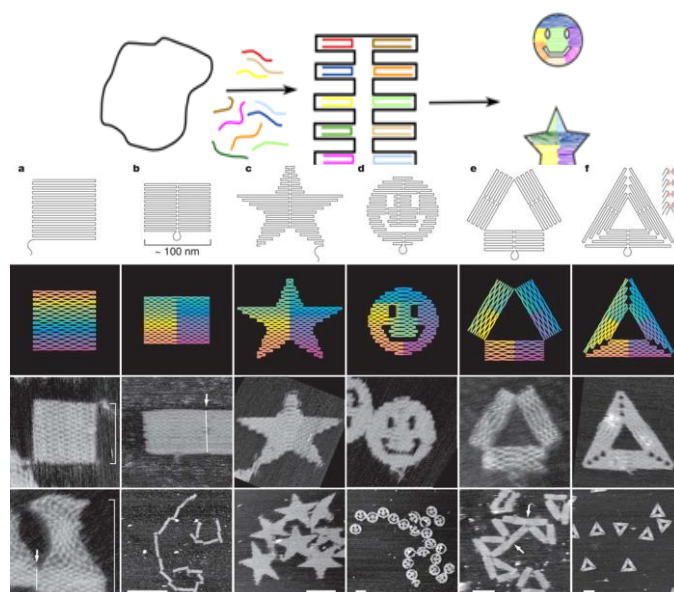


Figure 10. DNA origami shapes. Top row, folding paths. a, square; b, rectangle; c, star; d, disk with three holes; e, triangle with rectangular domains; f, sharp triangle with trapezoidal domains.²³

In the case of the preparation of 3D structures using DNA origami it is remarkable the preparation of a box with a lid described by Kjems and colleagues.²⁴ In this case, they folded the standard single-stranded DNA from the bacteriophage M13 into six sheets of DNA (Figure 11), which are employed in the preparation of the lidded box. Interestingly, the lid could

²⁴ E. S. Andersen, M. Dong, M. M. Nielsen, K. Jahn, R. Subramani, W. Mamdough, M. M. Golas, B. Sander, H. Stark, C. L. P. Oliveira, J. S. Pedersen, V. Birkedal, F. Besenbacher, K. V. Gothelf, J. Kjems, *Nature*. **2009**, *459*, 73–76.

be opened by the addition of DNA strands containing the complementary sequences of the ones used in the lock of this nanostructure (Figure 11).

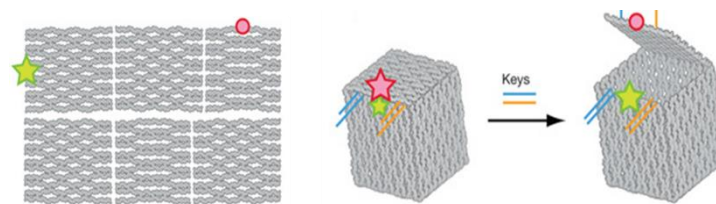


Figure 11. Design of a DNA origami box with lid. Molecular models of the six DNA sheets employed in a flat and cubic arrangement.

Another remarkable example of DNA origami was reported by Shih and colleagues.²⁵ They described a versatile method for the preparation of 3D structures. In their approach a 2D structure is generated with "discontinuous" sequences, which is refolded by the intramolecular annealing of those "discontinuous" regions. An example of these structures, is the formation of multilayer structures as described in Figure 12.²⁶

²⁵ S. M. Douglas, H. Dietz, T. Lied, B. Högberg, F. Graf, W. M. Shih, *Nature*, **2009**, 459, 414-418.

²⁶ M. Endo, H. I. Suiyama, *ChemBioChem*, **2009**, 10, 2420 – 2443.

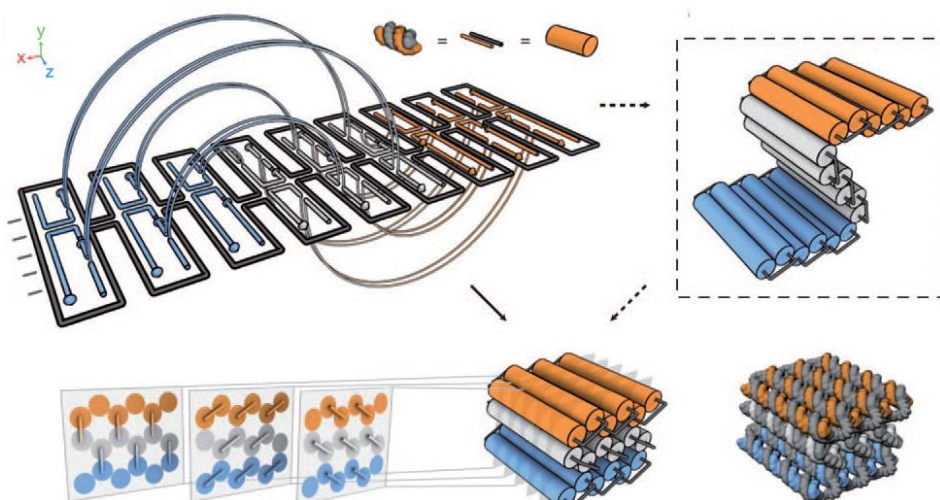


Figure 12. DNA origami plates were folded layer-by-layer into 3D structures by connecting faces and bottoms of the plates with the aid of designed DNA strands.

26

Besides the different reports dealing with the preparation of 2D and 3D structures based on DNA, there is a great interest in the preparation of 1D structures, due to their potential in the field of nanoelectronics. Particularly, DNA has been used mainly as a template for the production of conductors or semiconductor nanowires. In this regard, Lee et al.²⁷ described a new way to generate DNA structures where the imine proton involved in the base pairs of DNA is replaced by different cations, such as Zn^{2+} , Ni^{2+} , Co^{2+} , among others (Figure 13)²⁸. These new structures are known as metallic DNA (M-DNA), and can work as a molecular wires

²⁷ J. S. Lee, L. J. P Latimer, *Biochem. Cell Biol.* **1993**, 71, 162- 168

²⁸ T. H. LaBean, H. Li, *Nanotoday*, **2007**, 2, 26-35.

and have a great potential for further development of electronic molecular devices.^{29, 30}

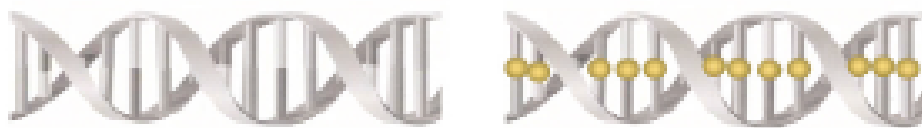


Figure 13. Schematic view of DNA double-helix and M-DNA, where metal ions are bound and stacked into the DNA base pairs.

Additionally the incorporation of organic molecules in the DNA provides a convenient approach to increase the functionality and architecture of this versatile molecule, which has generated great advances in various fields, such as biomedicine and materials science.^{31,32} In this sense, chemically modified DNA has been applied in the preparation of complex nanodevices,³³ nanomechanical motors,^{34,35,36} as well as in directed organic synthesis.^{37,38}

²⁹ P. Aich, S. L. Labiuk, L. W. Tari, L. J. T. Delbaere, W. J. Roesler, K. J. Falk, R. P. Steer, J. S. Lee, *J. Mol. Biol.* **1999**, 294, 477-485

³⁰ A. Rakitin, P. Aich, C. Papadopoulos, Yu. Kobzar, A. S. Vedenev, J. S. Lee, and J. M. Xu, *Phys. Rev. Lett.* **2001**, 86, 16, 3670-3676

³¹ G.K. Such, A.P.R. Johnston, K. Liang, F. Caruso, *Progress in Polymer Science*, **2012**, 37, 985–1003.

³² C. S. McKay, M.G. Finn, *Chemistry & Biology*, **2014**, 21, 1075-1101.

³³ S. Beyer, F. C. Simmel, *Nucleic Acids Res.* **2006**, 34, 1581-1587

³⁴ C. Mao, W. Sun, Z. Shen, N. C. Seeman, *Nature*, **1999**, 397, 144-146

³⁵ B. Yurke, A. J. Turberfield, A. P. Mills Jr, F. C. Simmel, J. L. Neumann, *Nature*, **2000**, 406, 605-608

³⁶ A. J. Turberfield, J. C. Mitchell, B. Yurke, A. P. Mills, Jr., M. I. Blakey, and F. C. Simmel, *Phys. Rev. Lett.* **2003**, 90, 118102-1- 118102-4,

³⁷ D. R. Liu, *PLoS Biol.* **2004**, 2, E223, 0906-0906

³⁸ K. V. Gothelf, T. H. LaBean, *Org. Biomol. Chem.* **2005**, 3, 4023-4037

Nanostructures Based on Chemically Modified Oligonucleotides

Over the last years, modified oligonucleotides are being extensively used in different applications in nanotechnology, besides DNA origami. Particularly, the preparation of hybrid structures containing organic molecules and DNA,³⁹⁻⁵⁰ as well as the modification and stabilization of different nanostructures, such as metallic nanoparticles⁴¹⁻⁵⁴ or carbon nanotubes.⁵⁵⁻⁵⁹

Hybrid structures based on organic molecules and modified oligonucleotides have been touted as promising building blocks to nanoscale.^{39,40} Although the preparation of hybrids of organic molecules and DNA can provide novel functionalities and applications, the synthesis is difficult due to the low solubility of DNA in organic solvents, the low reactivity of the terminal functional groups, and electrostatic interactions. For these reasons different synthetic approaches have been developed to prepare hybrid structures containing oligonucleotides and organic molecules, such as DNA templated cross-coupling strategies,⁴¹ or the standard phosphoramidite chemistry used in DNA synthesizers.^{42,43,44} However, the directionality of the obtained ssDNA sequences is limited, hampering their subsequent use for DNA extension in both directions. In

³⁹ H Korri-Youssoufi, F. Garnier, P. Srivastava, P. Godillot, A. Yassar, *J. Am. Chem. Soc.* **1997**, *119*, 7388–7389.

⁴⁰ K. P. R. Nilsson, O. Inganäs, *Nat. Mater.* **2003**, *2*, 419–424.

⁴¹ X. Y. Li, D. R. Liu, *Angew. Chem., Int. Ed.* **2004**, *43*, 4848–4870.

⁴² M. Nielsen, V. Dauksaite, J. Kjems, K. V. Gothelf, *Bioconjugate Chem.* **2005**, *16*, 981–985.

⁴³ T. Kuroda, Y. Sakurai, Y. Suzuki, A. O. Nakamura, M. Kuwahara, H. Ozaki, H. Sawai, *Chem. Asian J.* **2006**, *1*, 575–580.

⁴⁴ M. F. Jacobsen, J. B. Ravnsbaek, K. V. Gothelf, *Org. Biomol. Chem.* **2010**, *8*, 50–52.

contrast, conventional cross-coupling reaction allows choosing the direction of each sequence of ssDNA and therefore provides a more versatile approach.^{45,46,47,48}

In this regard, the standard Click reaction has proven very useful for the preparation of a variety of materials. This reaction implies the cycloaddition between an azide and alkyne moiety catalyzed by Cu^+ (Figure 14) and has been applied in the orthogonal ligation of a variety of biomolecules, including oligonucleotides for preparation of hybrid nanostructures based on DNA.^{49, 50}

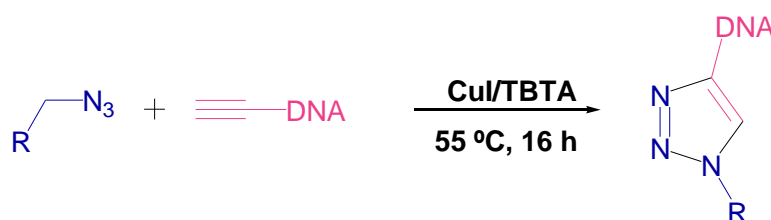


Figure 14. Scheme of synthesis click reaction catalyzed by Cu^+ the cycloaddition between an azide group and alkyne terminal present in DNA.

The use of oligonucleotides in the functionalization of nanoparticles have been intense, but particularly with gold nanoparticles, due to their ease of

⁴⁵ J. K. Lee, Y. H. Jung, J.B.-H. Tok, Z. Bao, *ACS Nano.*, **2011**, 5, 2067–2074.

⁴⁶ J. K. Lee, F. Jackel, W. E. Moerner, Z. A. Bao, *Small*, **2009**, 5, 2418–2423.

⁴⁷ J. K. Lee, Y. H. Jung, R. M. Stoltenberg, J. B. H. Tok, Z. N. Bao, *J. Am. Chem. Soc.* **2008**, 130, 12854–12855.

⁴⁸ A. V. Ustinov, V. V. Dubnyakova, V. A. Korshun, *Tetrahedron*, **2008**, 64, 1467–1473.

⁴⁹ J. K. Lee, Y. H. Jung, J. B.-H. Tok, and Z. Bao, *ACS. Nano.*, **2011**, 5, 2067–2074

⁵⁰ M. A. Abdalla, J. Bayer, J. O. Radler, K. Mullen, *Angew. Chem., Int. Ed.* **2004**, 43, 3967–3970.

conjugation through thiol groups. In this sense, it is remarkable the contributions of Mirkin and coworkers,^{51,52} who have reported most of the key applications within this area of research. In this sense, they have defined the nanostructure generated after the functionalization of gold nanoparticles with oligonucleotides as Spherical Nucleic Acid Nanoparticle Conjugates, which have been used in multiple applications. For instance, they have reported the controlled assembly of gold nanoparticles (AuNPs) modified with oligonucleotides to create crystal structures (Figure 15 A).⁵³ As well as the assembly of small AuNPs (8 nm) around a larger one (31 nm) (Figure 15 B).⁵⁴

In addition, systems based on DNA-AuNPs have been employed in the development of sensors. In this case the sequences employed in the functionalization of the particles are able to bind a complementary sequence present in a target DNA or RNA⁵⁵ as well as small molecules.⁵⁶ Due to this binding the optical properties of the nanoparticles change dramatically, which can be easily detected providing a convenient strategy for the detection of molecules at low concentrations.^{52, 54}

⁵¹ E. Auyeung, J. I. Cutler, R. J. MacFarlane, M. R. Jones, J. Wu, G. Liu, K. Zhang, K. D. Osberg, C. A. Mirkin, *Nat Nano.* **2012**, 7, 24–28

⁵² C. A. Mirkin, *Inorg. Chem.* **2000**, 39, 2258-2272.

⁵³ C. A. Mirkin, R. L. Letsinger, R. C. Mucic, J. J. Storhoff, *Nature*, **1996**, 382, 607-609.

⁵⁴ R. C. Mucic, J. J. Storhoff, C. A. Mirkin, R. L. Letsinger, *J. Am. Chem. Soc.* **1998**, 120, 12674-12675.

⁵⁵ P. Liu, X. Yang, S. Sun, Q. Wang, K. Wang, J. Huang, J. Liu, L. He, *Anal. Chem.*, **2013**, 85, 16, 7689–7695.

⁵⁶ F. Xia, X. Zuob, R. Yangc, Y. Xiaob, D. Kangb, A. Vallée-Bélisleb, X. Gongc, J.D. Yuenac, B. B. Y. Hsua, A.J. Heegera, K. W. Plaxcob, *PNAS*, **2010**, 107, 10837–10841.

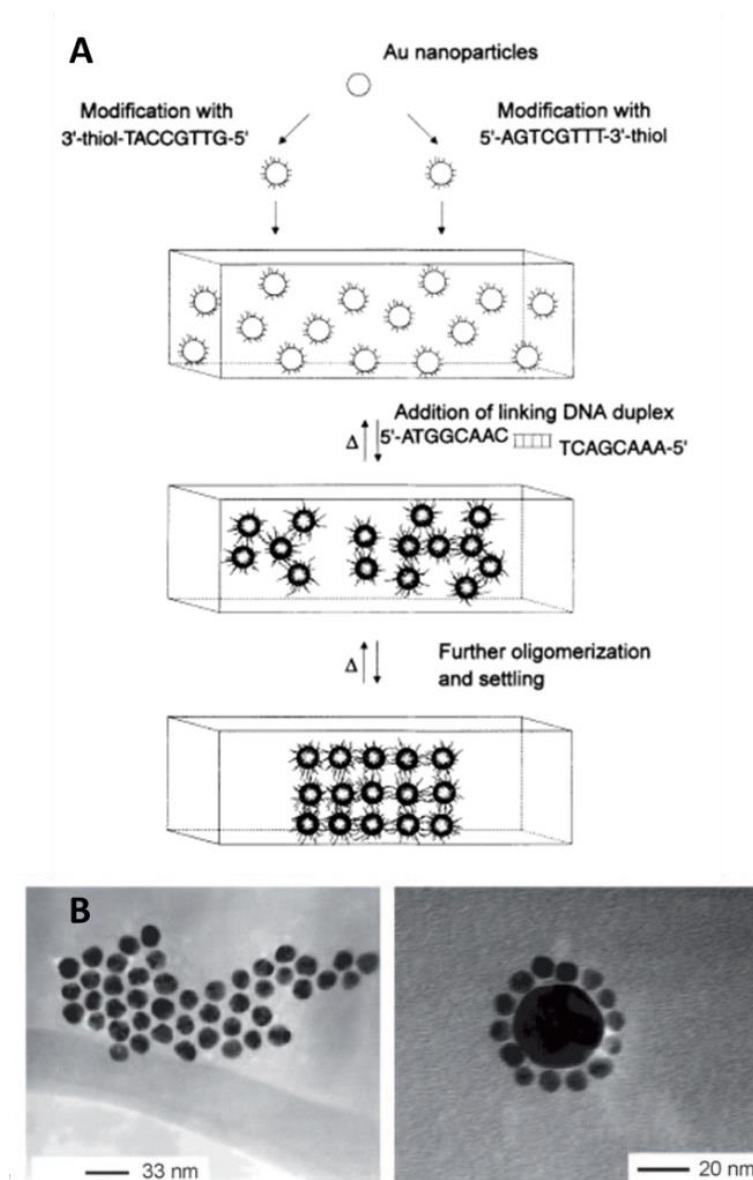


Figure 15. A) Scheme showing the DNA-based colloidal nanoparticles assemble strategy.⁵³ B) TEM image of DNA-directed 13 nm Au NP assembly and TEM image of DNA-induced Au NP assembly with 31 and 8 nm NPs.⁵⁴

Carbon nanotubes are very attractive materials due to its unique conductive properties and toughness, with multiple applications in a variety of fields. For instance, their functionalization with biomolecules has allowed the preparation of a variety sensors^{57,58} and devices with therapeutic applications.^{59,60} The electronic properties of single wall carbon nanotubes (SWCNT) have been exploited by Jacqueline K. Barton and coworkers to measure the conductivity of DNA along 100 bp (34 nm).^{61, 62}

In the last years other materials that have been employed in combination with oligonucleotides are silver nanoclusters (AgNCs). In this case the oligonucleotides are able to stabilize and tune the fluorescent properties of AgNCs.

The standard fluorescent structures currently employed are mainly three: fluorescent proteins,^{63, 64, 65} organic dyes^{66, 67} and fluorescent nanocrystals.^{68, 69} All of them have some limitations and for this reason new fluorescent materials are welcome. Particularly, fluorescent proteins

⁵⁷ X. Tang, S. Bansaruntip, N. Nakayama, E. Yenilmez, Y. I. Chang, Q. Wang, *Nano Lett.*, **2006**, 6, 1632–1636.

⁵⁸ N. J. Kybert, M. B. Lerner, J. S. Yodh, G. Preti, A. T. C. Johnson, *ACS Nano*, **2013**, 7, 2800–2807.

⁵⁹ K. A. Williams, P. T. Veenhuizen, B. G. de La Torre, R. Eritja, C. Dekker, *Nature* **2002**, 420, 761.

⁶⁰ H. Dai, *Acc. Chem. Res.* **2002**, 35, 1035–1044.

⁶¹ X. Guo, A. A. Gorodetsky, J. Hone, J. K. Barton, C. Nuckolls, *Nat Nanotechnology*, **2008**, 4, 163–167.

⁶² J. D. Slinker, N. B. Muren, S. E. Renfrew, J. K. Barton, *Nat Chem.* **2011**, 3, 228–233.

⁶³ R. H. Newman, M. D. Fosbrink, J. Zhang, *Chem. Rev.*, **2011**, 111, 3614–3666.

⁶⁴ W. B. Frommer, M. W. Davidsonb, R. E. Campbell, *Chem. Soc. Rev.*, **2009**, 38, 2833–2841.

⁶⁵ V. Sample, R. H. Newman and J. Zhang, *Chem. Soc. Rev.*, **2009**, 38, 2852–2864.

⁶⁶ F. Wang, W. B. Tan, Y. Zhang, X. Fan and M. Wang, *Nanotechnology*, **2006**, 17, R1–R13.

⁶⁷ A. Waggoner, *Curr. Opin. Chem. Biol.*, **2006**, 10, 62–66.

⁶⁸ H. Mattoussi, G. Palui and H. Bin Na, *Adv. Drug Delivery Rev.*, **2012**, 64, 138–166.

⁶⁹ L. W. Zhang, W. Baumer, N. A. Monteiro-Riviere, *Nanomedicine*, **2011**, 6, 777–791.

have been successfully used in many applications such as protein expression or protein–protein interaction studies.^{70,71} However their size may interfere with some internal cell processes, as well as some aggregation events, which can cause cellular toxicity. The use of organic dyes is limited by their poor photostability and toxicity.⁷² In the case of quantum dots, their size and toxicity are important drawbacks that prevent their use in live cells and animals.^{63,64} In this context, DNA-stabilized silver nanoclusters (DNA-AgNCs) are being intensively studied as alternative fluorescent materials for multiple applications.^{73,74,75,76}

⁷⁰ A. Bavec, *Mol. Biol. Rep.*, **2010**, 37, 2749–2755.

⁷¹ T. J. Magliery, C. G. M. Wilson, W. Pan, D. Mishler, I. Ghosh, A. D. Hamilton, L. Regan, *J. Am. Chem. Soc.*, **2005**, 127, 146–157.

⁷² U. Resch-Genger, M. Grabolle, S. Cavaliere-Jaricot, R. Nitschke, T. Nann, *Nat. Methods*, **2008**, 763–775.

⁷³ A. Latorre, A. Somoza, *ChemBioChem*, **2012**, 13, 951–958.

⁷⁴ B. Han, E. Wang, *Anal. Bioanal. Chem.*, **2012**, 402, 129–138.

⁷⁵ I. Diez, R. H. Ras, *Nanoscale*, **2011**, 3, 1963–1970.

⁷⁶ C. I. Richards, S. Choi, J.-C. Hsiang, Y. Antoku, T. Vosch, A. Bongiorno, Y.-L. Tzeng, R. M. Dickson, *J. Am. Chem. Soc.*, **2008**, 130, 5038–5039.

CHAPTER 1.

DNA Silver Nanocluster (DNA-AgNCs).

Introduction

Silver Nanoclusters.

Silver nanoclusters (AgNCs), are small metallic nanostructures (≤ 2 nm)^{77,78} composed of a few silver atoms (4-10), which can have fluorescent properties. The electronic and optical properties of these metallic structures rely on their size and shape. It is well known that metallic nanoparticles (i. e., size ≥ 2 nm) have intense colours due to the surface plasmon resonance, a feature attributed to the collective oscillation of the conduction electrons and their interaction with light.⁷⁵ The colour of these structures can be modulated by increasing their size in one direction, giving rise to nanoparticles or nanorods with different colours. When the size of these structures is reduced close to the Fermi level (≤ 2 nm), as is the case of nanoclusters, the continuous density of states breaks up into discrete energy levels, leading to large changes in their electrical, optical and chemical properties compared to nanoparticles.^{75, 77, 79, 80, 81, 82} Nanoclusters do not present the characteristic plasmon resonance band of the nanoparticles, however, the energy levels of the electronic transitions of metal nanocluster have shown a strong absorption of light and very good emissions.^{75,77,78 and 80-82-} In this regard, the fluorescence emission

⁷⁷ H. Xu and K. S. Suslick, *Adv. Mater.* **2010**, 22, 1078–1082

⁷⁸ D. Santhakumar, S. Varghese, T. P. Rao, *Electrochimica Acta*, **2013**, 102, 299–305.

⁷⁹ I. Diez, R. H. A. Ras, in *Advanced Fluorescence Reporters in Chemistry and Biology II*, ed. A. P. Demchenko, Springer Berlin Heidelberg, **2010**, 307–332.

⁸⁰ J. Zheng, P. R. Nicovick and R. M. Dickson, *Annu. Rev. Phys. Chem.* **2007**, 58, 409–431.

⁸¹ M. Walter, J. Akola, O. Lopez-Acevedo, P. D. Jadzinsky, G. Calero, C. J. Ackerson, R. L. Whetten, H. Gronbeck, H. Hakkinen, *Proc. Natl. Acad. Sci. U. S. A.*, **2008**, 105, 9157–9162.

⁸² R. C. Jin, *Nanoscale*, **2010**, 2, 343–362.

strongly depends on their size, and is usually excited in the UV-visible range.⁸⁰

In addition, AgNCs, have excellent photo stability and are non-toxic,⁸³ which makes them an attractive alternative to the standard fluorescent probes commonly employed in biological applications,^{83, 84, 85} such as fluorescent proteins,⁶³⁻⁶⁵ organic dyes^{66, 67} and quantum dots.^{63, 68-69} Fluorescent proteins have been successfully used in many applications such as protein expression or protein–protein interaction studies.^{70, 71} However the size of these structures may interfere with some internal cell processes, and aggregation events cause cellular toxicity. The use of organic dyes is limited by their poor photostability and toxicity.⁷² In the case of quantum dots, their size and toxicity are important drawbacks that prevent their use in live cells and animals.^{66, 67}

Fluorescent AgNCs, have been prepared and studied in gas phase,^{86, 87} and in solution through different stabilizing ligands such as dendrimers,⁸⁸ peptides,⁸⁹ polymers⁹⁰ and microgels.⁹¹ The use of oligonucleotides in the stabilization of AgNCs can provide a new layer of versatility to this material due to the self-assembly properties of oligonucleotides.

⁸³ T. Vosch, Y. Antoku, J.-C. Hsiang, C. I. Richards, J. I. Gonzalez, R. M. Dickson, *Proc. Natl. Acad. Sci. U. S. A.*, **2007**, 104, 12616–12621.

⁸⁴ N. de Souza, *Nat. Methods*, **2007**, 4, 540.

⁸⁵ C. A. J. Lin, C.-H. Lee, J.-T. Hsieh, H.-H. Wang, J. K. Li, J.-L. Shen, W.-H. Chan, H.-I. Yeh, W. H. Chang, *J. Med. Biol. Eng.*, **2009**, 29, 276–283.

⁸⁶ F. Conus, V. Rodrigues, S. Lecoultré, A. Rydlo, C. Felix, *J. Chem. Phys.* **2006**, 125, 024511.

⁸⁷ T. Sun, K. Seff, *Chem. Rev.* **1994**, 94, 857–870.

⁸⁸ (a) J. Zheng, R. M. Dickson, *J. Am. Chem. Soc.* **2002**, 124, 13982–13983.; (b) W. Lesniak, A. U. Bielinska, K. Sun, K. W. Janczak, X. Shi, J. R. Baker Jr., L. P. Balogh, *Nano Lett.* **2005**, 5, 2123–2130.; (c) Z. Shen, H. Duan, H. Frey, *Adv. Mater.* **2007**, 19, 349–352; (d) L. Shang, S. Dong, *Chem. Commun.* **2008**, 1088–1090.

⁸⁹ J. Yu, S. A. Patel, R. M. Dickson, *Angew. Chem.* **2007**, 119, 2074–2076; *Angew. Chem. Int. Ed.* **2007**, 46, 2028–2030.

⁹⁰ B. G. Ershov, A. Henglein, *J. Phys. Chem. B* **1998**, 102, 10663–10666.

⁹¹ J. Zhang, S. Xu, E. Kumacheva, *Adv. Mater.* **2005**, 17, 2336–2340.

Silver nanocluster stabilized by Oligonucleotides.

AgNCs stabilized by DNA (DNA-AgNCs) were reported for the first time in 1998 by Braun and co-workers, who prepared a DNA-templated silver wire, although the metallic species generated were not characterized.⁹² Later, in 2004, Dickson and colleagues provided a detailed description of these fluorescent systems,⁹³ which has led to new area of research devoted to the preparation, characterization and application of DNA-AgNCs.

DNA-AgNCs are being intensively studied in the last years as alternative fluorescent probes for the detection of a variety of structures such as peptides, protein, small molecules or metal ions.^{73, 74, 76, 94, 95, 96} The use of DNA as a template for the generation of AgNCs and stabilizing agent, enhances the biocompatibility and water solubility of silver clusters. Interestingly, the selective binding properties of some oligonucleotides (aptamers) make them promising candidates for specific biolabeling.⁹⁷

The preparation of DNA-AgNCs is relatively simple. It requires a silver salt, an oligonucleotide with an appropriate sequence and a reducing reagent. These reagents when mixed in correct order and stoichiometric ratio yield fluorescent AgNCs. An experimental procedure that works for most cases requires an oligonucleotide of 12 nucleotides (nt) with several

⁹² E. Braun, Y. Eichen, U. Sivan, G. Ben-Yoseph, *Nature* **1998**, 391, 775–778.

⁹³ J. T. Petty, J. Zheng, N. V. Hud, R. M. Dickson, *J. Am. Chem. Soc.* **2004**, 126, 5207–5212.

⁹⁴ A. Latorre and A. Somoza, *ChemBioChem*, **2012**, 13, 951–958.

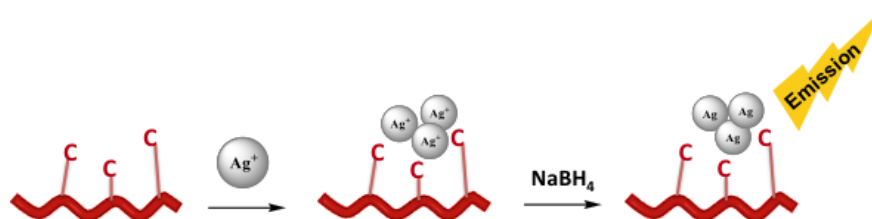
⁹⁵ B. Han and E. Wang, *Anal. Bioanal. Chem.*, **2012**, 402, 129–138.

⁹⁶ C. I. Richards, S. Choi, J.-C. Hsiang, Y. Antoku, T. Vosch, A. Bongiorno, Y.-L. Tzeng and R. M. Dickson, *J. Am. Chem. Soc.*, **2008**, 130, 5038–5039.

⁹⁷ J. Sharma, H.-C. Yeh, H. Yoo, J. H. Werner and J. S. Martinez, *Chem. Commun.*, **2011**, 47, 2294–2296.

cytosines in the sequence. Typically, a micromolar solution of DNA is mixed and incubated with six equivalents of silver nitrate (AgNO_3) for 10 to 15 minutes. Then, six equivalents of sodium borohydride (NaBH_4) are added, the mixture stirred for one minute and incubated in the dark for 12 hours (Scheme 1). This reaction can be performed in water or buffer, such as phosphate buffered saline, citrate, or ammonium acetate, pH 6-7. It is particularly important to prevent the use of halogens, such as chloride, which lead to the formation of their corresponding insoluble salts.

During the incubation of the silver salt with oligonucleotides, Ag^+ ions bind exclusively to the nucleobases and not to negatively charged phosphates of the backbone.^{98, 99} This interaction takes place mainly at two sites, the N3 of pyrimidines and the N7 in purines. When several Ag^+ ions are close to each other, the generation of AgNCs is favoured during the reduction step by NaBH_4 , compared to the generation of AgNPs.¹⁰⁰



Scheme 1.1. DNA–AgNCs preparation. A DNA strand is incubated with silver ions then sequentially reduced with sodium borohydride.

The fluorescence properties of DNA-AgNCs depend on multiple parameters, such as buffer employed, pH, concentration of reagents, size

⁹⁸ R. M. Izatt, J. J. Christensen, J. H. Rytting, *Chem. Rev.* **1971**, 71, 439–481.

⁹⁹ K. F. S. Luk, A. H. Maki, R. J. Hoover, *J. Am. Chem. Soc.* **1975**, 97, 1241–1242.

¹⁰⁰ L. Berti, G. A. Burley, *Nat. Nanotechnol.* **2008**, 3, 81–87.

and oxidation state of the silver clusters.^{101, 102} Remarkably, the emission of DNA-AgNCs depends strongly on the DNA sequence used during their synthesis,^{103, 104, 105} allowing the preparation of a wide palette of colours by changing the nucleotide sequence. In this regard, Dickson and co-workers managed to obtain emitters from blue to red and near infrared using different oligonucleotide sequences (Figure 1).⁷⁶ Nowadays, it is possible to obtain almost any colour from blue to near infrared just by selecting the proper oligonucleotide.⁹³

Blue: 5'-CCCTTTAACCCC-3'
 Green: 5'-CCCTCTTAACCC-3'
 Yellow: 5'-CCCTTAATCCCC-3'
 Red: 5'-CCTCCTTCCTCC-3'

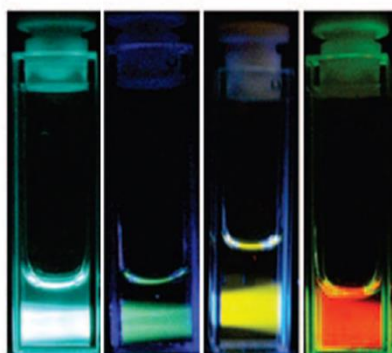


Figure 1.1. Sequences used by Dickson to obtained DNA-AgNCs with different emission wavelengths (left) and pictures of emissive solutions (right).

¹⁰¹ C. Ritchie, K. Johnsen, J. Kiser, Y. Antoku, R. Dickson and J. Petty, *J. Phys. Chem. C*, **2007**, 111, 175–181.

¹⁰² B. Sengupta, C. M. Ritchie, J. G. Buckman, K. R. Johnsen, P. M. Goodwin and J. T. Petty, *J. Phys. Chem. C*, **2008**, 112, 18776–18782.

¹⁰³ S. Choi, J. Yu, S. A. Patel, Y.-L. Tzeng and R. M. Dickson, *Photochem. Photobiol. Sci.*, **2011**, 10, 109–115.

¹⁰⁴ J. Sharma, H.-C. Yeh, H. Yoo, J. H. Werner and J. S. Martinez, *Chem. Commun.*, **2010**, 46, 3280–3282.

¹⁰⁵ P. R. O'Neill, L. R. Velazquez, D. G. Dunn, E. G. Gwinn and D. F. Fygenson, *J. Phys. Chem. C*, **2009**, 113, 4229–4233.

Interestingly, some of these fluorescent materials have shown good pH, temperature and oxidation resistance, preserving 31% of the initial emission intensity after 10 months.¹⁰⁶

In addition, minor structural changes of DNA-AgNCs due to the interaction with other molecules can also affect their fluorescent properties. This property has been exploited to develop sensors for different entities such as ions,^{107, 108} small molecules,^{109, 110, 111, 112} DNA,^{113, 114, 115, 116} microRNAs,^{117, 118, 119} proteins^{120, 121} or tumour cells.¹²²

On the other hand, the use of hybrid materials containing multiple oligonucleotide strands have afforded significant improvements in the selectivity and sensitivity of several orders of magnitude compared to the standard molecular probes.^{79, 83, 84, 123, 124, 125} This is mainly due to the

¹⁰⁶ J. Sharma, R. C. Rocha, M. L. Phipps, H.-C. Yeh, K. A. Balatsky, D. M. Vu, A. P. Shreve, J. H. Werner and J. S. Martinez, *Nanoscale*, **2012**, 4, 4107–4110.

¹⁰⁷ L. Deng, Z. Zhou, J. Li, T. Li and S. Dong, *Chem. Commun.*, **2011**, 47, 11065–11067.

¹⁰⁸ W.-Y. Chen, G.-Y. Lan and H.-T. Chang, *Anal. Chem.*, **2011**, 83, 9450–9455.

¹⁰⁹ S. Han, S. Zhu, Z. Liu, L. Hu, S. Parveen and G. Xu, *Biosens. Bioelectron.*, **2012**, 36, 267–270.

¹¹⁰ K. Ma, Q. Cui, Y. Shao, F. Wu, S. Xu and G. Liu, *J. Nanosci. Nanotechnol.*, **2012**, 12, 861–869.

¹¹¹ G.-Y. Lan, W.-Y. Chen and H.-T. Chang, *RSC Adv.*, **2011**, 1, 802–807.

¹¹² Z. Zhou, Y. Du and S. Dong, *Biosens. Bioelectron.*, **2011**, 28, 33–37.

¹¹³ H.-C. Yeh, J. Sharma, I.-M. Shih, D. M. Vu, J. S. Martinez and J. H. Werner, *J. Am. Chem. Soc.*, **2012**, 134, 11550–11558.

¹¹⁴ G.-Y. Lan, W.-Y. Chen and H.-T. Chang, *Biosens. Bioelectron.*, **2011**, 26, 2431–2435.

¹¹⁵ H.-C. Yeh, J. Sharma, J. J. Han, J. S. Martinez and J. H. Werner, *Nano Lett.*, **2010**, 10, 3106–3110.

¹¹⁶ W. Guo, J. Yuan, Q. Dong and E. Wang, *J. Am. Chem. Soc.*, **2010**, 132, 932–934.

¹¹⁷ P. Shah, A. Rørvig-Lund, S. B. Chaabane, P. W. Thulstrup, H. G. Kjaergaard, E. Fron, J. Hofkens, S. W. Yang and T. Vosch, *ACS Nano*, **2012**, 6, 8803–8814.

¹¹⁸ Y.-Q. Liu, M. Zhang, B.-C. Yin and B.-C. Ye, *Anal. Chem.*, **2012**, 84, 5165–5169.

¹¹⁹ S. W. Yang and T. Vosch, *Anal. Chem.*, **2011**, 83, 6935–6939.

¹²⁰ J. Li, X. Zhong, H. Zhang, C. X. Le and J.-J. Zhu, *Anal. Chem.*, **2012**, 84, 5170–5174.

¹²¹ G.-Y. Lan, W.-Y. Chen and H.-T. Chang, *Analyst*, **2011**, 136, 3623–3638.

¹²² J. Yin, X. He, K. Wang, Z. Qing, X. Wu, H. Shi and X. Yang, *Nanoscale*, **2012**, 4, 110–112.

¹²³ M. L. Collins, B. Irvine, B. D. Tyner, E. Fine, C. Zayati, C. Chang, T. Horn, D. Ahle, J. Detmer, L.-P. Shen, J. Kolberg, S. Bushnell, M. S. Urdea, D. D. Ho, *Nucleic Acids Res.* **1997**, 25, 2979–2984.

¹²⁴ T. A. Taton, G. Lu, C. A. Mirkin, *J. Am. Chem. Soc.* **2001**, 123, 5164–5165.

¹²⁵ S. J. Park, T. A. Taton, C. A. Mirkin, *Science* **2002**, 295, 1503–1506.

interaction between neighbouring DNA ion clouds that enhances the binding between complementary strands. This behaviour can be observed in different hybrid structures such as nanoparticles^{126,127,128} or polymers¹²⁹ with a large number of strands, but it is also possible in hybrid materials with only three¹³⁰, or two¹³¹ strands around a rigid and small molecule core. However, the effects of neighbouring strands on the fluorescent properties of DNA stabilized silver nanoclusters have not been studied.

Objectives

Despite the multiple reports on the preparation and applications of DNA-AgNCs the use of modified oligonucleotides are scarce. In this sense, we aim to use modified oligonucleotides to stabilize AgNCs and modulate their properties. Particularly, we envision that the use of trimeric structures can wrap AgNCs and protect them from quenching improving their fluorescent properties. For this reason we plan to prepare DNA derivatives connected through a benzene derivative for the preparation and stabilization of AgNCs. Therefore, the specific objectives of this part are:

1. Synthesis of DNA trimers using a benzene scaffold
2. Preparation and evaluation of DNA-AgNCs.

¹²⁶ J.-Y. Kim and J.-S. Lee, *Nano Lett.*, **2009**, 9, 4564–4569.

¹²⁷ S. J. Hurst, H. D. Hill and C. A. Mirkin, *J. Am. Chem. Soc.*, **2008**, 130, 12192–12200.

¹²⁸ T. A. Taton, R. C. Mucic, C. A. Mirkin and R. L. Letsinger, *J. Am. Chem. Soc.*, **2000**, 122, 6305–6306.

¹²⁹ J. M. Gibbs, S.-J. Park, D. R. Anderson, K. J. Watson, C. A. Mirkin and S. T. Nguyen, *J. Am. Chem. Soc.*, **2005**, 127, 1170–1178.

¹³⁰ I. Eryazici, I. Yildirim, G. C. Schatz and S. T. Nguyen, *J. Am. Chem. Soc.*, **2012**, 134, 7450–7458.

¹³¹ I. Eryazici, T. R. Prytkova, G. C. Schatz and S. T. Nguyen, *J. Am. Chem. Soc.*, **2010**, 132, 17068–17070.

Result and discussion

Synthesis of DNA trimers

For the preparation of trimers we selected the benzene moiety as scaffold due to its rigid structure, and also to the accessibility of multiple derivatives with the required functional groups. Among the target derivatives we planned to prepare two different derivatives where the oligonucleotides are attached at alternating positions of the benzene ring (Figure 1.2). This scaffold should force a planar structure in order to minimize the electrostatic interaction between the phosphate groups of the DNA strands. To promote a different arrangement, or at least increase the rigidity of the structure, we planned as well to use a scaffold that contains ethyl groups at alternating positions. This kind of structure has been used previously to place groups at different sides of the benzene ring to study the effect of the functional groups in rigidity of the system.¹³²

¹³² (a) J. N. Moorthy, S. Saha, *Eur. J. Org. Chem.* **2010**, 6359–6365. ; (b) D. Y. Lee, N. Singh, M. J. Kim and D. O. Jang, *Org. Lett.*, **2011**, *13*, 3024–3027.

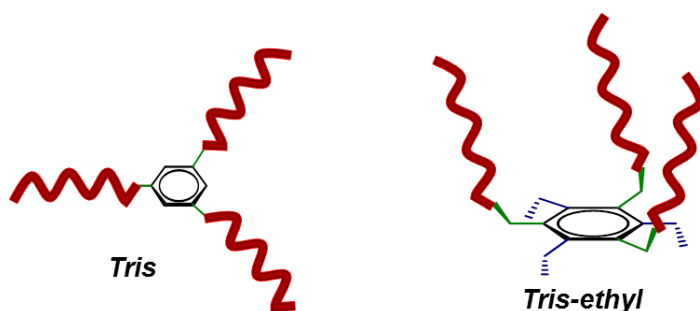


Figure 1.2. Representation of trimers synthesized

Our first attempt to prepare these derivatives was based in the formation of amides between the carboxylic acids present in a benzene derivative and amino modified oligonucleotides. In this case we evaluated the standard conditions employed in the formation of amides where biomolecules are employed. However, the incubation of the benzene derivative, with the amino modified oligonucleotide in the presence of *N*-hydroxy succinimide (NHS) and oligonucleotides modified with an amino group,⁴⁵ did not afforded the desired trimeric structure (Figure 1.3A).

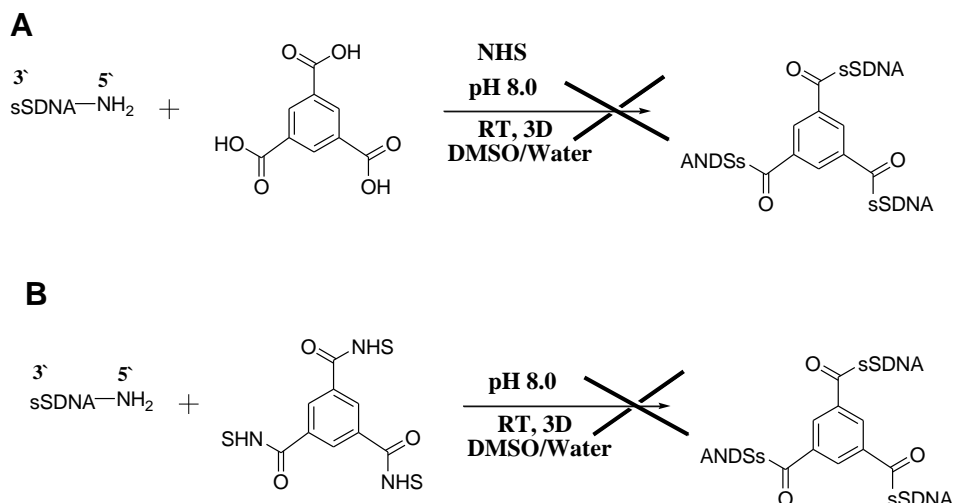


Figure 1.3. Synthetic scheme of preparation if trimeric structure by Amide-coupling reactions

We also prepared and isolated the derivative with all the esters activated and used afterwards in the conjugation with the oligonucleotides, although again, it did not yield the desired derivative (Figure 1.3B).

Then, we decided to use a different reaction for the conjugation of oligonucleotides to the benzene moiety, the copper (I)-catalyzed alkyne-azide cycloaddition (CuAAC), commonly known as “click” reaction.^{61, 133} In this case azide groups will be placed at alternating positions in the benzene ring and an alkyne moiety at the 3'-end of the oligonucleotides. This reaction have been used with oligonucleotides,⁶¹ however, the

¹³³ M. A. Abdalla, J. Bayer, J. O. Radler, K. Mullen, K. *Angew. Chem., Int. Ed.* **2004**, 43, 3967–3970.

conditions should be controlled to prevent the degradation of DNA¹³⁴ and achieve good yields.^{135,136} In our case, the preparation of the desired trimer through this approach implies three click reactions, which efficiency should be very high to achieve good final yields.

In order to evaluate this approach we prepared five benzene derivatives containing the azide moiety. The simplest one was modified with just an azido methyl group (**Azidomethyl benzene (1)**). We also prepared two bi-substituted benzene derivatives, one bearing the azide moieties in ortho and the other in meta (**1,2-bis(azidomethyl) benzene (2)** and **1,3-bis(azidomethyl) benzene (3)** respectively). Two different tri-substituted benzene derivatives were also prepared, one with three azidomethyl groups at alternating positions (**1,3,5-tris(azidomethyl) benzene (4)**) and other containing additionally three ethyl groups at positions 2, 4 and 6 (**1,3,5-tris(azidomethyl)-2,4,6-triethylbenzene (5)**). All these compounds were employed in a click reaction with oligonucleotides modified with a terminal alkyne group. Then, the derivatives obtained were used in the preparation of AgNCs and their properties evaluated. (Figure 1.4).

¹³⁴ J-F. Lutz, Z. Zarafshani, *Advanced Drug Delivery Reviews*, **2008**, 60, 958–970.

¹³⁵ J. Gierlich, G. A. Burley, P. M. E. Gramlich, D. M. Hammond, and T. Carell, *Org. Lett.*, **2006**, 8, 17, 3639-3642.

¹³⁶ N. K. Devaraj, G. P. Miller, W. Ebina, B. Kakaradov, J. P. Collman, E. T. Kool, and C. E. D. Chidsey, *J. Am. Chem. Soc.*, **2005**, 127, 8600-8601

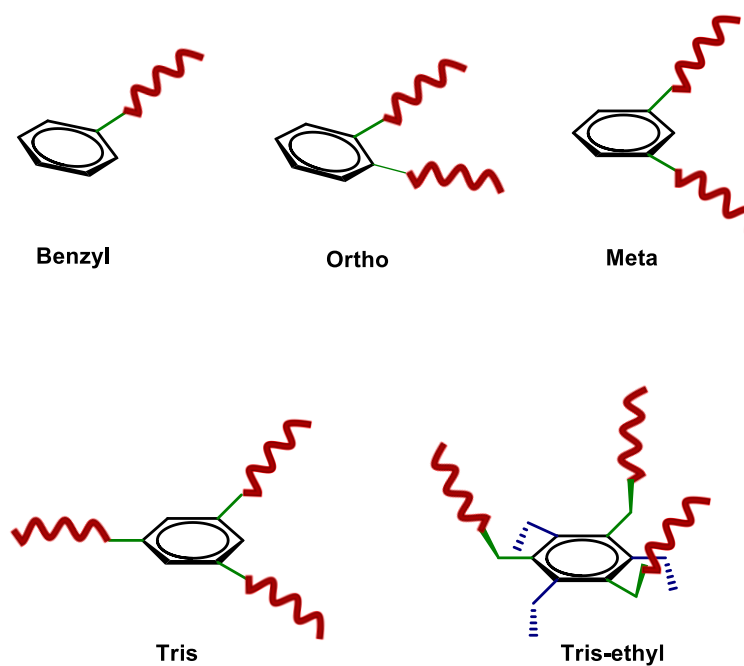
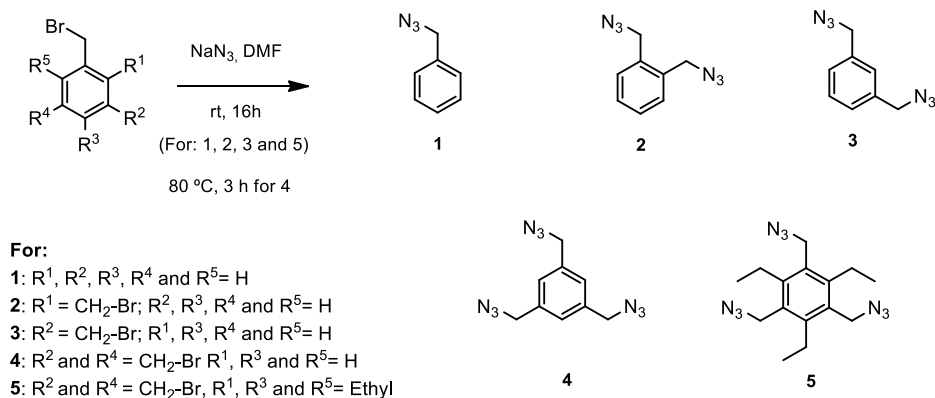


Figure 1.4. Schematic representation of the derivatives prepared.

Synthesis of benzene derivatives

The different benzene derivatives were obtained following previously reported methods (Scheme 1.2). Particularly, to a solution of the corresponding bromo aryl compound in DMF, NaN_3 was added at room temperature and stirred for 16 h to obtain compounds 1, 2, 3 and 5. In the case of compound 4 the temperature was raised to 80 °C and the reaction mixture stirred for 3 h.



Scheme 1.2. Synthetic route for preparation of benzene derivatives.

For these studies we selected a DNA strand composed of twelve cytosines (C12) because it is known that cytosines bind silver better than guanines and much better than adenines and thymine.¹³⁷ In addition, this sequence has been previously employed in the preparation of AgNCs, affording fluorescent AgNCs with a maximum absorption at 560 nm, and emission at 630 nm.^{73, 138}

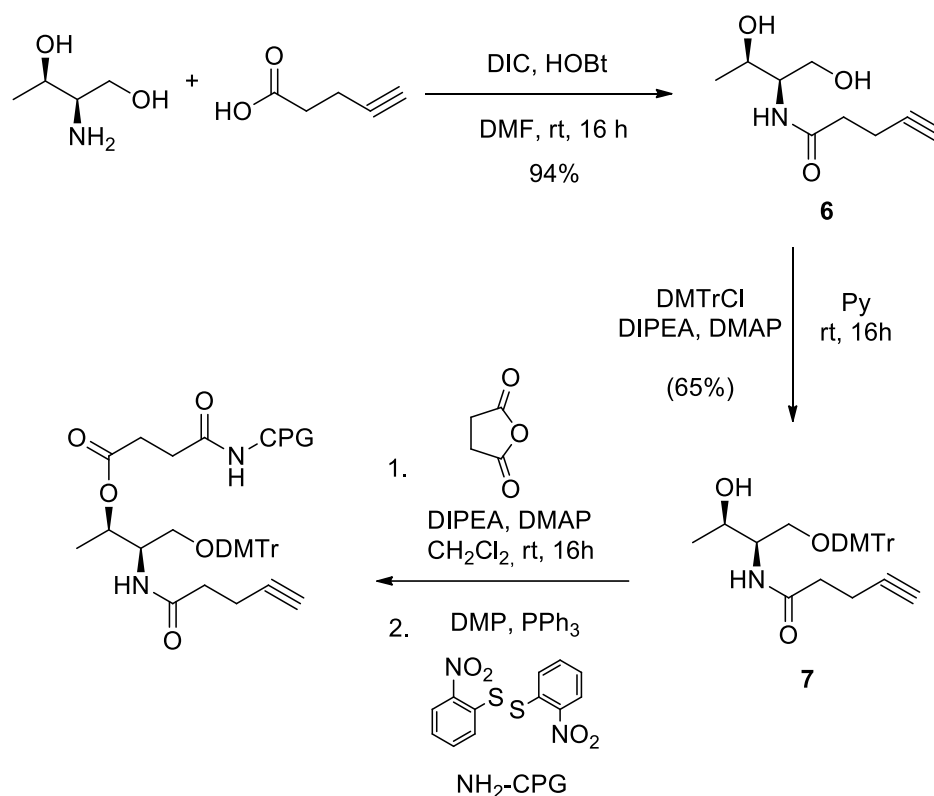
The required DNA strand (C12 sequence) was synthesized on a MerMade4 DNA synthesizer, using a modified solid support containing an alkyne moiety prepared in our laboratory.

¹³⁷ T.T. Zhao, Q. Y. Chen, H. Yang, *Spectrochimica Acta Part A: Molecular and Biomolecular Spectroscopy*, **2015**, 137, 66–69

¹³⁸ G.-Y. Lan, W.-Y. Chen, H.-T. Chang, *Biosens. Bioelectron.* **2011**, 26, 2431 – 2435

Synthesis of modified solid support

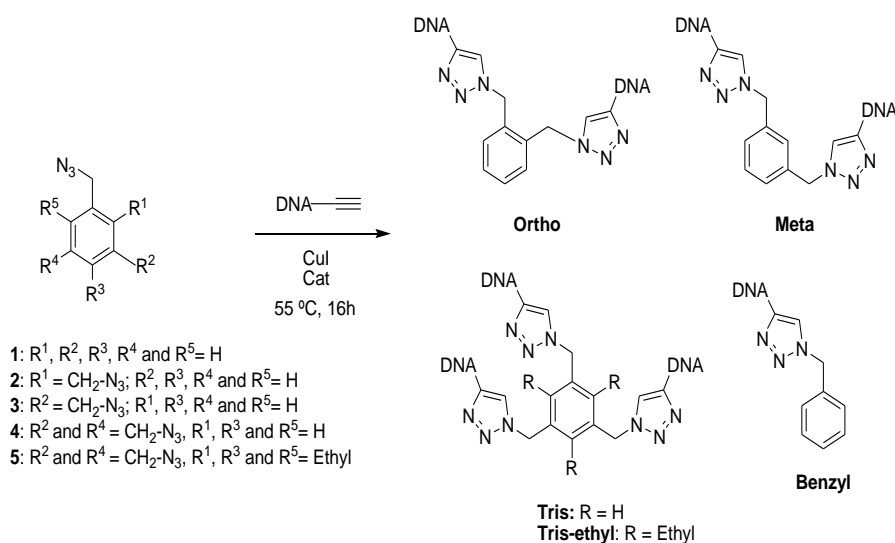
The synthesis of the modified solid support was performed by the procedure described in Scheme 1.3. It involves the reaction between 4-pentynoic acid and threoninol to yield the amide derivative **6**. Then, the secondary hydroxyl group was protected as dimethoxytrytyl group **7** and the primary hydroxyl group was treated with succinic anhydride to introduce a carboxylic acid moiety. This group was used to attach the alkyne molecule to the Controlled Pore Glass (CPG).



Scheme 1.3. Summary of solid support preparation

Click reaction between modified oligonucleotides and benzene derivatives

Once the benzene derivatives and the oligonucleotides were obtained we used the copper catalyzed cycloaddition reaction mentioned above to combine both elements into the final structures. In our case we used CuI as a source of copper, which was stabilized by a standard ligand, TBTA (tris[1-benzyl-1H-1,2,3-triazol-4yl)methyl] amine) (Scheme 1.4).



Scheme 1.4. Click reaction between modified DNA and benzene derivatives.

We found out that in order to obtain the desired products the addition of NaCl was required to reduce the electrostatic repulsion between the strands. The reaction was carried out at 55 °C for 16 hours. The products were purified by polyacrylamide gel electrophoresis (PAGE) and characterized by MALDI-TOF. In the purification gels we only detected

the presence of the final products and the remaining starting material, which was added in excess. It is worth mentioning that degradation of DNA was not observed. As an example a picture of the gel employed in the purification of the trimer **Tris** is included (Figure 1.5).

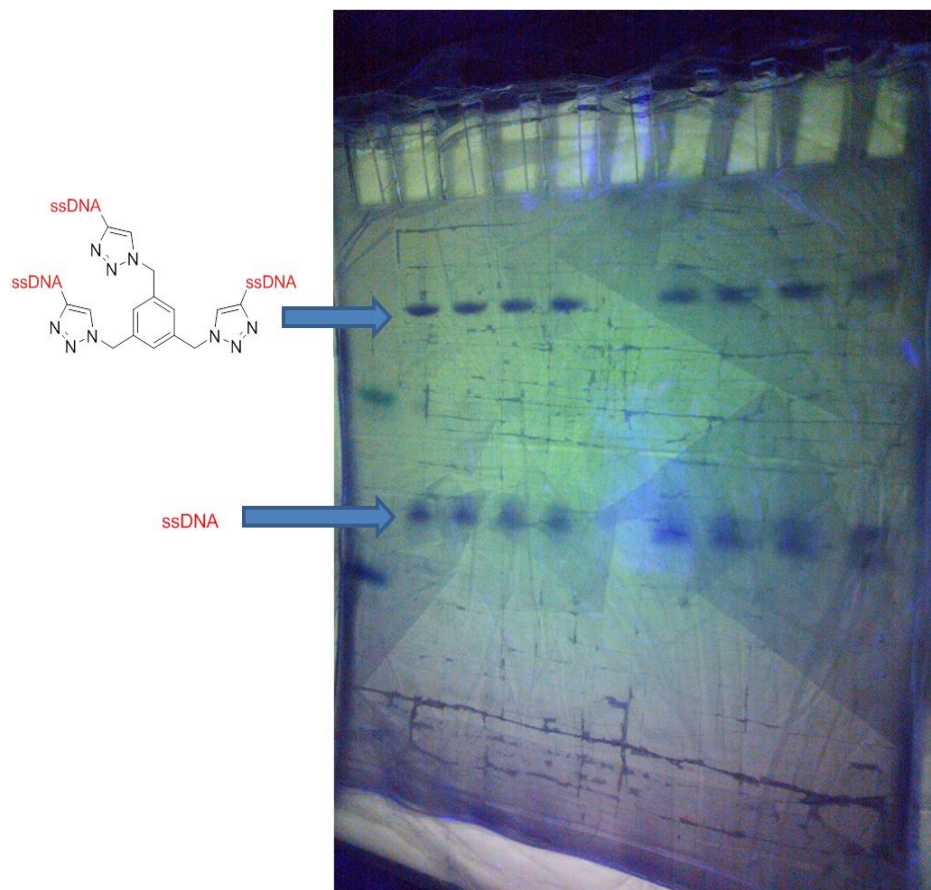
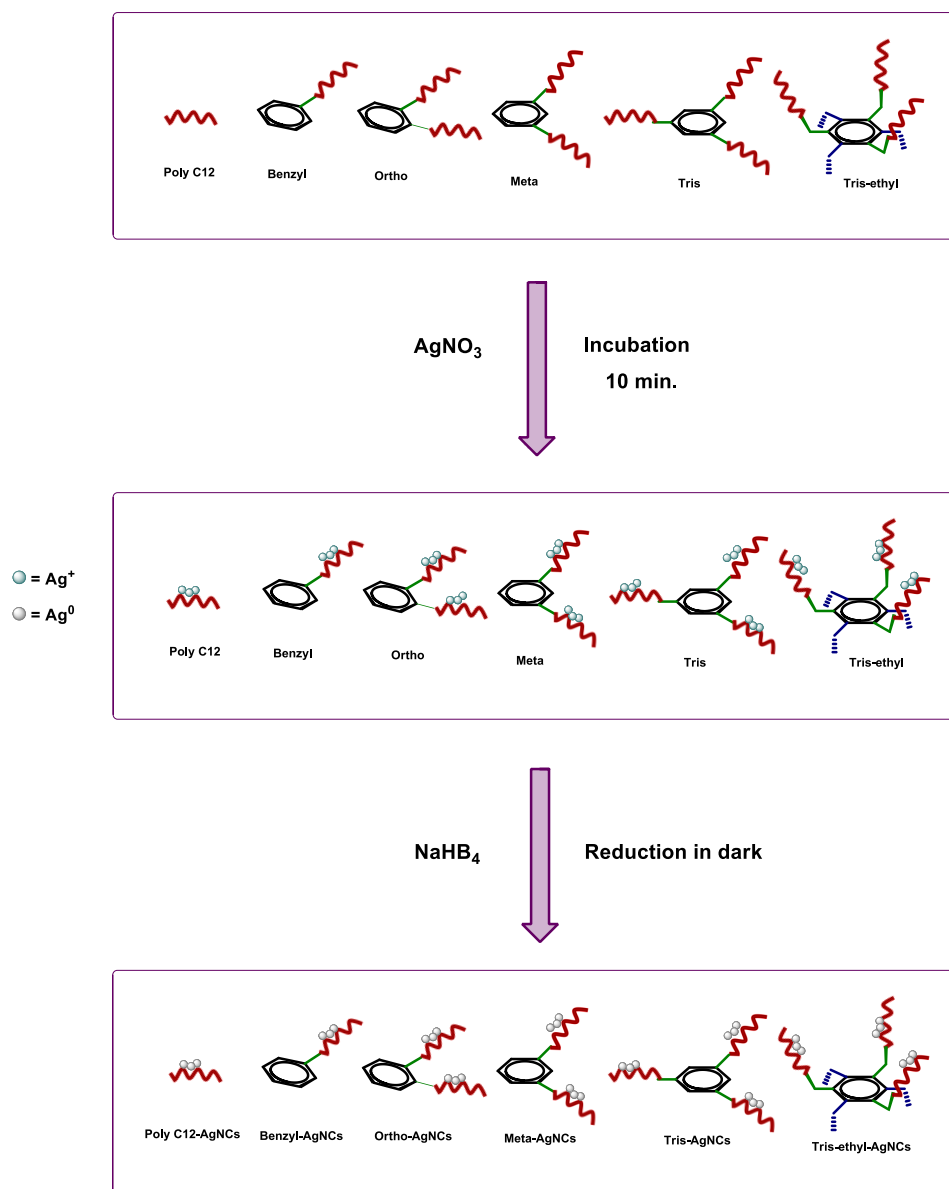


Figure 1.5. Polyacrylamide gel used in the purification of trimer **Tris**. Degradation was not observed after the click reaction.

DNA Silver Nanoclusters (DNA-AgNCs)

Once the conjugates were obtained we employed them in the preparation of AgNCs. The process is very simple it just requires the combination of an aqueous solution of each derivative with six equivalents of AgNO_3 (per oligonucleotide strand) and their incubation at room temperature for 10 min. Then, the silver salt is reduced by the addition of six equivalents of NaBH_4 and vortexed for 1 min. The resulting solutions were stored in the dark at room temperature to yield the corresponding DNA-AgNCs (Scheme 1.5).

**Scheme 1.5.** Synthesis of DNA-AgNCs

Characterization of DNA-AgNCs

The main characteristic of DNA-AgNCs is their fluorescence emission and therefore we check their fluorescence to confirm the presence of AgNCs. Particularly we measure the fluorescence of the AgNCs obtained with the compounds 1-5 after 4 hours. Additionally, we prepared AgNCs using single stranded oligonucleotides containing 12, 24 and 36 cytosines.

We observed that the fluorescence obtained with the branched derivatives was higher than the fluorescence obtained with a single strand of DNA (PolyC12) (Figure 1.6).

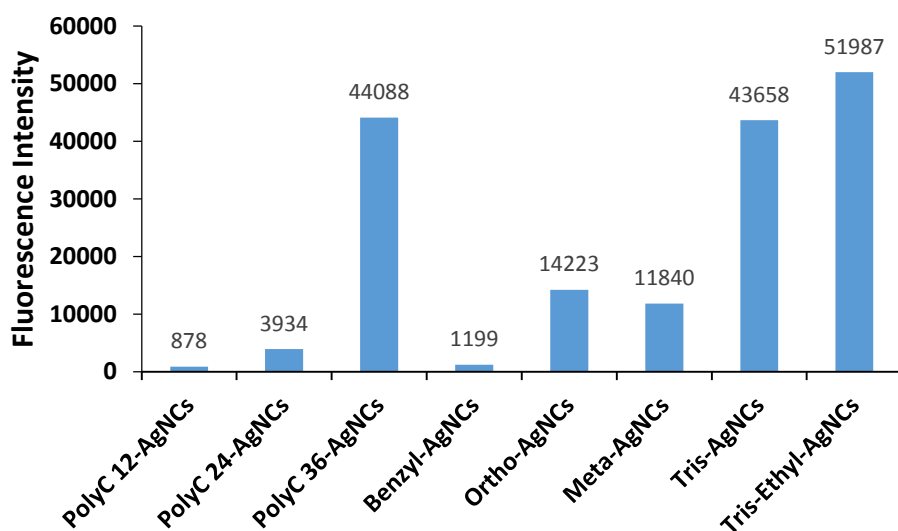


Figure 1.6. Fluorescence of the AgNCs obtained with all derivatives after 4 h.
Ex: 560 nm, Em: 630 nm.

In the case of the dimers, both derivatives yielded more fluorescence than the PolyC24, which has the same amount of nucleotides. Interestingly, the *ortho* derivative showed higher fluorescence than the *meta* derivative, suggesting that the close proximity between strands might enhance the formation of fluorescent AgNCs and/or its stabilization. The most striking results were obtained with the trimers where the fluorescence obtained was around 60 times higher than that obtained with the PolyC 12. Among the trimers, the one bearing the ethyl groups (Tris-ethyl-AgNCs) showed the highest fluorescence values compared with all the samples tested, including single strands of DNA with 24 and 36 cytosines.

It is worth mentioning that also, the fluorescence obtained with the trimers was more reliable than the one obtained with single strands of DNA, where the high values showed here were not obtained in every case.

Then, we studied the formation of the AgNCs complexes by fluorescence during the first hours to better understand the kinetics of AgNCs formation and their stability (Figure 1.7). We observed that the highest fluorescence was achieved after 10 hours, and then it decreased slowly.

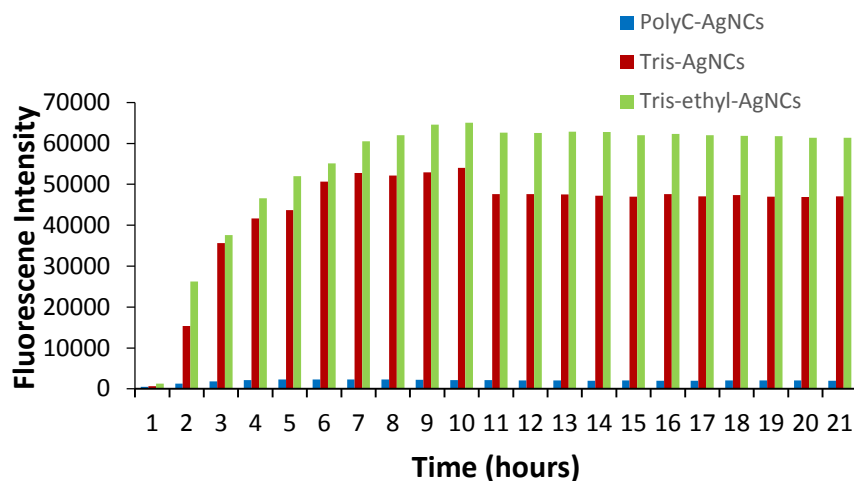


Figure 1.7. Fluorescence of AgNCs generated using PolyC12, Tris and Tris-Ethyl, monitored over 20 h. The maximum fluorescence was observed after 10 h. Ex: 560 nm, Em: 630 nm.

Interestingly, its fluorescence did not decay significantly during the first 21 h (Figure 1.7) and what is more, the fluorescence of the trimers was maintained after 20 days in the dark (Figure 1.8).

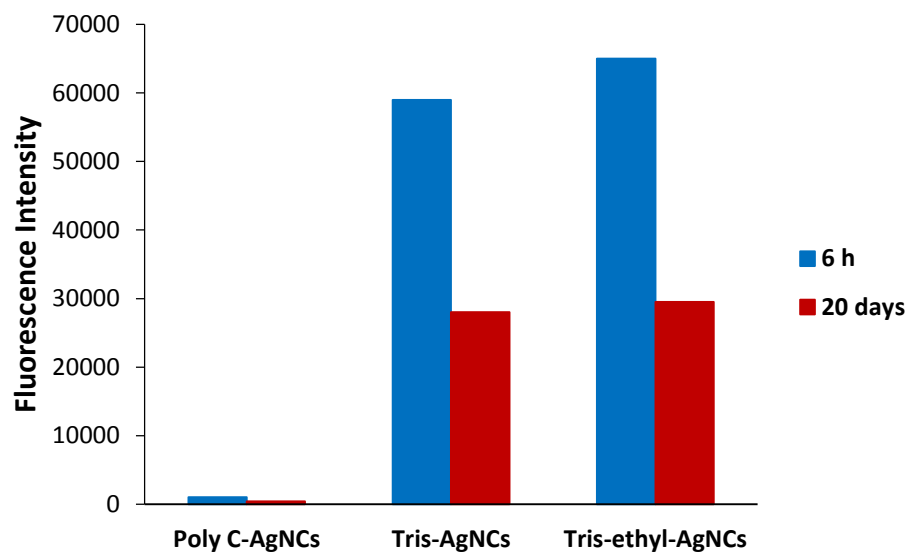


Figure 1.8. Fluorescence of the AgNCs obtained with PolyC, Tris and Tris-ethyl derivatives after 6 h and 20 days. Ex: 560 nm, Em: 630 nm.

We also recorded the absorbance spectrum to the AgNCs obtained with PolyC, Tris and Tris-ethyl derivatives after 6 hours (Figure 1.9). In all cases, two bands were observed, one band at 440 nm, that could be related to the formation of Ag nanoparticles and the other at 560 nm associated with the formation of AgNCs.

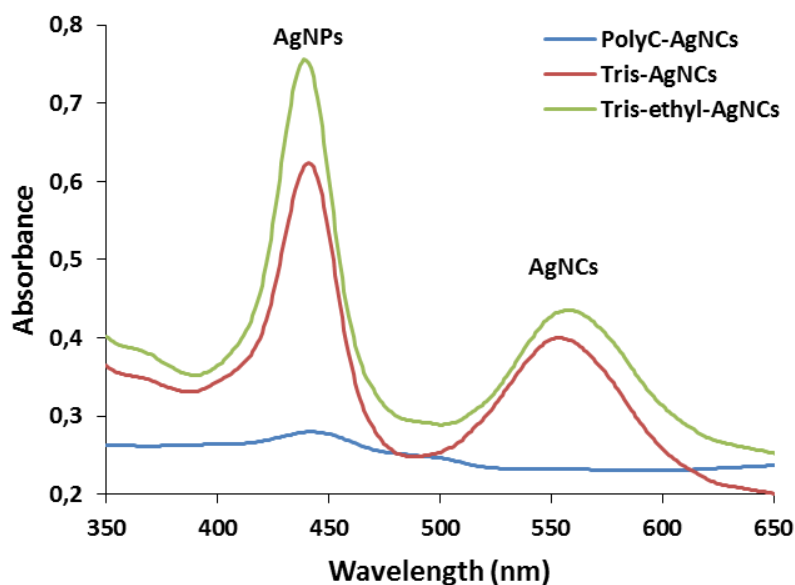


Figure 1.9. UV-Visible spectrum of the AgNCs obtained with PolyC, Tris and Tris-ethyl derivatives after 6 hours of reaction.

When these measurements were done overtime we observed that the band at 440 nm, related to Ag nanoparticles decreases, meanwhile the band associated to AgNCs (560 nm) increases (Figures 1.10 to 1.12). This process is less clear in the case of the PolyC (Figure 1.10) than when the modified oligonucleotides were employed (Figures 1.11 and 1.12) due to the low amount of AgNCs generated with the single stranded oligonucleotide.

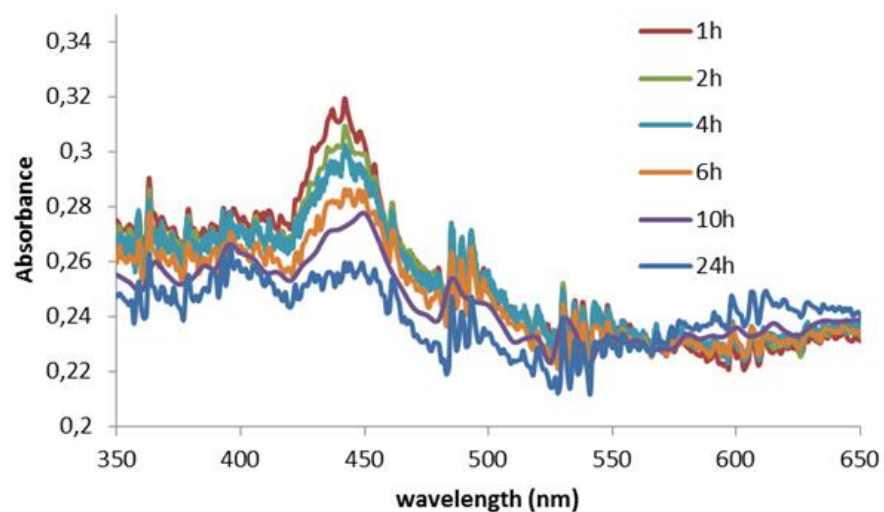


Figure 1.10. UV-Visible spectrum of the AgNCs generated with PolyC. The sample was monitored over 24 h.

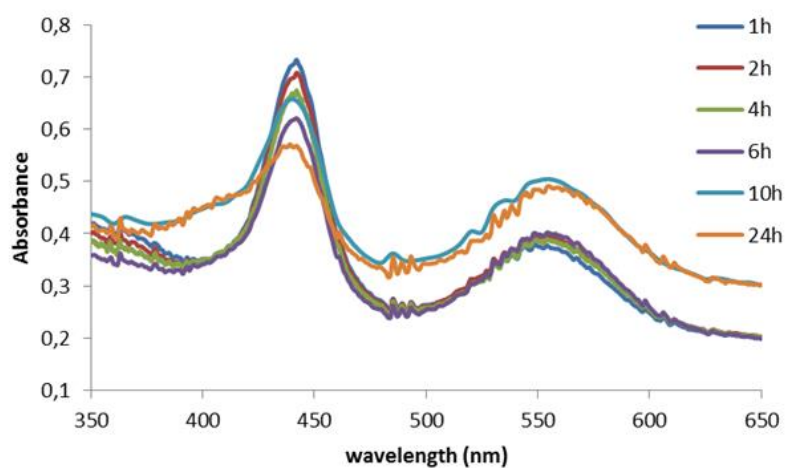


Figure 1.11. UV-Visible spectrum of the AgNCs generated with Tris. The sample was monitored over 24 h. The peak at 450 nm decreases over time meanwhile the peak at 560 nm increases.

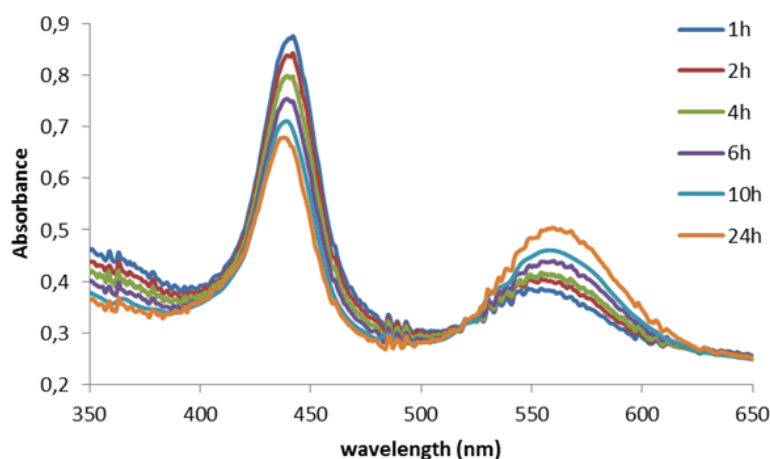


Figure 1.12. UV-Visible spectrum of the AgNCs generated with Tris-ethyl. The sample was monitored over 24h. The peak at 450 nm decreases over time meanwhile the peak at 560 nm increases.

These experiments revealed that during the generation of AgNCs a different structure (or structures) is obtained, which absorbs at 440. However, this structure evolves over time to the formation of the final fluorescent AgNCs. Unfortunately, the total conversion of the silver salt to silver nanoclusters was not possible.

We believe that the high fluorescence as well as the stability observed in the trimers is due to the spatial arrangement of the AgNCs and the DNA strands. In these cases AgNCs could be better protected from quenching and also the close proximity of the strands could result in a cooperative effect, leading to the high fluorescence. This effect is more intense in the

trimer bearing ethyl groups than in the other cases. This may be due to the presence of ethyl groups that force a better packing of the final structure, improving the stability of AgNCs. In the case of PolyC12 the low intensity of the bands observed in the UV-vis spectra correlate well with the low fluorescence observed.

We also monitored the structural changes in the oligonucleotides promoted by AgNCs formation using circular dichroism (CD). We observed that in all cases, the CD spectra of the sequences before the formation of AgNCs showed the characteristic bands of an i-motif structure. However, after the generation of AgNCs the positive band at 280 nm disappeared and the negative band at 265 increased. This change is much clear when the trimers are employed (Figures 1.17 and 1.18) compared to the single stranded sample (Figure 1.16). These data suggest that the structure of the oligonucleotides stabilizing fluorescent AgNCs is different from the structure of the oligonucleotides alone.

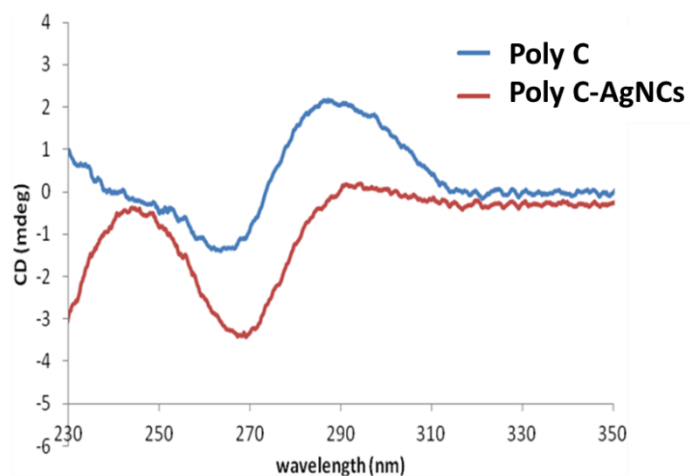


Figure 1.16. Circular dichroism spectra of the DNA strand PolyC12 before and after AgNCs synthesis.

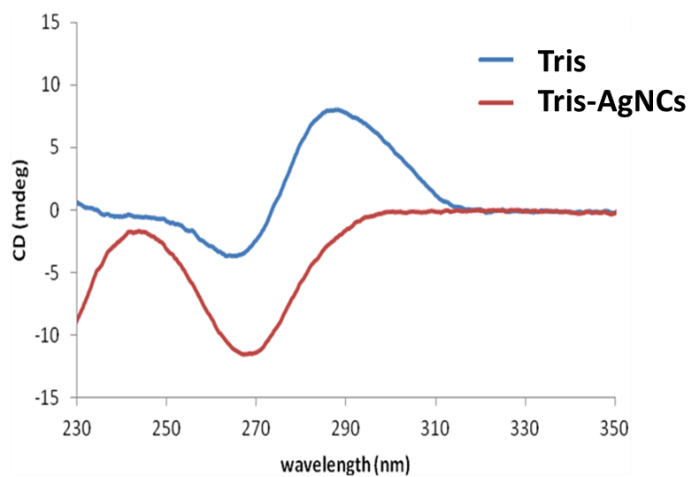


Figure 1.17. Circular dichroism spectra of Tris before and after AgNCs synthesis.

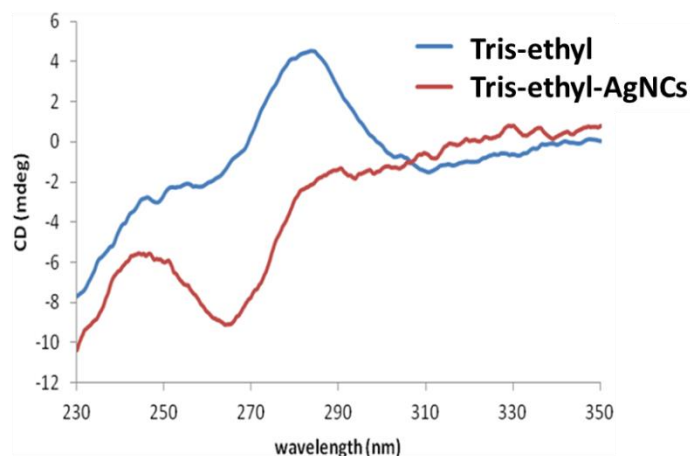


Figure 1.18. Circular dichroism spectra of Tris-ethyl before and after AgNCs synthesis

Finally, we analysed the samples by atomic force microscopy, which allows us to measure the height of the nanoclusters with excellent precision. However, AFM has not good lateral resolution at very low scales due to the size of the tip and the inherent characteristics of this technique. For this reason we used it mainly to analyse the height of the samples. We observed the formation of small particles (ca. 2 nm height) in the case of the both trimers, which could be due to AgNCs (Figure 1.19 and 1.21). In the case of PolyC12, larger structures (12 nm height) were observed, which could be due to the formation of silver nanoparticles during the reduction step (Figure 1.21).

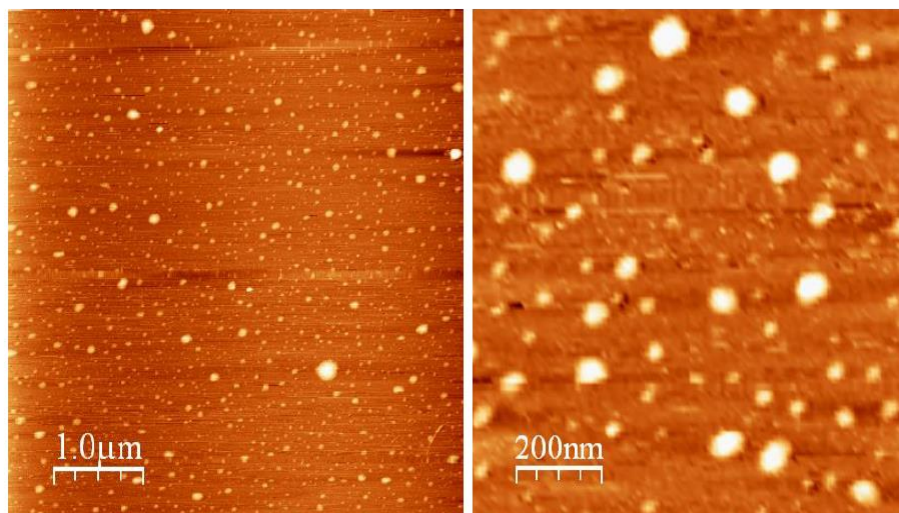


Figure 1.19. AFM images obtained after AgNCs preparation using the Tris derivative. In this case the surfaces showed mainly the presence of particles with an average height between 2 and 3 nm.

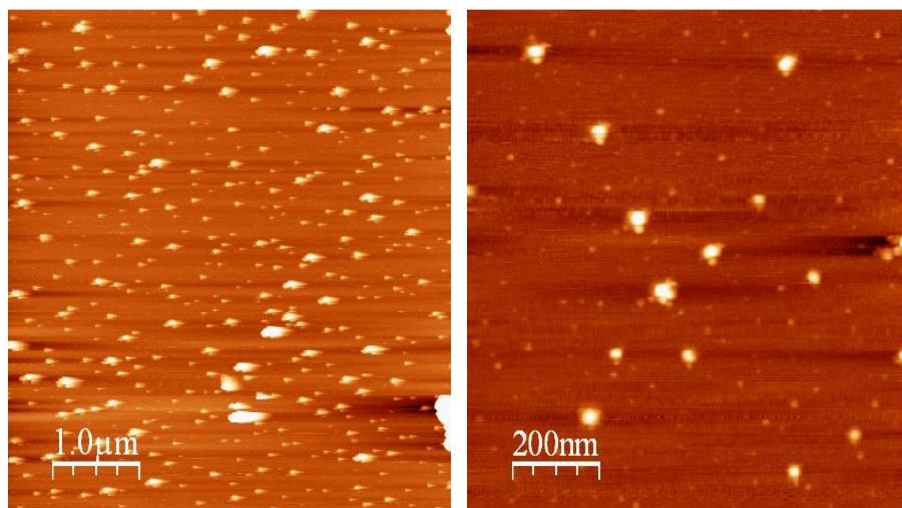


Figure 1.20. AFM images obtained after AgNCs preparation using the Tris-ethyl derivative. In this case, the surface studied showed excellent uniformity in the size and the distribution of the. The average height of the particles is around 2 nm.

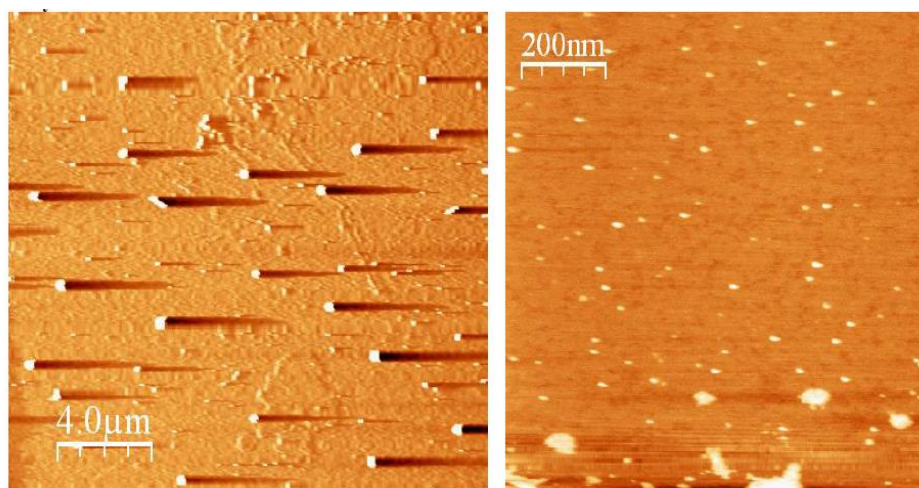


Figure 1.21. AFM images obtained after AgNCs preparation using the PolyC12. On the surfaces studied, we observed two particle sizes, with average height of 11.85 nm and 1.04 nm.

Conclusions

- We have prepared fluorescent silver nanoclusters using novel derivatives of oligonucleotides connected with a benzene molecule.
- DNA-AgNCs, obtained from these derivatives have excellent fluorescent properties, particularly the trimers.
- The fluorescence showed by the trimers was 60 times higher than the one obtained with a single strand.
- The great fluorescence obtained using the trimers might be due to a cooperative effect between vicinal strands, which could stabilize better the AgNCs and prevent their quenching.

Chapter 2.
Structural Characterization of DNA-AgNCs.

Introduction

As mentioned previously, it is known that the fluorescence obtained by DNA-AgNCs strongly depends on the oligonucleotide sequence employed, allowing the preparation of wide variety of emissive materials from blue to near infrared.^{73,76} However, the structure of DNA-AgNCs is still unclear, and its fluorescent properties depend on many variables, besides the oligonucleotide sequence, such as the buffer, pH, concentration of reactants, and the size and oxidation state of the silver clusters. For these reasons, it is not possible to predict the fluorescent properties of these structures. This area of research was initiated by Dickson and co-workers, who studied by mass spectrometry and CD the AgNCs obtained with a 12-mer oligonucleotide (5'-AGGTCGCCGCCC-3').⁹³ Using mass spectrometry they observed that the clusters contained mainly four silver atoms. In addition, the direct interaction between the oligonucleotide and the AgNCs was confirmed by CD, where new bands, one negative at 400 nm and one positive at 450 nm, due to AgNCs were observed.¹³⁹

Since their seminal work, multiple techniques have been employed to study DNA-AgNCs in order to unravel their structure and better understand the generation of the different emitters.

¹³⁹ G. Shemer, O. Krichovski, G. Markovich, T. Molotsky, I. Lubitz, A. B. Kotlyar, *J. Am. Chem. Soc.* **2006**, *128*, 11006–11007.

Fygenson and colleagues evaluated green and red emitters measuring their electrophoretic mobility and diffusivity and concluded that their main difference was its 3D structure.¹⁴⁰

X-ray absorption (EXAFS) was employed by Neidig and colleagues¹⁴¹ to obtain information on the size and bonding arrangement of different clusters. The results showed distances between atoms smaller than those present in metal silver (2.75 vs 2.89 Å), corroborating the generation of silver nanoclusters. This technique was also used to measure the distance between the silver atoms and DNA ($> 2.3\text{Å}$), which is consistent with a bond between the silver atoms and DNA. Interestingly, the nanoclusters evaluated exhibited different sizes depending on the sequence of DNA. However, the authors could not find any correlation between the size and the emission wavelengths.

The interaction between AgNCs and DNA, has also been observed by NMR. In this case the peaks corresponding to H5 and H6 of cytosines are specially affected by the formation of AgNCs. AgNCs interact mainly with cytosines (N3) and guanines (N7) and to a lesser extent with adenines and thymines.^{142,143} For these reasons, most of the oligonucleotides used in the preparation of AgNCs contain multiple cytosines in their sequences, which could induce the formation a stable secondary structure known as i-motif. This particular structure is stabilized by the formation of hydrogen bonds between cytosines at acidic pHs. The i-motif structure has been

¹⁴⁰ T. Driehorst, P. O'Neill, P. M. Goodwin, S. Pennathur, D. K. Fygenson, *Langmuir*, **2011**, 27, 8923–8933.

¹⁴¹ M. L. Neidig, J. Sharma, H.-C. Yeh, J. S. Martinez, S. D. Conradson, A. P. Shreve, *J. Am. Chem. Soc.* **2011**, 133, 11837–11839.

¹⁴² L. Berti, G. A. Burley, *Nat. Nanotechnol.* **2008**, 3, 81–87.

¹⁴³ C. M. Ritchie, K. R. Johnsen, J. R. Kiser, Y. Antoku, R. M. Dickson, J. T. Petty, *J. Phys. Chem. C*, **2007**, 111, 175–181.

studied, among others, by Petty and colleagues¹⁴⁴ who used a C-rich sequence to generate DNA-AgNCs. The sequence forms a stable i-motif structure at pH 6, which can be used to prepare red emitters. In contrast, at pH 9 a green emitter is generated, because at this pH the i-motif structure is destabilized. In this report the authors suggested that DNA-AgNCs are better stabilized when secondary structures are involved.

Recently, Zhao and colleagues studied the interaction between AgNCs and DNA by Raman spectroscopy.¹³⁷ In this case they employed a DNA sequence that folds into an anti-parallel i-motif structure made of four strands (C-Quadruplex). However, when the AgNCs are generated the structure disappears. These changes were well studied by Raman spectroscopy, where they observed that after the formation of the AgNCs, the DNA structure changed from B-form to Z-form. In this case the peaks from the O-P-O asymmetric vibration, 810 and 832 cm^{-1} , shifted to 810 cm^{-1} in the Raman spectrum. In addition, a peak at 240 cm^{-1} indicating the formation of Ag-N bonds was also observed. Therefore the changes observed in the C-quadruplexes may be caused by formation of the Ag-N bonds, which prevent the formation of the hydrogen bonds between cytosines.

In summary, despite the multiple studies the structure of DNA-AgNCs is not completely clear, and more important, there is not a clear correlation between the sequence of the oligonucleotide and the wavelength of the emitters. There are multiple parameters that can modulate the fluorescent properties of AgNCs, such as pH, temperature, oxidation state. However,

¹⁴⁴ B. Sengupta, K. Springer, J. G. Buckman, S. P. Story, O. H. Abe, Z. W. Hasan, Z. D. Prudowsky, S. E. Rudisill, N. N. Degtyareva, J. T. Petty, *J. Phys. Chem. C*, **2009**, *113*, 19518–19524.

the most important factor seems to be the oligonucleotide sequence and its secondary structure generated during the formation of AgNCs.

In this context, we decided to study the structure of different DNA-AgNCs using NMR and CD aiming to unravel any clue that might help in the design of DNA-AgNCs. For this study we selected six sequences, the PolyC, previously used in the preparation of dimers and trimers,¹⁴⁵ four sequences used by Dickson and co-workers⁷⁶ that yielded different emitters (Green, Yellow, Red and Ni-Red) and a sequence (L1Tcc), which secondary structure is known¹⁴⁶ although it has not been previously employed in the preparation of AgNCs. Therefore, the specific objectives of this part are:

1. Structural characterization by ¹H NMR and circular dichroism (CD) spectroscopy of the selected sequences.
2. Study of the secondary structures of these systems by CD spectroscopy under different concentration and temperatures.

¹⁴⁵ A. Latorre, R. Lorca, F. Zamora, A. Somoza, *Chem. Commun.*, **2013**, 49, 4950-4952

¹⁴⁶ N. Escaja, J. Viladoms, M. Garavís, A. Villasante, E. Pedroso, C. González. *Nucleic Acids Res*, **2012**, 40, 22, 11737-11747.

Results and Discussion

Characterization by ^1H -NMR

To evaluate the effect of the DNA structures after the formation of AgNCs, we recorded the ^1H -NMR of the DNA strands before and after the formation of the metallic clusters.

Table 2.1. Sequences employed in this study.

Name	Sequence
PolyC	5'-(dC) ₁₂ -ALK-3'
Green	CCCTCTTAACCC-3'
Yellow	5'-CCCTTAATCCCC-3'
Red	5'-CCTCCTTCCTCC-3'
NI-Red	5'-CCCTAACTCCCC-3'
L1tcc	5'-TCCGTTTCCGT-3'

In the case of PolyC (Figure 2.1) we observed the characteristic signals of an i-motif arrangement, which involves an interaction between cytosines in acidic pHs where the imine nitrogen of one cytosine is protonated.

Then the spectrum after the formation of the AgNCs was recorded. In this case, we did not observed signals from an i-motif structure, suggesting that the imine nitrogen was interacting with the AgNCs. In the aromatic region some changes were also observed, however, due to the symmetry of the sequence, we could not assign properly the signals. For this reason, we

decided to evaluate the L1Tcc sequence, which folds into a characteristic i-motif.

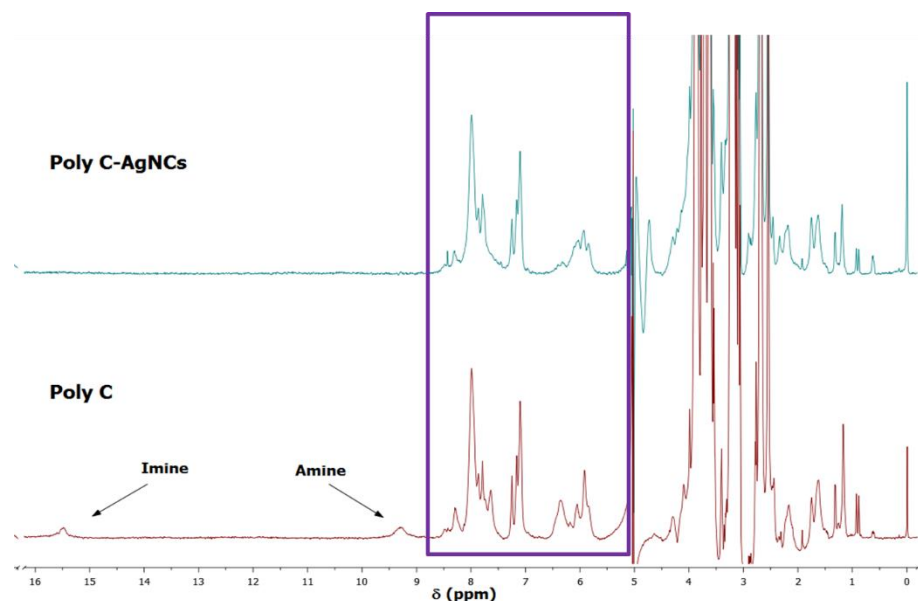


Figure 2.1. ^1H NMR spectrum measured at 5 °C for PolyC and PolyC-AgNCs 200 μM in $\text{H}_2\text{O}/\text{D}_2\text{O}$ 90/10 to pH = 5.3

We recorded the proton spectrum of the L1Tcc strand before and after formation of DNA-AgNCs (Figure 2.2). As expected, the characteristic signals of an i-motif were observed, although no changes were observed in the spectrum after the incubation with AgNO_3 and reduction with NaBH_4 . This result suggests that this sequence folds into a very stable structure that does not change during the protocol employed to generate AgNCs. What is more, this sequence did not yield fluorescence materials, pointing out that this sequence is not suitable for the generation of AgNCs.

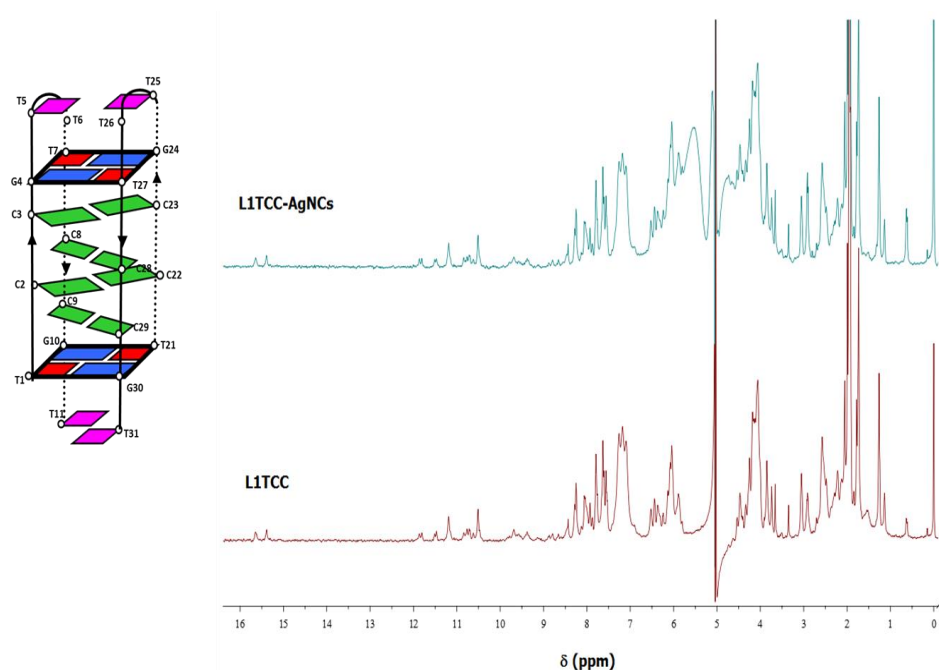


Figure 2.2. ^1H NMR spectrum measured at 5 °C for L1TCC and L1TCC-AgNCs 120 μM in Na Pi 25 μM , pH=4.8.

Different results were obtained with the sequences reported by Dickson.¹ (Green, Yellow, Red and NI-Red sequences) (Figures 2.4-2.7). In all these cases, it was observed the characteristic signals of an i-motif before the formation of AgNCs. However, the changes observed after the formation of AgNCs depend on the sequence employed. We observed that the intensity of the change observed seems to be related to the fluorescence intensity reported by these systems (Figure 2.3). I.e. in the case of the sequence that generates green emitting AgNCs we observed small changes between the two spectra and in this case the fluorescence intensity was the

lowest. On the other hand, the other three sequences reported significant changes in the spectra and their fluorescence intensity was much higher

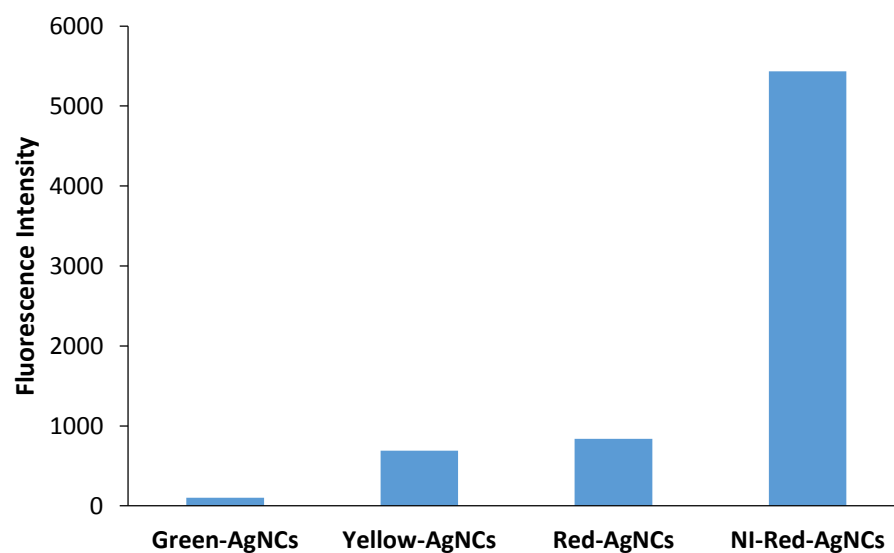


Figure 2.3. Comparison of fluorescence intensity of DNA-AgNCs obtained with different sequences reported by Dickson. (Green, Yellow, Red and NI-Red sequences).

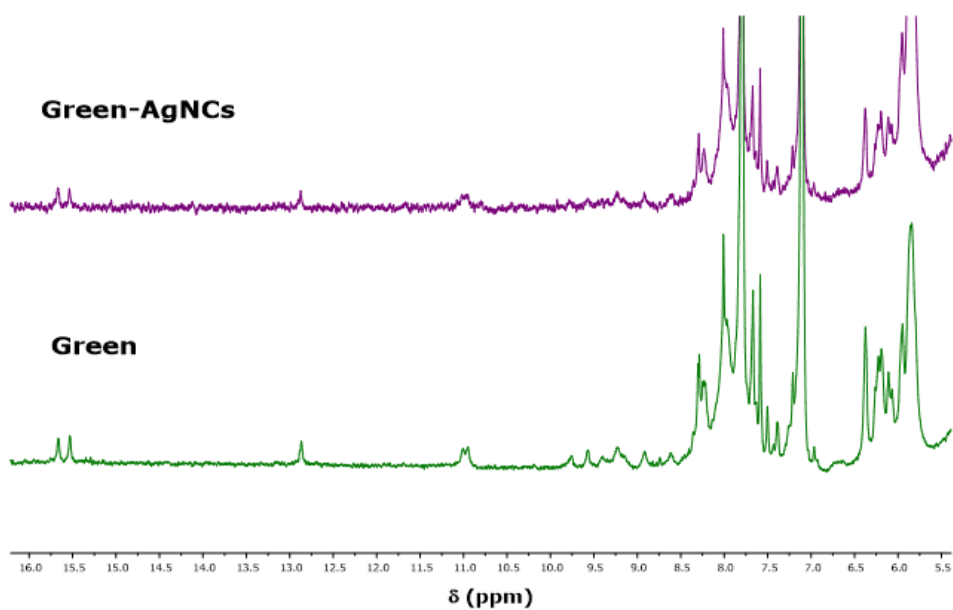


Figure 2.4. ^1H NMR spectrum measured at 5 ° C for Green and Green-AgNCs
200 μM in $\text{H}_2\text{O}/\text{D}_2\text{O}$ 90/10 to pH = 4.4.

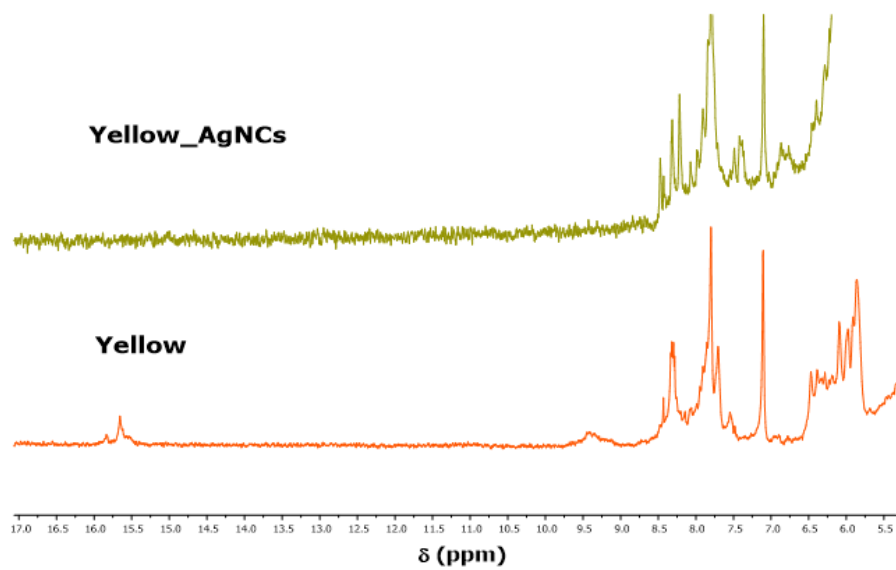


Figure 2.5. ^1H NMR spectrum measured at 5 ° C for Yellow and Yellow-AgNCs
200 μM in $\text{H}_2\text{O}/\text{D}_2\text{O}$ 90/10 to pH = 5.4.

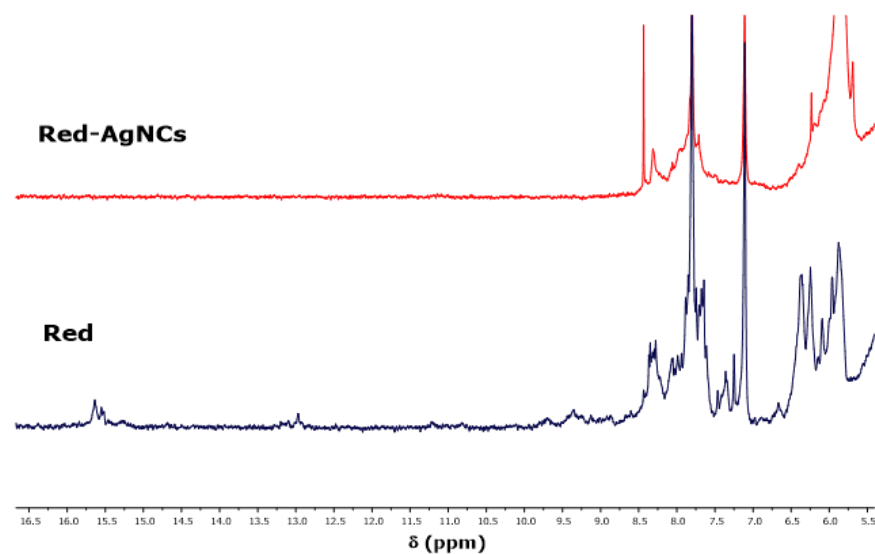


Figure 2.6. ^1H NMR spectrum measured at 5 ° C for Red and Red-AgNCs 200 μM in $\text{H}_2\text{O}/\text{D}_2\text{O}$ 90/10 to pH = 5.4.

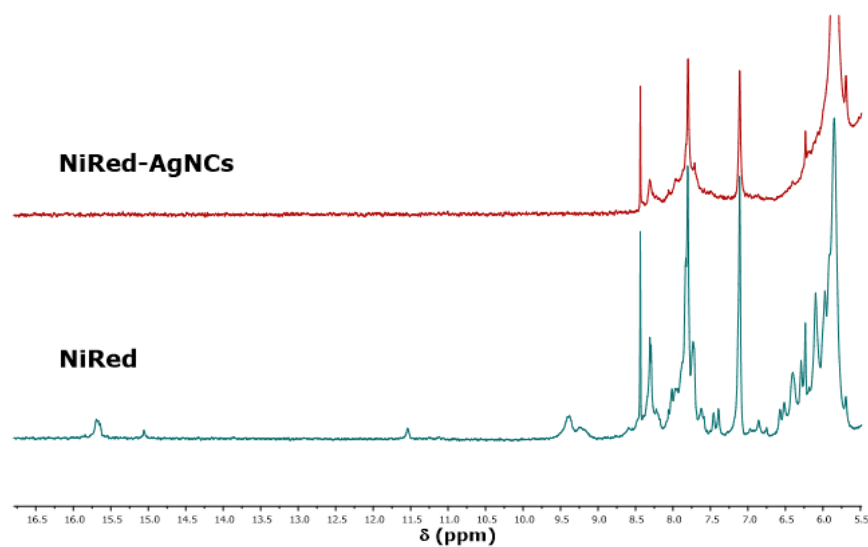


Figure 2.7. ^1H NMR spectrum measured at 5 ° C for Ni-Red and Ni-Red-AgNCs 200 μM in $\text{H}_2\text{O}/\text{D}_2\text{O}$ 90/10 to pH = 5.4.

Another technique commonly used in structural studies of DNA is CD spectroscopy. This technique provides important information on the secondary structure adopted by the DNA sequences. For this reason, we have also recorded the CD spectra of the different sequences used before and after the formation of the AgNCs.

Characterization by CD Spectroscopy

We recorded the CD spectra before and after the formation of the AgNCs (Figure 2.8 to 2.13). As in the NMR experiments, all sequences showed the characteristic peaks of an i-motif structure with a dominant positive band around 290 nm and a negative one about 260 nm. In all cases the presence of silver atoms induces large changes in the CD spectra, although not all the samples yielded fluorescent AgNCs, such as L1Tcc.

In the case of PolyC, Green, Yellow, Red and NI-Red (Figure 2.8, 2.10 to 2.13), the band around 260 nm is shifted to 270 nm and the band at 290 nm decreases significantly. This decrease was more pronounced when the Red and Ni-Red sequences were employed. (Figure 2.12 and 2.13). In the case of the green emitter, a new positive band near 240 nm was observed (Figure 2.10). However in the case of L1Tcc (Figure 2.9) the CD spectrum changes notably, where the CD signals almost disappear after the formation of AgNCs. This result does not correlate well with information obtained by ^1H -NMR, where we did not observe significant variations. It might mean that although the secondary structure changes after the

formation of AgNCs the C:C base pairs remain intact. Anyhow, further studies need to be done to solve these discrepancies.

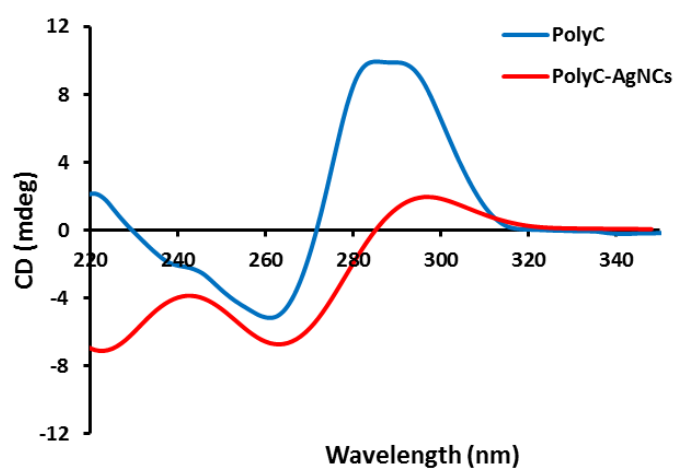


Figure 2.8. Circular dichroism spectra to room temperature of the PolyC sequences before and after preparation of DNA-AgNCs, to 25 μ M and pH = 5.3.

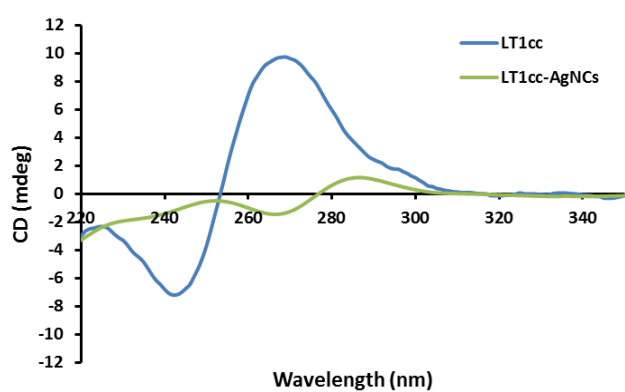


Figure 2.9. Circular dichroism spectra to room temperature of the LT1cc sequences before and after preparation of DNA-AgNCs, in Na Pi 25 μ M, pH=4.8.

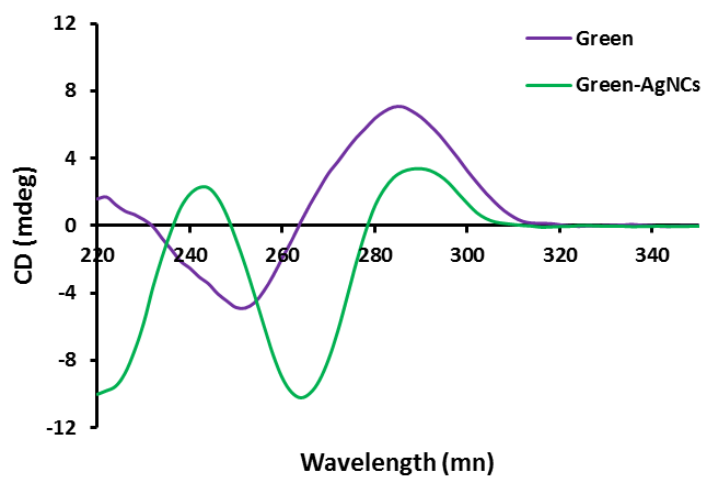


Figure 2.10. Circular dichroism spectra to room temperature of the Green sequences before and after preparation of DNA-AgNCs, to 25 μ M and pH = 4.4.

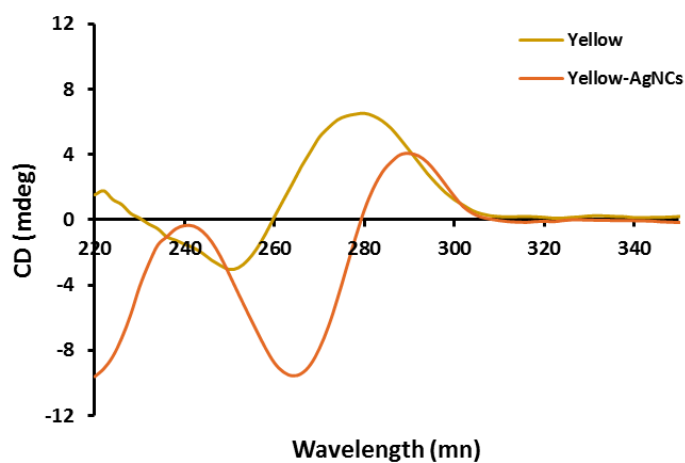


Figure 2.11. Circular dichroism spectra to room temperature of the Yellow sequences before and after preparation of DNA-AgNCs, to 25 μ M and pH = 5.4.

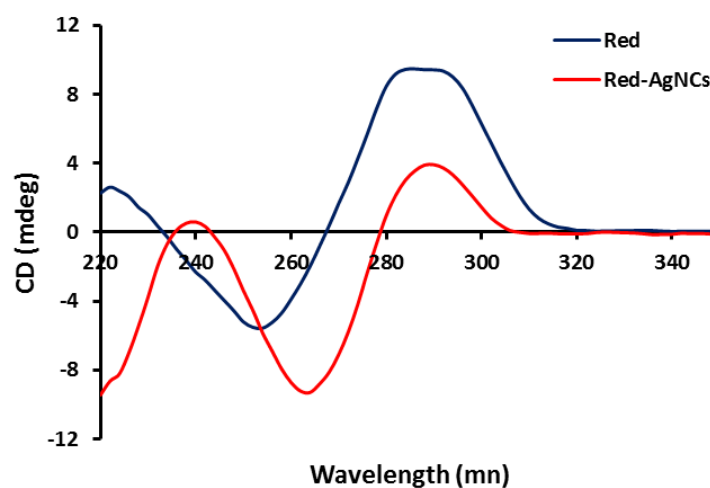


Figure 2.12. Circular dichroism spectra to room temperature of the Red sequences before and after preparation of DNA-AgNCs, to 25 μ M and pH = 5.4.

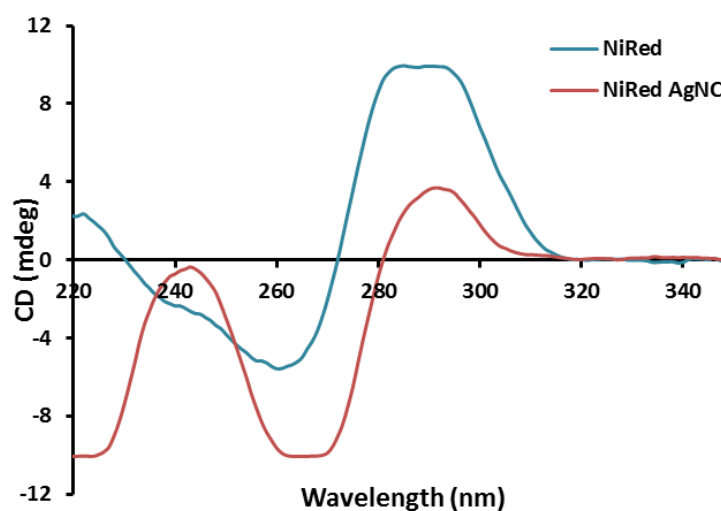


Figure 2.13. Circular dichroism spectra to room temperature of the Ni-red sequences before and after preparation of DNA-AgNCs, to 25 μ M and pH = 5.4.

Based on these results, we decided to continue the study using just two sequences, one that generates emitters with low intensity (green) and other with high intensity (Ni-Red). These derivatives showed different behaviour by CD and NMR and can represent sequences that yield bad and good emitters respectively. In this regard, we have evaluated by CD the effect of concentration and temperature to assess the stability of the structures generated.

To evaluate the effect of the concentration we recorded the spectrum before and after formation of AgNCs at different concentrations (15, 25 and 50 μM), using the Green (Figure 2.14) and Ni-red sequences (Figure 2.15). In both cases, the concentration only resulted in an increase in the intensity of the bands, without shifting their position. This result suggests that tertiary structures are not formed under these conditions and therefore the molecularity of the complexes is simple.

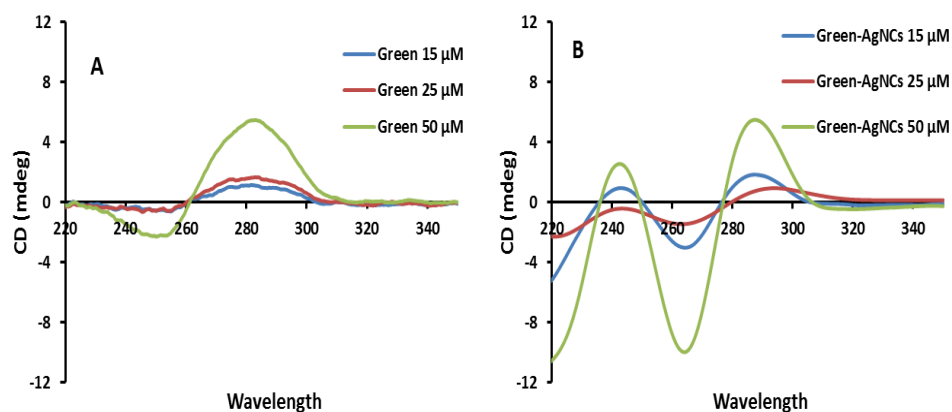


Figure 2.14. Circular dichroism spectra to room temperature of the Green sequences A) before and B) after of preparation DNA-AgNCs, to 15, 25 and 50 μ M and pH = 4.4.

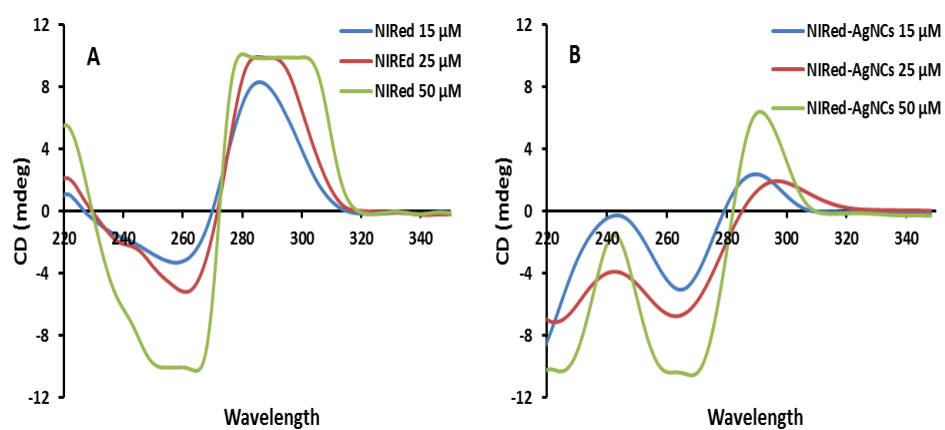


Figure 2.15. Circular dichroism spectra to room temperature of the Ni-Red sequences A) before and B) after of preparation DNA-AgNCs, to 15, 25 and 50 μ M and pH = 5.4.

Then, the structural stability of these two sequences by CD at variable temperature before and after the formation of AgNCs was evaluated. In the case of the Green sequence (Figure 2.16 A) we observed that the secondary structure is quite stable because only a small change in the spectrum at high temperature was observed. On the other hand, the Red sequence (Figure 2.17 A), showed a large change at high temperature, suggesting that the secondary structure is less stable. However, once the AgNCs are formed a different pattern is observed, where Ni-Red AgNCs seem to be more stable than Green-AgNCs. (Figure 2.16 B and 2.17 B).

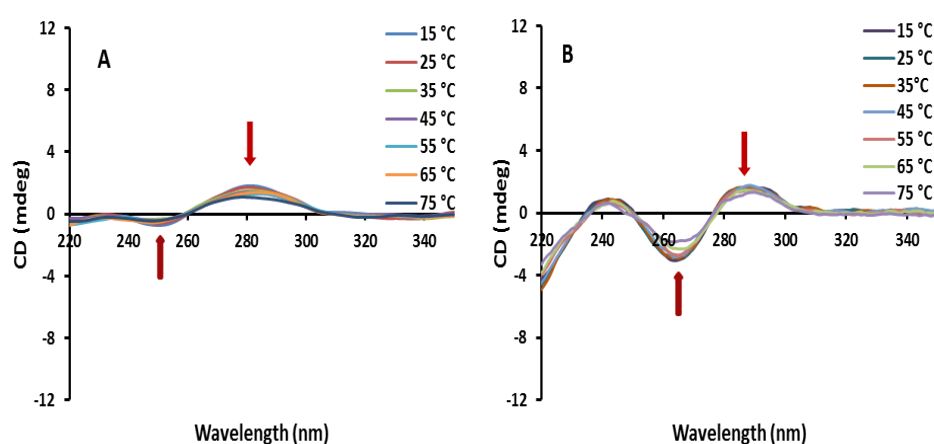


Figure 16. Circular dichroism spectra to variable temperature of Green sequence A) before and B) after preparation of DNA-AgNCs, to 25 μM in water and pH=4.4.

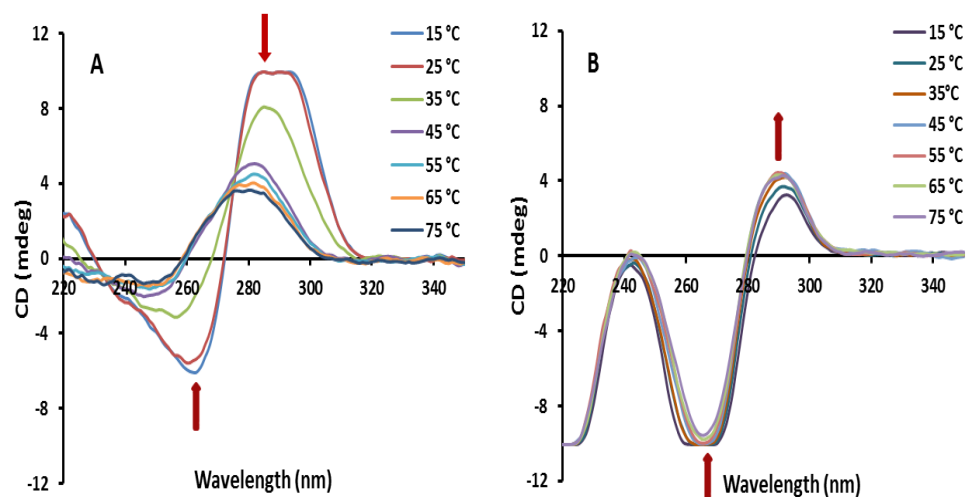


Figure 17. Circular dichroism spectra to variable temperature of Ni-Red sequence A) before and B) after preparation of DNA-AgNCs, to 25 μ M in 25 μ M in Buffer sodium acetate pH=5.4.

Conclusions

- The relationship between sequence and fluorescent properties is difficult to find, however it seems that the secondary structure plays an important role.
- In this sense, we have observed that oligonucleotides with a stable secondary structure yield AgNCs with low fluorescent intensity.
- On the other hand, when secondary structure is less stable, AgNCs have higher fluorescent intensities.
- In addition to the standard parameters that control the fluorescence (sequence, concentration, salt or secondary structure), we hypothesize that some differences in fluorescence maybe also due to the formation of tertiary structures.

Chapter 3.
Novel Catalyst for Click Reaction.

Introduction

The development of nanomaterials and biomaterials with precise control in composition, architecture and functionality has generated great advances in various fields, such as, biomedicine and materials science.^{147, 148} In addition, strategies that allow the connection of different molecules or materials in a straightforward manner have expanded the functional diversity of these materials significantly. In this regard, the ligations known as “Click Chemistries” are particularly relevant due to their ease of use and efficiency and include a variety of reactions such as Diels-Alder,^{149, 150} Staudinger,¹⁵¹ oxime,¹⁵² hydrazine,¹⁵³ thiol-ene,¹⁵⁴ aza-Wittig¹⁵⁵ and 1,3-dipolar cycloadditions.^{156, 157, 158} In the latter case, the cycloaddition between azides and alkynes have been widely explored in

¹⁴⁷ G.K. Such, A.P.R. Johnston, K. Liang, F. Caruso, *Progress in Polymer Science*, **2012**, 37, 985–1003.

¹⁴⁸ C. S. McKay, M.G. Finn, *Chemistry & Biology*, **2014**, 21, 1075–1101.

¹⁴⁹ M. A. Tasdelen, *Polym. Chem.* **2011**, 2, 2133–2145.

¹⁵⁰ S. Kotha, S. Banerjee, *RSC Adv.* **2013**, 3, 7642–7666.

¹⁵¹ F. L. Lin, H. M. Hoyt, H. v. Halbeek, R. G. Bergman, C. R. Bertozzi, *J. Am. Chem. Soc.*, **2005**, 127, 8, 2686–2695.

¹⁵² S. Ulrich, D. Boturyn, A. Marra, O. Renaudet, P. Dumy, *Chem. Eur. J.* **2014**, 20, 1, 34–41.

¹⁵³ T. Ganguly, B. B. Kasten, D. K. Bucar, L. R. MacGillivray, C. E. Berkman, P. D. Benny, *Chem. Commun.*, **2011**, 47, 12846–12848.

¹⁵⁴ C. E. Hoyle, T. Y. Lee, T. J. Roper, *Polym. Sci., Part A: Polym. Chem.* **2004**, 42, 21, 301–5338.

¹⁵⁵ J. W. Lee, U. Y. Lee, S. C. Han, J. H. Kim, *Bull. Korean Chem. Soc.* **2009**, 30, 5, 1001–1002.

¹⁵⁶ V. D. Bock, H. Hiemstra, J. H. Van Maarseveen, *Eur J Org Chem*, **2006**, 51–68

¹⁵⁷ M. Meldal, C. W. Tornøe, *Chem. Rev.* **2008**, 108, 2952–3015.

¹⁵⁸ V. V. Fokin, *CuAAC: The Quintessential Click Reaction. In Organic Chemistry-Breakthroughs and Perspectives*, 1st ed.; Ding, K., Dai, L.-X., Eds.; Wiley-VCH: Weinheim, Germany, **2012**, Chapter 7, pp 247–277

the preparation of a variety of materials and biomaterials^{159, 160} and particularly those catalysed by Cu.

This reaction implies the cycloaddition between an organic azide and a terminal alkyne in the presence of Cu (I) (CuAAC) to form a 1,4-disubstituted 1,2,3-triazole (Figure 3.1).

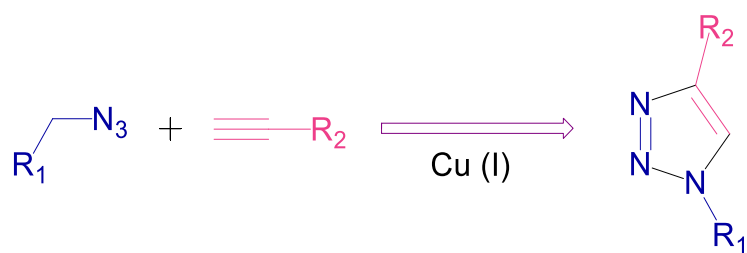


Figure 3.1. Cycloaddition between azide and alkyne group catalysed by Cu (I).

The use of Cu (I) in the cycloaddition makes the process more efficient, up to 10^7 times faster, than the conventional reaction without the catalyst. In addition, the reaction can be done at room temperature and is regioselective.^{156,161} The mechanism of the CuAAC reaction is complex and some aspects remain unclear, such as the formation of the copper acetylene intermediate. It consists of three basic steps: 1) the formation of copper acetylene complex, 2) azide displacement to yield the acetylene-

¹⁵⁹ J. Lahann, *Click chemistry for biotechnology and material science*. West Sussex, UK: John Wiley and Sons Pty Ltd.; **2009**.

¹⁶⁰ J. C. Jewett, C. R. Bertozzi, *Chem Soc Rev.* **2010**, 39, 4, 1272–1279.

¹⁶¹ R. Das, N. Majumdar, A. Lahiri, *IJRPC* **2014**, 4, 2, 467-472.

azide complex and 3) metallocycle ring contraction with subsequent dissociation of the product to regenerate the catalyst⁴ (Figure 3.2).

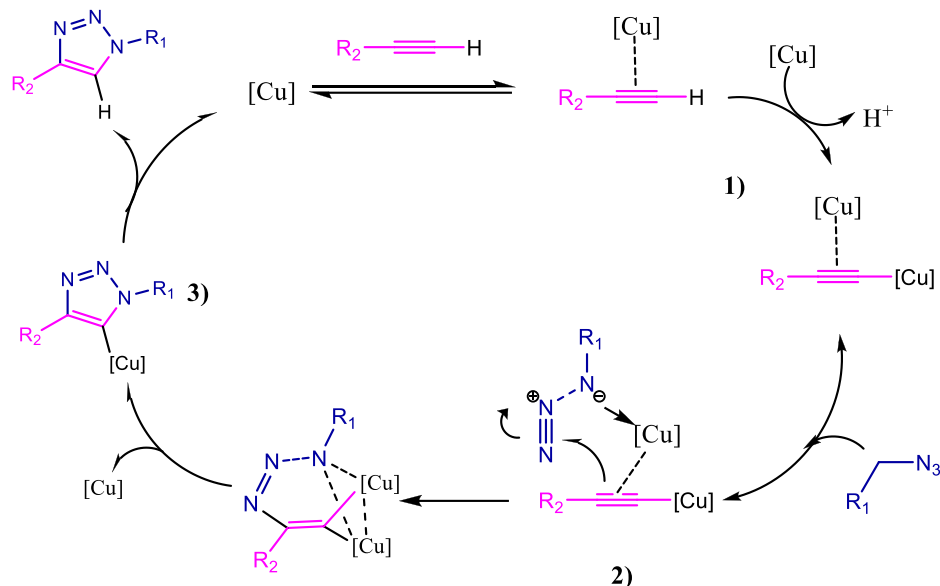


Figure 3.2. Scheme of the reaction mechanism of CuAAC reactions.

This reaction can be performed in different protic and aprotic solvents, including water, and is not affected by the presence of other inorganic and organic functional groups, making it ideal for different applications. Generally, a salt of Cu (I) is used, such as copper iodide, chloride or acetate. However, it is difficult to keep the Cu (I) active throughout the reaction since within the common oxidation states of copper (0, +1 and +2) the +1 is the least favoured thermodynamically. For this reason Cu (I) is easily oxidized to Cu (II) or disproportionate into Cu (II) and Cu

(0).^{162,163} Therefore, when Cu (I) is used directly, is often necessary to carry out the reaction under an inert atmosphere to prevent its oxidation

An alternative to the use of Cu (I) that eliminates the need for oxygen-free conditions, was developed by Hein and Fokin. This process involves a combination of salts of Cu (II) such as copper sulphate pentahydrate (II) acetate or copper (II), with a mild reductant such as sodium ascorbate. Besides the reduction of Cu (II) to Cu (I), the ascorbate also reduces any oxidized species present in the reaction, thus preventing the formation of any oxidative subproduct. Other reducing agents that have been used as well are hydroquinone and tris (carboxyethyl) phosphine.¹⁶⁴

The reaction can also be carried out using metallic copper, in this case it is catalyzed by the Cu (I) species liberated from the metallic structure overtime. In this approach a small piece of metallic copper, a copper wire for instance, is added to the reaction mixture, and stirred for 12 to 48 h.^{165,166,167} Although this procedure is efficient the reaction times are much longer.

To improve the speed of reaction different ligands have been used to prevent the degradation of the Cu (I) required in the reaction. The main role of the ligands employed are (i) promote the formation of copper acetylene; (ii) facilitate the coordination of the azide to intermediary

¹⁶² J. E. Hein, V. V. Fokin, *Chem Soc Rev.*, **2010**, 39, 1302–1315.

¹⁶³ C. J. Fahrni, *Curr. Opin. Chem. Biol.*, **2007**, 11, 121–127.

¹⁶⁴ Q. Wang, T. R. Chan, R. Hilgraf, V. V. Fokin, K. B. Sharpless, M. G. Finn, *J Am Chem Soc* **2003**;125:3192–3.

¹⁶⁵ V. V. Rostovtsev, L. G. Green, V. V. Fokin, K. B. Sharpless, *Angew. Chem., Int. Ed.*, **2002**, 41, 2596–2599.

¹⁶⁶ F. Himo, T. Lovell, R. Hilgraf, V. V. Rostovtsev, L. Noodleman, K. B. Sharpless, V. V. Fokin, *J. Am. Chem. Soc.*, **2005**, 127, 210–216.

¹⁶⁷ P. Appukkuttan, W. Dehaen, V. V. Fokin, E. Van der Eycken, *Org. Lett.*, **2004**, 6, 4223–4225.

copper acetylene; and (iii) increase the solubility of Cu (I) in the reaction mixture.

The ligands that accelerate the reaction more are not particularly “hard” or “soft”, such as those containing *N*-heterocyclic donors, such as pyridines,¹⁶⁸ or triazoles.^{169,170}

The development of ligands for the CuAAC reaction was particularly needed when biological molecules were involved, which structures could be damaged by the Cu and the solvent employed (aqueous) might speed-up the oxidation of Cu (I).

In this regard, tris(benzyltriazolyl) methyl amine TBTA has been proven to accelerate the reaction significantly and prevent the oxidation of Cu (I) in water-containing mixtures (Figure 3.3A).¹⁶⁹ Its potential application in the conjugation of biomolecules through the CuAAC reaction was illustrated by the conjugation of sixty fluorescent molecules in azide-labeled cowpea mosaic virus.¹⁷¹ However, its poor solubility in water has motivated the development of more polar analogues, such as THPTA (Figure 3.3B)¹⁷⁰ or bathophenanthroline disulfonate (Figure 3.3C).¹⁶⁸ Unfortunately, the intermediate complexes generated with this ligands are electron rich and therefore are highly susceptible to oxidation in air. Therefore, the reaction needs to be conducted under inert atmosphere, which can be inconvenient in particular settings.

¹⁶⁸ W. G. Lewis, F. G. Magallon, V. V. Fokin and M. G. Finn, *J. Am. Chem. Soc.*, **2004**, 126, 9152–9153.

¹⁶⁹ T. R. Chan, R. Hilgraf, K. B. Sharpless, V. V. Fokin, *Org. Lett.*, **2004**, 6, 2853–2855.

¹⁷⁰ V. Hong, A. K. Udit, R. A. Evans, M. G. Finn, *ChemBioChem*, **2008**, 9, 1481–1486.

¹⁷¹ Q. Wang, T. R. Chan, R. Hilgraf, V. V. Fokin, K. B. Sharpless, M. G. Finn, *J. Am. Chem. Soc.*, **2003**, 125, 3192–3193.

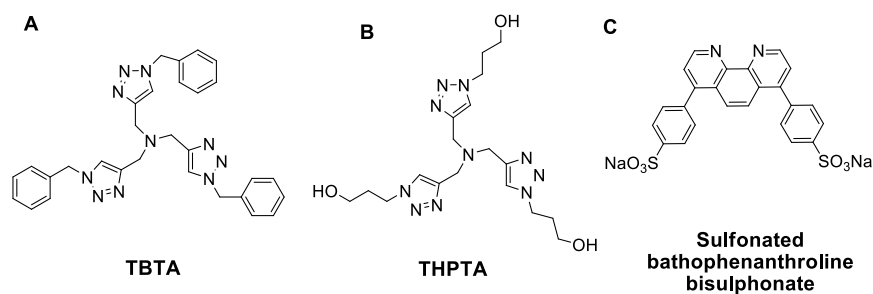


Figure 3.3. Ligands commonly used as catalyst in click reactions.

For this reason TBTA is still the preferred ligand in the orthogonal ligation of a variety of biomolecules, including oligonucleotides for preparation of hybrid nanostructures based on DNA.^{172, 173}

Another interesting approach for the ligation of biomolecules, particularly in *in vivo* settings, is the copper-free click reaction. This strategy was promoted by Carolyn Bertozzy and exploits the ring strain of cyclooctynes to promote the cycloaddition without the need of the copper catalyst. However, the preparation of these derivatives can be complicated and the use of compatible ligands for *in vivo* experiments might be a preferable choice in some cases.

¹⁷² C. Uttamapinant, A. Tangpeerachaikul, S. Grecian, S. Clarke, U. Singh, P. Slade, K. R. Gee, A. Y. Ting, *Angew. Chem. Int. Ed.*, **2012**, 51, 5852–5856.

¹⁷³ J. K. Lee, Y. H. Jung, J.B.-H. Tok, Z. Bao, *ACS Nano.*, **2011**, 5, 3, 2067–2074.

Objectives

As discussed above the use of ligands to catalyze CuAAC reactions is key to achieve good efficiencies. In this regard, in our research group we have observed that the efficiency of the conjugations when oligonucleotides were involved was sequence-dependent (Chapter 1 page 49). For this reason, we decided to study this process in more detail, and develop a new catalyst based on gold nanoparticles modified with oligonucleotides to run the CuAAC reaction in water. With the new system we expected to improve the efficiency of the process and also protect the DNA from degradation. Therefore, the specific objectives of this part are:

1. Prepare gold nanoparticles modified with oligonucleotides.
2. Evaluate the nanostructure as new ligand.
3. Apply this system for the preparation of new 2D DNA hybrids nanostructures.
4. Study of the Morphology of new materials by Atomic Force Microscopy (AFM).

Result and discussions

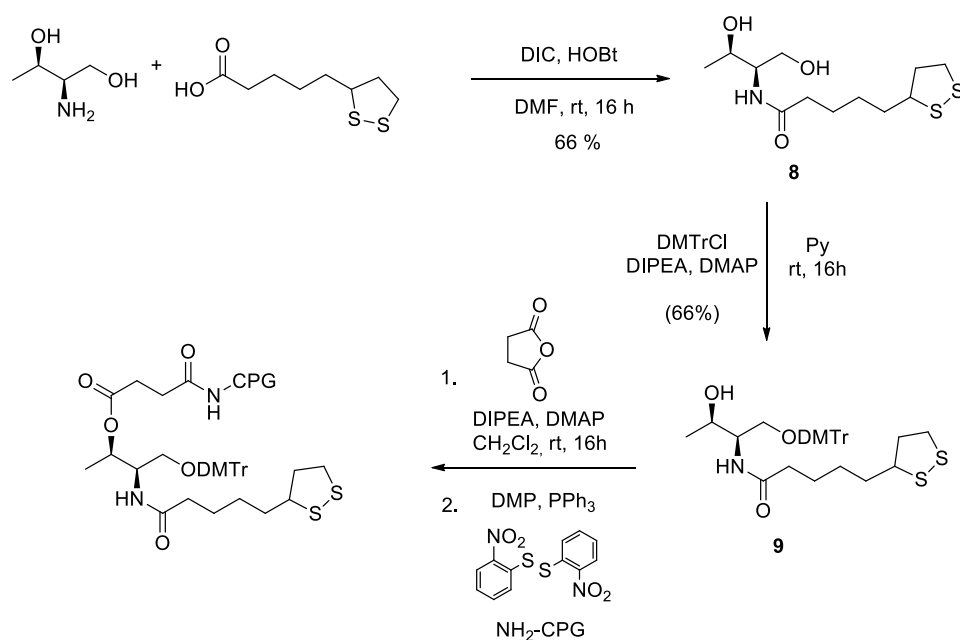
Based on the previous results obtained for the formation of dimers and trimers by click reaction, where the efficiency of the CuAAC reaction was clearly improved, we decided to prepare a system with higher number of strands. In this sense, we selected gold nanoparticles, which can be easily functionalized with 100-200 oligonucleotides.¹⁷⁴ The conjugation of oligonucleotides to gold nanoparticles is very easy, it requires the presence of a sulfur derivative, such as thiol, at one end of the oligonucleotide. The incubation of the oligonucleotides with gold nanoparticles provides the corresponding modified nanostructures, due to the high affinity of sulfur to gold. However, to increase the number of strands decorating the nanoparticle it is required the addition of salt to neutralize the phosphate charges of the oligonucleotides to improve their packing. The nanostructures obtained are known as *Spherical Nucleic Acid Nanoparticle Conjugates* and present excellent properties for biological applications, such as good stability, low toxicity and excellent internalization capabilities.¹⁷⁵ In our case we introduced a dithiolane moiety at the 3'-end to ease the conjugation to the nanoparticle. Using this derivative the deprotection step required in other sulfur modifications is not necessary. In addition, the conjugation is faster and yields very stable nanoparticles. In order to introduce this group we have prepared a modified solid support as described below.

¹⁷⁴ J. I Cutler, E. Auyeung, C. A. Mirkin, *J. Am. Chem. Soc.* **2012**, *134*, 1376.

¹⁷⁵ A. Latorre, C. Posch, Y. Garcimartín, S. Ortiz-Urda, Álvaro Somoza, *Chem. Commun.*, **2014**, 50, 3018—3020.

Synthesis of modified solid support

The synthesis of the modified solid support¹⁷⁵ was carried out as described in Scheme 3.1. It involves the reaction between (*R*)-(+)-1,2-dithiolane-3-pentanoic acid and L-threoninol to yield the corresponding amide derivative **8**. Then, the secondary hydroxyl group was protected as dimethoxytrytyl group **9** and the primary hydroxyl group was treated with succinic anhydride to introduce a carboxylic acid moiety. This group was used to attach the diol molecule to the Controlled Pore Glass (CPG).



Scheme 3.1. Summary of solid support preparation.

This modified CPG¹⁷⁵ was employed in the preparation of an oligonucleotide with twelve cytosines, since this sequence showed good activity in our previous click experiments. In addition, cytosines bind better than the other nucleobases to different metallic salts, such as silver, lead or copper, and for this reason this sequence could be a good ligand for this reaction.¹⁴⁵

The conjugation of AuNP with this modified oligonucleotide is straightforward; it just requires their incubation during a few hours in the presence of NaCl to neutralize the negative charges of the phosphate groups and improve the loading of the nanoparticle.¹⁷⁴

Comparison of different ligands.

Once the new system was obtained, its activity was evaluated and compared to the commercial ligand TBTA, usually employed in this transformation. In addition, a dimer previously obtained was also included in the comparative study. (Figure 3.4).

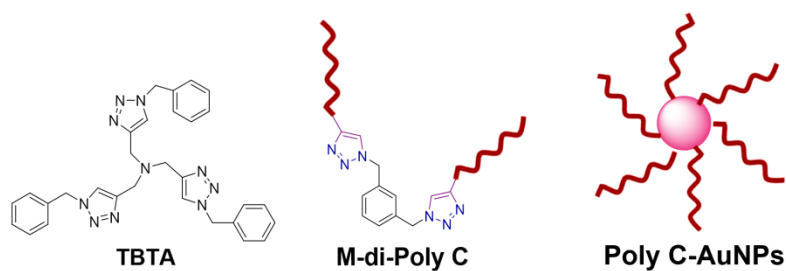


Figure 3.4 Ligands employed.

As a model reaction to evaluate the activity of the ligands we have employed the previous cross-coupling reaction between a tri-azide derivative and an oligonucleotide bearing an alkyne group (Figure 3.5).

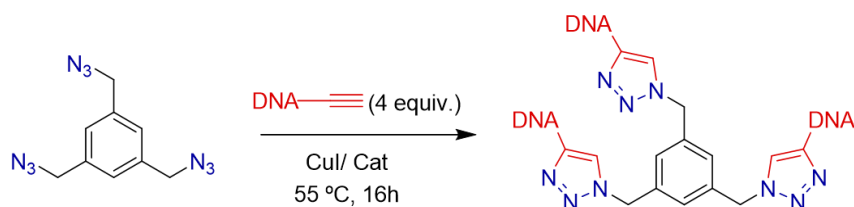


Figure 3.5. Click reaction between modified DNA and benzene derivatives using different ligands as catalyst

After 16 h at 55 °C the reaction mixtures were loaded into an analytical gel (Figure 3.6). In the case of TBTA a larger amount of starting material (ssDNA) and the intermediate dimeric structure was observed compared with the other two cases. The best result was obtained with the gold based catalysis, where a slightly higher presence of the final product was observed.

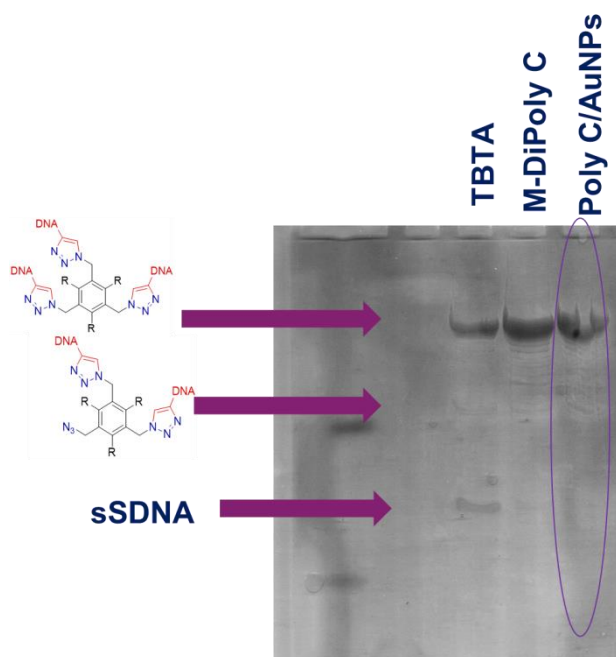


Figure 3.6. Analytical acrylamide gel electrophoresis.

Optimization of Reaction used Gold NPs Ligand

After the good results obtained with the AuNPs-based catalyst we decided to evaluate its activity at different conditions, particularly, using less amount of catalyst and copper and lower temperatures. First, we carried out the reaction using a lower amount of the AuNPs. In this case we did not observed any significant change in its efficiency when the reaction was carried out at 0.3 nM (Figure 3.7 left). Then, keeping the concentration of the AuNP at 0.3 nM, the amount of CuI was reduced. In our procedure CuI is added from a suspension containing 10 mg of CuI in 1mL of water.

In these experiments we reduced the volume from 6 mL to 2.5 mL and the activity was retained (Figure 3.7 right).

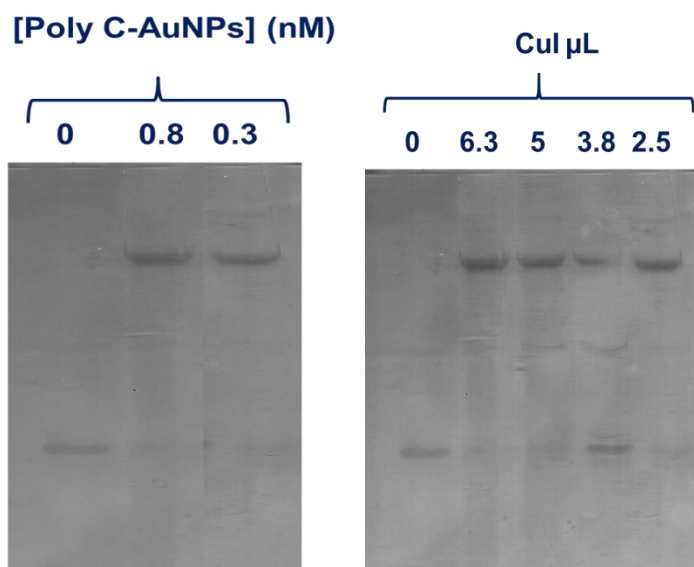


Figure 3.7. Gels of samples treated with the different amounts of AuNPs (left) and CuI (right).

After that, the temperature required to achieve good efficiency was also assessed. The standard temperature employed in this reaction (55 °C) was compared with the optimum temperature employed in cell culture experiments (37 °C) and also to room temperature. Interestingly the system was very efficient at room temperature, and what is more, it yielded less degradation compared with the reaction at 55 °C (figure 3.8).

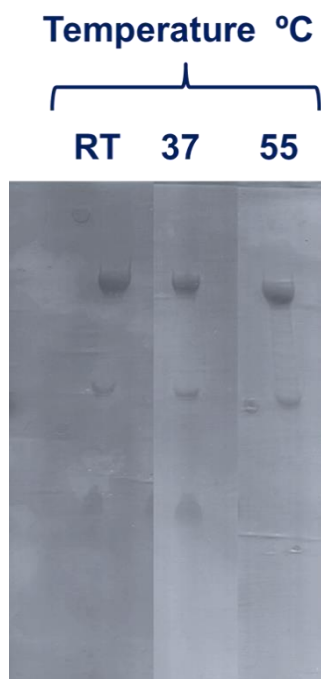


Figure 3.8. Gel of samples prepared at different temperatures.

Then, the system was employed in the preparation of a trimer in a preparative scale to isolate it for further experiments. The following sequence bearing an alkyne group at the 3'-end was employed (CCCTTAATCCCC). Interestingly, when the same reaction was carried out with TBTA only starting material was observed. The trimer obtained was purified by preparative gel electrophoresis (Figure 3.9 left). Remarkably, even at this scale the system was very efficient and moreover degradation products were not observed. In addition, the catalyst was easily recovered from the reaction mixture through centrifugation and used in other reaction. However, in this case some starting material was observed (Figure 3.9 right).

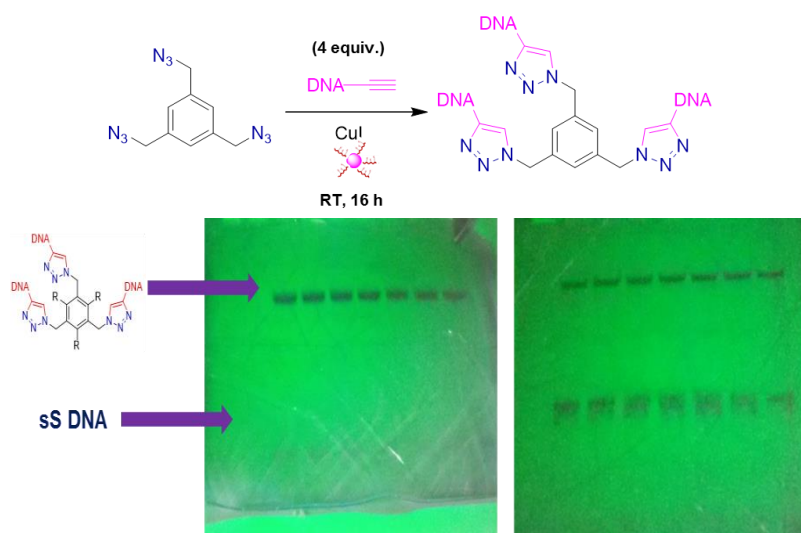


Figure 3.9. Polyacrylamide gel used in the purification of the trimer obtained after the click reaction at room temperature: (right) using Poly C-AuNPs and (left) using recovered nanoparticles from the previous reaction.

Since the methodology employed here to evaluate the activity of the ligands is time-consuming we decided to use a different model with a faster read-out. Thus, we used a coumarine derivative bearing an azide group as substrate for the click reaction. Interestingly, this derivative becomes highly fluorescent once the cycloaddition has taken place, allowing an easy monitorization of the reaction by fluorescence.

In this case, we evaluated the cycloaddition reaction between 3-azido-7-hydroxycoumarine and 5-hexyn-1-ol (Figure 3.10).

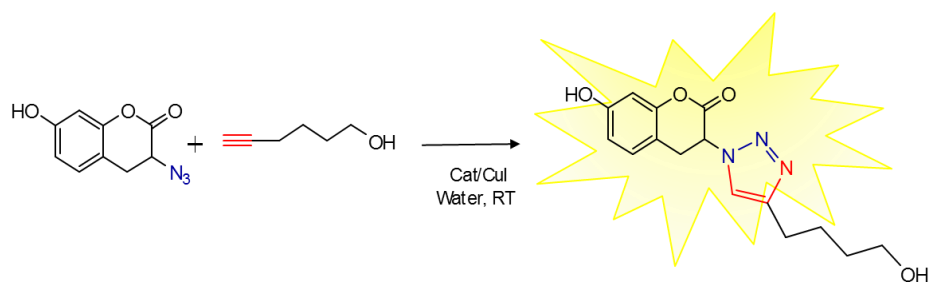


Figure 3.10. Click reaction with Fluoreogenic reagent.

The reaction was carried out at room temperature using 2.5 μL of our stock CuI mixture (10 mg / mL) and the different ligands previously evaluated. The course of the reactions was followed by their fluorescence intensity. After two hours the catalytic activity of DNA-AuNPs was clearly better than the other ligands, which did not provide a significant increase in the fluorescent intensity (Figure 3.11).

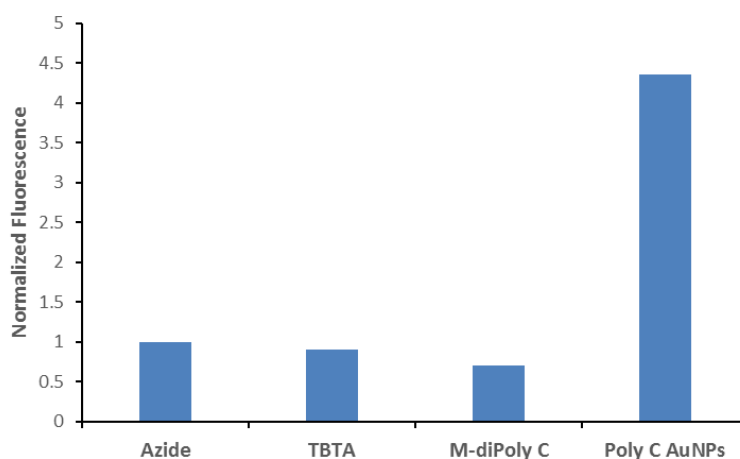


Figure 3.11. Comparison of the catalytic effect of different ligands employed.

Due to the great efficiency of the system developed we decided to apply it to the preparation of new materials based on hybrid structures containing oligonucleotides and small organic molecules. Particularly, we are exploring two different approaches. The first one is based on the assembly of complementary oligonucleotides and the second strategy is based on the formation of covalent bonds. Through this strategy we hope to obtain structures related to those found in covalent organic frameworks (COFs) and therefore we have named these new structures **BioCOFs**, since they could be considered COF made of biomolecules.

2D Hybrid Nanostructures by Self-Assembly of complementary sequences

This approach is based on the assembly of units with complementary oligonucleotides. In this case the forces that control their assembly are mainly hydrogen bonds between complementary nucleobases (Watson-Crick). Each unit is composed of a benzene ring bearing oligonucleotides at alternating positions (1, 3 and 5). As described before the preparation of these derivatives implies a cycloaddition reaction between the alkyne groups present in the oligonucleotides and the azides present in the benzene moiety (Figure 3.12). Using this strategy we prepared two trimers with complementary sequences (A and B) and different lengths one with 12 oligonucleotides (**Short**) and the other with 30 oligonucleotides (**Long**).

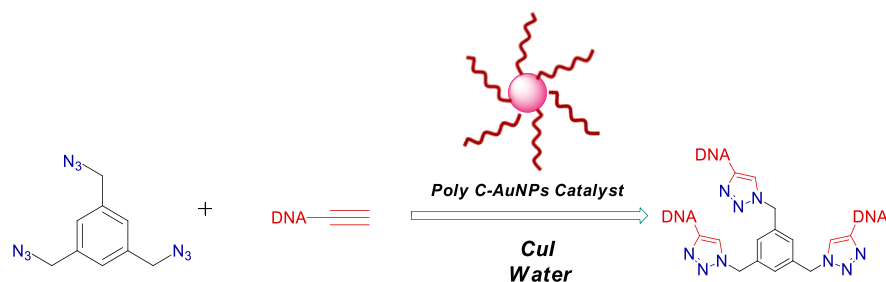


Figure 3.12. Click reaction between modified oligonucleotides and a benzene derivative bearing three azides for the preparation of trimers.

Once the complementary units were prepared and purified their assembly was carried out at different concentrations (0.1, 0.05 and 0.01 μM) in MgCl_2 (10 mM). The mixtures were heated up to 95 $^{\circ}\text{C}$, and cooled down slowly for sixty hours to ensure the self-assembly of the complementary strands (Figure 3.13).

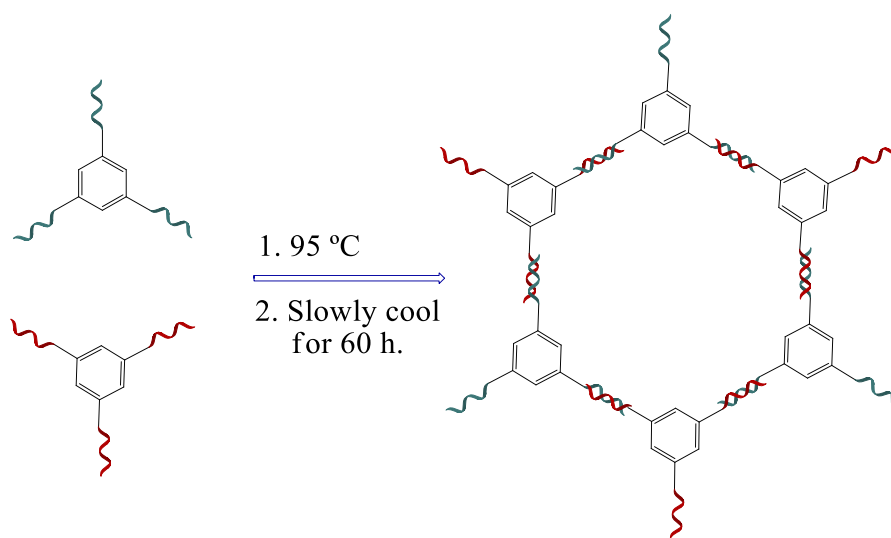


Figure 3.13. Assembly reactions of complementary trimers.

The products obtained at different concentrations were morphological characterized used Atomic Force Microscopy (AFM) operating at room temperature in ambient air conditions and in solution.

The images obtained at ambient air (figure 3.14) show the formation of small disks with around 2 nm height. However, the diameter of the disks depended on the length of the sequence employed. Particularly, larger structures were obtained using complementary units with short oligonucleotides. We also observed that the diameter depended as well on the concentration employed in the assembly of the complementary units. In this regard, larger structures were obtained at low concentrations. Particularly, the diameters obtained for the short sequence at 0.1, 0.05 and 0.01 μM were 75.7, 135.8 and 172.8 nm respectively and in the case of the long sequence the diameters obtained were 43.7, 65.2 and 97.2 nm.

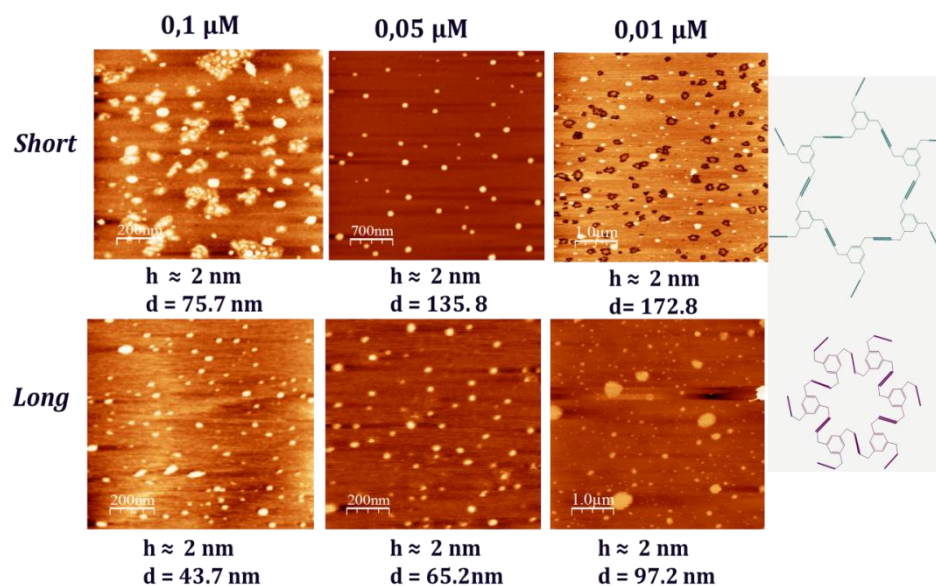


Figure 3.14. AFM images in air of nanostructures obtained by assembly of complementary units at different concentrations.

The different sizes observed between the short and large oligonucleotides could be due to the different flexibility of the duplex generated in both systems. When short oligonucleotides are employed the structures obtained should be more rigid than those prepared with larger oligonucleotides. Under the conditions employed in these experiments, the DNA structures could collapse and due to the higher flexibility of long oligonucleotides they should afford better packed structures (smaller).

When the samples were analysed in solution similar structures were observed (Figure 3.15). But in this case, the dependence of the length of the diameter of the structures with concentration is different. In the case of

the short sequence the diameter decreases at lower concentration. This may be associated to higher molecular dispersion since there is less interaction between the DNA strands. In the case of the long sequence the diameter does not change significantly, however, at high concentration the height of the structures generated increases from 3 to 10 nm, which should be due to the unspecific interaction between DNA strands.

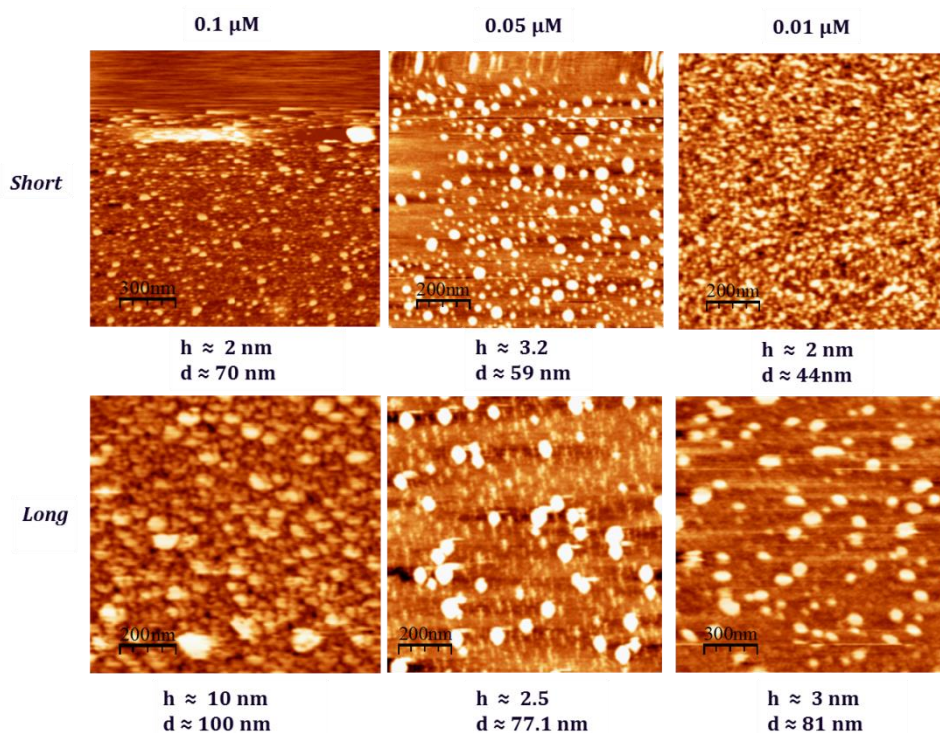


Figure 3.15. AFM images in liquid of nanostructures obtained by assembly of complementary units at different concentrations.

In these experiments we did not observed the formation large structures as reported by other approaches. In addition, we did not observed any

specific pattern within of the nanostructures generated, probably due to settings of the AFM employed.

2D Hybrid Nanostructures by covalent bonds

In this case the oligonucleotide employed have been synthesized bearing alkyne groups at both ends. Thus, the cycloaddition (Click reaction) with the functional groups presented in the organic benzene core could yield a 2D structure since the reaction can go on if the required reagents are in the mixture (Figure 3.16).

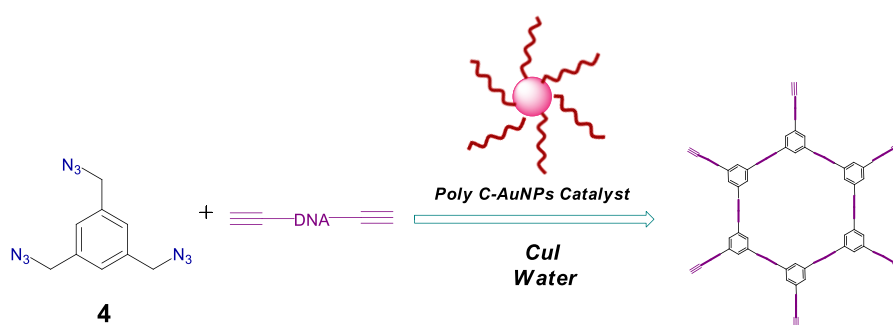


Figure 3.16. Preparation of 2D Hybrid nanostructures by covalent bonds by Click reaction.

In this case, the 2D structure was obtained by a click reaction catalyzed by CuI, using our nanoparticle-based ligand as before. In the process the benzene derivative **4** and an oligonucleotide with 20 thymidines modified at both ends with alkyne groups (PolyT-20-Bis-alk) were incubated with CuI and the modified nanoparticles at room temperature for 16 h.

The solution was deposited on mica in the presence MgCl₂ and studied by AFM in air. The presence of different of laminar structures of about 1 nm

height was observed in the same sample (Figure 3.17). One type was very large, with diameters about 800 nm (Figure 3.17 B). Other structures were smaller, with diameters around 100 nm (Figure 3.17 C). It was also observed the formation of porous structures (Figure 3.17 D and E) with pore sizes around 50 nm (Figure 3.17 F).

$$h \approx 1 \text{ nm}$$

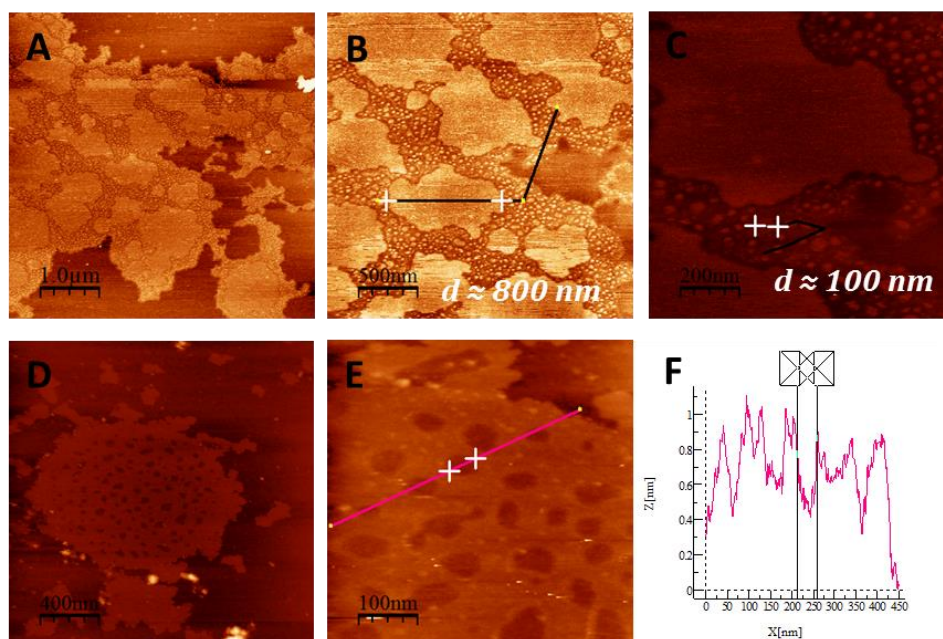


Figure 3.17. AFM images obtained after click reaction.

Here again we did not observed the formation of honeycomb structures, however very large structures were formed compared with the previous approach. It is possible that due to the speed and irreversibility of the reaction employed (click), multiple defects are introduced in the network, preventing the formation of the desired defined structures and leading to a

heterogeneous mixture of structures (large, small and porous). With this idea in mind we are evaluating other reactions where the products are in equilibrium with the starting materials, and therefore, the most stable structures will be mainly generated.

Conclusions

- Oligonucleotides, and particularly a PolyC sequence, are a good catalyst for click reactions.
- The use of AuNPs nanoparticles functionalized with PolyC significantly improves the reaction.
- The PolyC-AuNPs can catalyze the click reaction even at room temperature and protects the DNA from degradation.
- Using this novel catalyst has been possible to obtain 2D hybrid nanostructures based on small organic molecules and oligonucleotides.
- We have evaluated two strategies for the preparation of two-dimensional hybrid nanostructures based on modified oligonucleotides.
- Through self-assembly of complementary sequences circular nanostructures were obtained, where their diameter could be modulated by the sequence employed and the conditions of assembly.
- The preparation of BioCOFs by click reaction yielded different laminar structures.

Experimental Procedures.

Experimental procedures

1. General methods.

^1H and ^{13}C NMR spectra of organic molecules were recorded in CDCl_3 at 300 and 75 MHz, respectively. ^1H NMR (1D and 2D) of oligonucleotides were recorded in $\text{H}_2\text{O}/\text{D}_2\text{O}$ 9/1 at 600 MHz. All reactions of organic molecules were monitored by thin layer chromatography using precoated sheets of silica gel 60. Flash column chromatography was done using silica gel 60 (230-400 mesh, Merck). Eluting solvents are indicated in the text. All other reagent were purchased from Aldrich, Fluorochem or ABCR and used without further purification. Ultrapure reagent grade water (18.2 M Ω , Wasserlab), was used in all experiments.

The UV/VIS spectra were recorded in a Varian Cary 50 spectrophotometer using 1 cm path length quartz cells at room temperature. The fluorescence spectra were recorded in a Synergy H4 microplate reader, using 96-well plates at room temperature. CD spectra were determined using a Jasco J-815 CD spectrometer and 1 mm path length quartz cells at room temperature. The scanning speed was adjusted to 200 nm/min, and three accumulations were acquired.

The AFM images were acquired in dynamic mode using a Nanotec Electronic system. Olympus cantilevers were used with a nominal force constant of 0.75 N m $^{-1}$ and a resonance frequency of 70 kHz. The images were processed using WSxM¹⁷⁶ (freely downloadable scanning probe

¹⁷⁶ I. Horcas, R. Fernández, JM Gómez Rodríguez, J. Colchero, J. Gómez Herrero, A. M. Baro, Rev. Sci. Instrum. 2007, 78, 013705

microscopy software from www.nanotec.es) operating at room temperature in ambient air and in solution conditions.

Preparation of AFM samples

Measurements in air

Aqueous solutions of DNA samples (20 μL) containing MgCl_2 (20 mM), were deposited by drop-casting on a mica surface. The surface was allowed to air dry at room temperature for 5 min and washed three times with ultrapure H_2O (200 μL) to remove unbound material from the surface and dried under argon. The muscovite mica surface was prepared just before deposition and was cleaved with adhesive tape.

Measurements in buffer

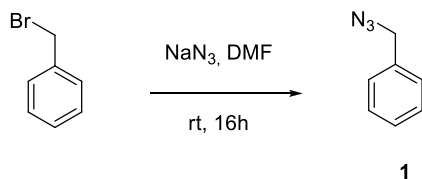
The muscovite mica surface was previously treated with (3-aminopropyl)triethoxysilane (APTES). The substrates were submerged in a solution of APTES (0.1%) in ultrapure H_2O during 15 minutes, then washed three times with 2-propanol (200 μL) and ultrapure water (200 μL) and finally dried under argon. The samples (20 μL), were deposited just before performing the measurement and a solution of MgCl_2 (30 μL , 10 mM) to cover the cantilever in the liquid cell.

2. Synthesis of azides:

General procedure for synthesis of azides. Procedure A

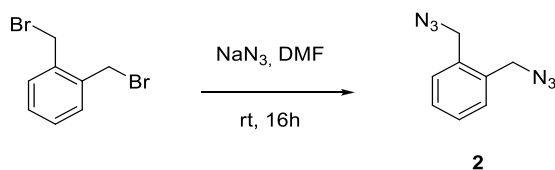
To a solution of corresponding bromo aryl derivative (0.34 mmol) in DMF (2 mL), NaN₃ was added at room temperature and stirred for 16h. The mixture was diluted with brine, and extracted with CH₂Cl₂ to obtain the corresponding azide as colorless oil. Those compounds were used without further purifications.

Benzyl azide¹⁷⁷ (1)



Compound **1** was obtained from benzyl bromide following the general procedure A, using 23.4 mg of NaN₃ (1.1 Eq) ; ¹H NMR (300 MHz, CDCl₃) δ 7.47-7.37 (m, 5H), 4.40 (s, 2H).

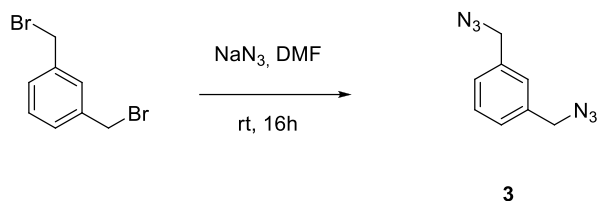
1,2-bis(azidomethyl) benzene¹⁷⁸ (2)



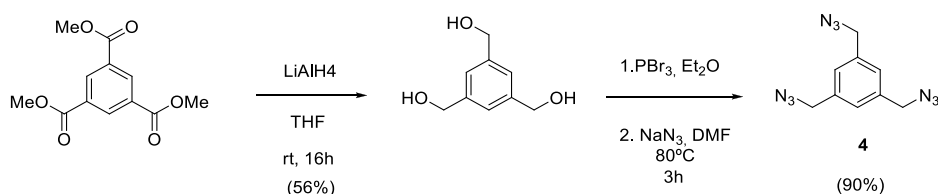
Compound **2** was obtained from 1,2-bis(bromomethyl)benzene following the general procedure A, using 48.6 mg of NaN₃ (2.2 Eq); ¹H NMR (300 MHz, CDCl₃) δ 7.35 (s, 4H), 4.36 (s, 4H).

¹⁷⁷ K.-C. Tiew, D. Dou, T. Teramoto, H. Lai, K. R. Alliston, G. H. Lushington, R. Padmanabhan, W. C. Groutas, *Bioorg. Med. Chem.* **2012**, *20*, 1213–1221.

¹⁷⁸ N. Gigant, E. Claveau, P. Bouyssou, I. Gillaizeau, *Org. Lett.*, 2012, *14*, 844-847.

1,3-bis(azidomethyl) benzene¹⁷⁹ (3)

Compound **3** was obtained from 1,3-bis(bromomethyl)benzene following the general procedure A, using 48.6 mg of NaN₃ (2.2 Eq); ¹H NMR (300 MHz, CDCl₃) δ 7.44-7.39 (m, 1H), 7.31-7.26 (m, 3H), 4.37 (s, 4H).

1,3,5-tris(azidomethyl) benzene¹⁸⁰ (4)

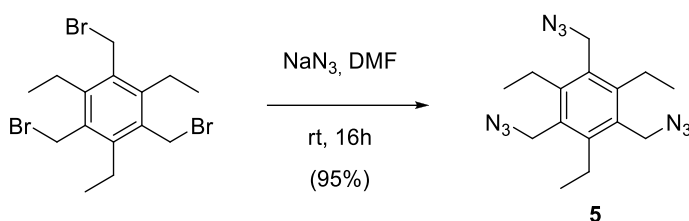
To a suspension of LiAlH₄ (247 mg, 6.5 mmol) in THF (5 mL) under N₂, was added slowly a solution of trimethyl benzene-1,3,5-tricarboxylate (500 mg, 1.97 mmol) in THF (5mL) and stirred for 16 h at rt. The reaction mixture was hydrolyzed with MeOH at 0 °C and then with a saturated solution of sodium tartrate during 2 h. The mixture was washed with AcOEt and the aqueous phase acidified with HCl until neutral pH. Then, it was extracted with AcOEt and after solvent evaporation the 1,3,5-tribenzyl alcohol was obtained and used without further purification as a colorless oil with 56% yield.

¹⁷⁹ J. R. Thomas, X. Liu, P. J. Hergenrother *J. Am. Chem. Soc.* **2005**, 127, 12434-12435.

¹⁸⁰ J. E. Moses, D. J. Ritson, F. Zhang, C. M. Lombardo, S. Haider, N. Oldhama, S. Neidle, *Org. Biomol. Chem.* **2010**, 8, 2926-2930.

To a suspension of 1,3,5-tribenzyl alcohol (205 mg, 1.22 mmol) in (Et₂O 10 mL), PBr₃ (285 μ L, 3 mmol) was added and stirred for 16h. The mixture was hydrolyzed with a saturated solution of NaHCO₃ and extracted with AcOEt. After solvent evaporation, the white solid obtained was dissolved in DMF (5 mL) and NaN₃ (253 mg, 3.9 mmol) added and heated at 80 °C during 3 h. The mixture was washed with water, brine and extracted with AcOEt. After flash chromatography (eluent Hexane/AcOEt 8:1) 1,3,5-tris(azidomethyl) benzene **4** was obtained as a colorless oil in 90% yield; ¹H NMR (300 MHz, CDCl₃) δ 7.26 (s, 3H), 4.40 (s, 6H).

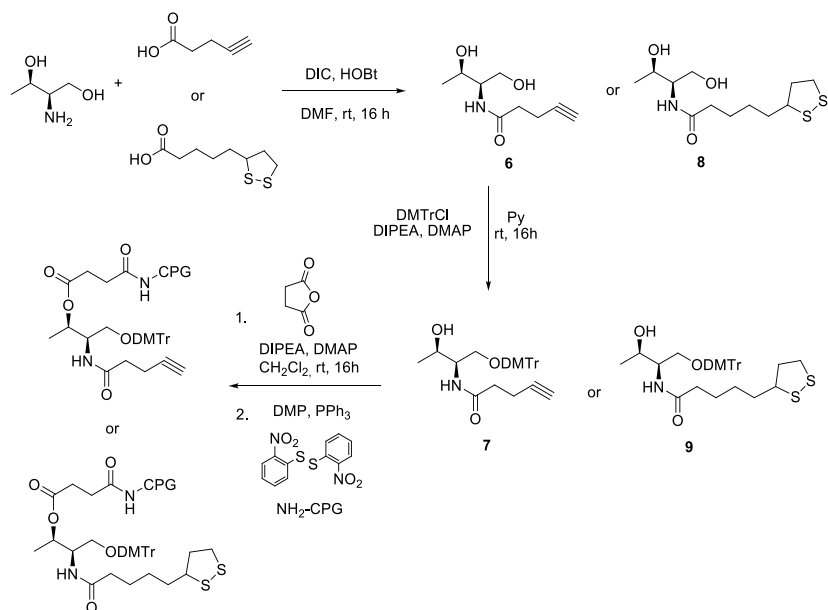
1,3,5-tris(azidomethyl)-2,4,6-triethylbenzene¹⁸¹ (5)



Compound **5** was obtained from 1,3,5-tris(bromomethyl)-2,4,6-triethylbenzene following the general procedure A, using 72.9 mg of NaN₃ (3.3 Eq); ¹H NMR (300 MHz, CDCl₃) δ 4.49 (s, 6H), 2.85 (q, J = 7.6 Hz, 6H), 1.24 (t, J = 7.6 Hz, 9H).

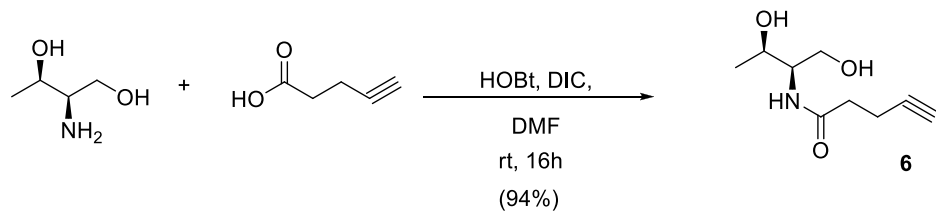
¹⁸¹ J. N. Moorthy, S. Saha, *Eur. J. Org. Chem.* **2010**, 6359–6365.

3. Synthesis of modified solid support:



Scheme 1. Summary of CPG preparation.

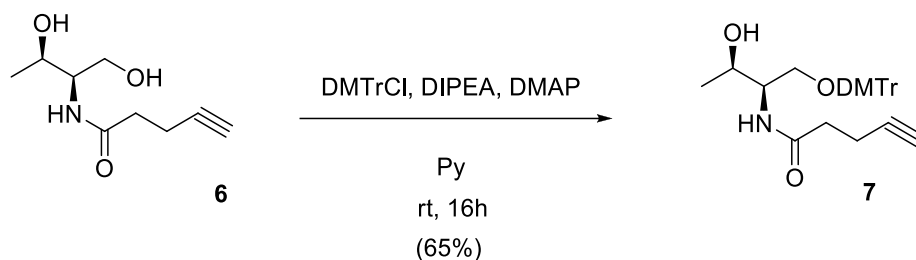
***N*-((2*R*,3*R*)-1,3-dihydroxybutan-2-yl)pent-4-ynamide (6).**



To a stirred mixture of 4-pentynoic acid (294 mg, 3.6 mmol), *N*-hydroxybenzotriazole (444 mg, 3.1 mmol) and *N,N'*-

diisopropylcarbodiimide (510 μ L, 3.1 mmol) in DMF (7.2 mL) under N_2 , L-threoninol (315 mg, 3 mmol) was added at room temperature. After 16 h the reaction mixture was quenched with MeOH and the solvent evaporated in vacuum. After solvent evaporation and flash chromatography (eluent CH_2Cl_2 /Hexane/MeOH 10:1:1) compound **6** was obtained as a colorless oil, in 94% yield; 1H NMR (300 MHz, $CDCl_3$) δ 6.47 (s, 1H), 4.18 (d, J = 5.9 Hz, 1H), 3.82 (bs, 3H), 2.66 – 2.35 (m, 5H), 1.21 (d, J = 6.1 Hz, 3H); ^{13}C NMR (75 MHz, $CDCl_3$) δ 172.4, 82.8, 69.6, 67.7, 63.9, 55.1, 35.4, 20.2, 15.0; MS (ESI): m/z (%) 136 (27), 168 (M^+ -OH, 39), 186 (M^+ +H, 25), 208 (M^+ +Na, 100); HRMS (ESI) calcd for $C_9H_{15}NO_3$ (M^+ +H) 186.1124, found 186.1141.

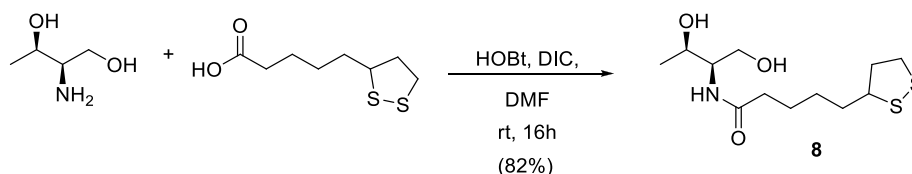
***N*-((2*R*,3*R*)-1-(bis(4-methoxyphenyl)(phenyl)methoxy)-3-hydroxybutan-2-yl)pent-4-ynamide (**7**).**



To a solution of compound **6** (525 mg, 2.83 mmol) in pyridine (14 mL) at 0 °C, DIPEA (730 μ L, 4.2 mmol), 4,4'-dimethoxytritylchloride (1.15 g, 3.4 mmol) and DMAP (catalytic amount) were added. The mixture was stirred and allowed to reach room temperature slowly. After 16 h, the solvent was evaporated and the residue purified by flash chromatography (

Hex/AcOEt 1:5), using silica gel deactivated with Et₃N. Compound 7 was obtained in 65% yield as a yellow solid; ¹H NMR (300 MHz, CDCl₃) δ 7.42 (d, *J* = 7.2 Hz, 2H), 7.32 (d, *J* = 8.8 Hz, 4H), 7.38 – 7.22 (m, 3H), 6.88 (d, *J* = 8.8 Hz, 4H), 6.31 (d, *J* = 8.6 Hz, 1H), 4.22 – 4.09 (m, 1H), 3.99 (dd, *J* = 8.3, 2.4 Hz, 1H), 3.83 (s, 6H), 3.41 (ddd, *J* = 13.0, 9.6, 3.8 Hz, 2H), 2.63 – 2.44 (m, 4H), 2.02 (t, *J* = 2.4 Hz, 1H), 1.18 (d, *J* = 6.3 Hz, 3H); ¹³C NMR (75 MHz, CDCl₃) δ 171.3, 158.6, 144.3, 135.5, 135.3, 129.9, 129.9, 128.0, 127.9, 127.0, 113.3, 86.8, 82.9, 69.5, 68.6, 65.3, 55.2, 53.4, 35.5, 19.8, 15.0; MS (ESI): *m/z* (%) 303 (100), 510 (M⁺+Na, 23); HRMS (ESI) calcd for C₃₀H₃₃NO₅ (M⁺+Na) 510.2250, found 510.2249.

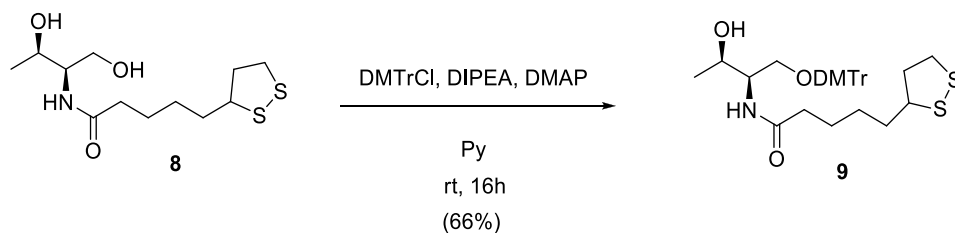
5-[(3*S*)-1,2-dithiolan-3-yl]-N-[(1*R*,2*S*)-2-hydroxy-1-(hydroxymethyl)propyl]pentanamide (8)



To a solution of (*R*)-(+)-1,2-dithiolane-3-pentanoic acid (3.301 mmol, 680 mg, 1.2 eq.) in DMF (0.5 M) at room temperature, *N*-hydroxybenzotriazole (3.027 mmol, 409 mg, 1.1 eq.) and diisopropylcarbodiimide (3.026 mmol, 468 μl, 1.1 eq.) were added. After stirring the mixture 10 min. L-threoninol (2.752 mmol, 289 mg, 1 eq.) was added. The resulting mixture was stirred overnight and then quenched by the addition of methanol. The solvent was evaporated under vacuum and the residue purified by flash chromatography 20:1 (CH₂Cl₂: MeOH)

to yield 660 mg as a pale yellow oil (82%). $^1\text{H-NMR}$ (300 MHz, CDCl_3): δ 6.26 (d, $J = 6.7$ Hz, 1H), 4.17 (d, $J = 6.2$ Hz, 1H), 3.95 – 3.71 (m, 3H), 3.58 (dt, $J = 13.1, 6.5$ Hz, 1H), 3.48 (s, 1H), 3.26 – 3.04 (m, 2H), 2.46 (td, $J = 12.4, 6.4$ Hz, 1H), 2.27 (t, $J = 7.4$ Hz, 2H), 1.91 (dq, $J = 13.7, 6.9$ Hz, 1H), 1.80 – 1.60 (m, 5H), 1.57 – 1.41 (m, 2H), 1.19 (d, $J = 6.4$ Hz, 3H). $^{13}\text{C-NMR}$ (75 MHz, CDCl_3): δ 174.1 (C), 68.7 (CH), 65.0 (CH₂), 56.4 (CH), 54.7 (CH), 40.3 (CH₂), 38.5 (CH₂), 36.5 (CH₂), 34.6 (CH₂), 28.8 (CH₂), 25.5 (CH₂), 20.6 (CH₃). HR-MS (ESI): m/z calculated for $\text{C}_{12}\text{H}_{24}\text{NO}_3\text{S}_2$ 294.1192 $[\text{M}+\text{H}]^+$, found 294.1186.

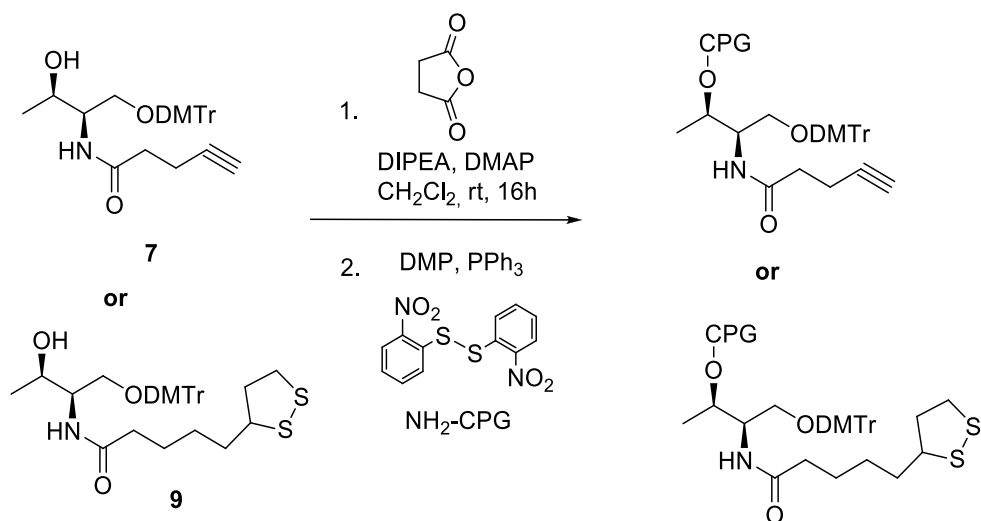
N-((1R,2S)-1-[[bis(4-methoxyphenyl)(phenyl)methoxy]methyl]-2-hydroxypropyl)-5-[(3S)-1,2-dithiolan-3-yl]pentanamide (9).



To a solution of the corresponding diol (0.682 mmol, 200 mg, 1 eq.) in pyridine (0.2 M) at 0°C, diisopropylethylamine (1.023 mmol, 179 μl , 1.5 eq), 4,4'-dimethoxytritylchloride (0.819 mmol, 277 mg, 1.2 eq) and dimethylaminopyridine (catalytic amount) were added. After 15 min. the mixture was allowed to reach room temperature. The mixture was stirred overnight and then quenched by the addition of methanol. The solvent was evaporated under vacuum and the residue purified by flash

chromatography 1:2 (hexane: EtOAc) to yield 270 mg as a white to light yellow foam (66%). $^1\text{H-NMR}$ (300 MHz, CDCl_3): δ 7.28 (m, 9H), 6.83 (d, $J = 8.8$ Hz, 4H), 6.03 (d, $J = 8.7$ Hz, 1H), 4.10 (m, 1H), 3.93 (dd, $J = 8.4, 2.5$ Hz, 1H), 3.79 (s, 6H), 3.62 – 3.48 (m, 1H), 3.41 (dd, $J = 9.6, 4.3$ Hz, 1H), 3.29 (dd, $J = 9.6, 3.5$ Hz, 1H), 3.23 – 3.05 (m, 3H), 2.44 (td, $J = 12.4, 6.4$ Hz, 1H), 2.23 (t, $J = 7.3$ Hz, 2H), 1.90 (td, $J = 13.7, 6.9$ Hz, 1H), 1.76 – 1.62 (m, 4H), 1.56 – 1.41 (m, 2H), 1.12 (d, $J = 6.4$ Hz, 3H). $^{13}\text{C-NMR}$ (75MHz, CDCl_3): δ 173.0 (C), 158.6 (2C) (C), 144.3 (C), 135.5 (C), 135.3 (C), 129.9 (2C) (CH), 129.8 (2C) (CH), 127.9 (2C) (CH), 127.8 (2C) (CH), 127.0 (CH), 113.3 (4C) (CH₃), 86.7, 68.6 (CH), 65.2 (CH₂), 60.3, 56.3 (CH), 55.2 (CH), 53.3 (CH), 40.2 (CH₂), 38.4 (CH₂), 36.5 (CH₂), 34.6 (CH₂), 28.9 (CH₂), 25.5 (CH₂), 19.9 (CH₃). HR-MS (ESI): m/z calculated for $\text{C}_{33}\text{H}_{41}\text{NNaO}_5\text{S}_2$ 618.2324 $[\text{M}+\text{Na}]^+$, found 618.2296.

Solid Support preparation.



To a solution of compound **7** or **9** (27 mg, 0.055 mmol) in CH_2Cl_2 (0.4 mL), succinic anhydride (7.2 mg, 0.072 mmol), DIPEA (14 μL , 0.077 mmol) and DMAP (catalytic amount) were added under N_2 at room temperature. The mixture was stirred during 16 h, washed with water and dried with MgSO_4 . After solvent evaporation, the residue obtained was dissolved in CH_3CN (1.2 mL) and DMAP was added. This solution was added to an eppendorf containing 2,2'-dithiobis(5-nitropyridine) (25 mg, 0.08 mmol) and vortexed. This solution was added to a second eppendorf containing PPh_3 (21 mg, 0.08 mmol) and vortexed until complete dissolution. This mixture was added to 200 mg of aminopropyl-CPG (500 Å) and stirred during 2h. The solvent was removed and the CPG washed with MeOH and CH_3CN . Once the CPG was dried, 2 mL of a 1:1 mixture of capping reagents CAP-A and CAP-B, commonly used in oligonucleotide synthesis was added [CAP MIX A: Acetic anhydride (400 μL)/ Py (600 μL)/ THF (500 μL); CAP MIX B: 1-Methylimidazol (400 μL)/ THF (1 mL)] . After 25 min, the modified CPG was washed with MeOH, CH_3CN , and dried.

The CPG loading was calculated using the trityl quantification method. Particularly, 10 mg of the modified CPG was treated with 5 mL of a detritylation solution (3 mL of perchloric acid and 2 mL of EtOH) during 30 min. Then, 100 μL of the mixture was diluted to 2.5 mL, and the absorbance was measured at 498 nm to quantify the trityl cation. Functionalization (F) was determined by Lambert-Beer law. The extinction coefficient (ϵ) at this wavelength is $70000 \text{ mol}^{-1} \text{ dm}^3 \text{ cm}^{-1}$. The

loading obtained was 73.6 $\mu\text{M}/\text{gr}$ in the case of alkyne modification and 183 $\mu\text{M}/\text{gr}$ in the case of diol modification.

4. Oligonucleotide Synthesis

Oligonucleotides were prepared using a MerMade4 DNA Synthesizer using standard phosphoramidites (Link Technologies) and the modified solid support described above. After solid-phase synthesis, the solid support was transferred to a screw-cap glass vial and incubated at 55 °C for 4 h with 2 mL of ammonia solution (33%). After the vial was cooled on ice the supernatant was transferred by pipet to microcentrifuge tubes and the solid support and the vial were rinsed with water. The combined solutions were evaporated to dryness using an evaporating centrifuge.

The samples were purified by polyacrylamide gel electrophoresis 20% and the oligonucleotides were eluted from gel fractions using an elutrap system. The solutions were desalted using a NAP-10 column and concentrated in an evaporating centrifuge and characterized by MALDI-TOF

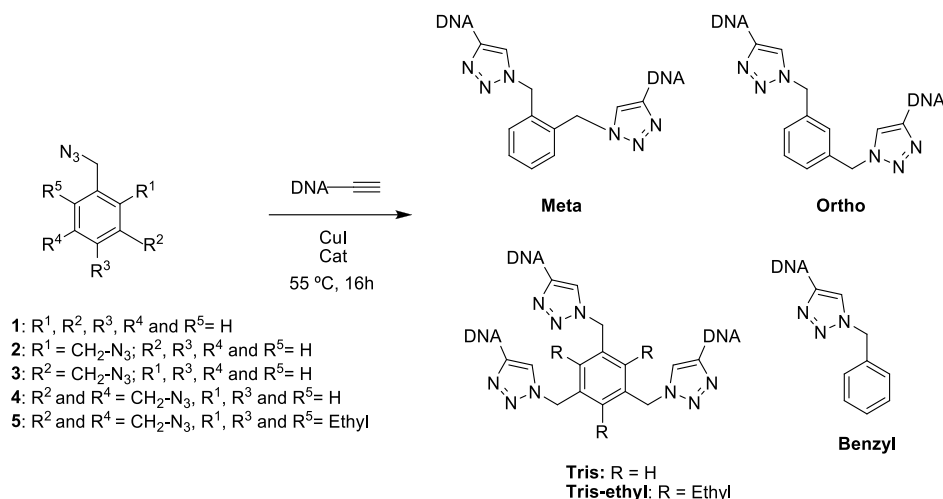
Table 1 Sequences employed.

Name	Sequence
Poly C	5`-(dC) ₁₂ -ALK-3`
Poly C 24	5`-(dC) ₂₄ -ALK-3`
Poly C 36	5`-(dC) ₃₆ -ALK-3`
Green	5`-CCCTCTTAACCC-3`
Yellow	5`-CCCTTAATCCCC-3`
Red	5`-CCTCCTTCCTCC-3`
NI-Red	5`-CCCTAACTCCCC-3`
L1tcc	5`-TCCGTTTCCGT-3`
Short A	5`-GGGCAAGGACTA-ALK-3`
Short B	5`-TAGTCCTTGCCC-ALK-3`
Long A	5`-TTCTAATACGACTCACTATAGGTGCGACTA-ALK-3`
Long B	5`-TAGTCGCACCTATAGTGAGTCGTATTAGAA-ALK-3`
Poly T 20	5`-ALK-(dT) ₂₀ -ALK-3`
Bis-Alk	

Table 2 Maldi-TOF of the sequences modified

Sample	Calculated mass	Found
Poly C	3655.3	3653.4
Poly C 24	7124.6	7122.5
Poly C36	10595.8	10597.8
Short A	3965.6	3966.6
Short B	3818.5	3821.8
Long A	9411.1	9402.1
Long B	9491.2	9497.2
Poly T 20 BisALK	4080.6	3987.3

5. Click reaction between modified DNA and benzene derivatives:



To an aqueous solution of each azide (**1-5**) (0.075 μmol), PolyC12 or short A, B and long A, B (amounts used in table 3 (0.038 μmol , 1 equiv.) in the case of **1**; (0.225 μmol , 3 equiv) in the case of **2** and **3**; (0.30 μmol , 4 equiv) in the case of **4** and **5**), NaCl (0.13M), CuI (1.78 mg, 9.35 μmol) and a solution of TBTA (tris[1-benzyl-1H-1,2,3-triazol-4yl)methyl] amine) (7.14 mg, 13.46 μmol) in DMF (357 μL) were added. The reaction was maintained at 55 $^{\circ}\text{C}$ for 16 hours. The products were purified by polyacrylamide gel electrophoresis 20% and eluted from gel fractions using an elutrap system. The solutions were desalted using a NAP-10 column and concentrated in an evaporating centrifuge. The trimers were characterized by MALDI-TOF (table 4).

Table 3 amounts of oligonucleotide used

Sequence employed	Number of Equiv.	Dimer or Trimer obtained
Poly C	1	Benzyl
	2	<i>Meta</i>
		<i>Ortho</i>
	3	Tris
		Tris.ethyl
		Tris-Short A
		Tris-short B
		Tris-long A
Short A		<u>Tris-long B</u>
Short B		
long A		
Long B		

Table 4 Maldi-TOF of the samples

Sample	Calculated mass	Found
Benzyl	3787.5	3785.2
Orto	7596.8	7497.9
Meta	7496.8	7491.2
Tris	11206.1	11200.3
Tris-ethyl	11290.3	11286.5
Tris Short A	12137.0	11398.7
Tris Short B	11695.7	11698. 5
Tris long A	28473.5	28209.6
Tris Long B	28713.8	28364.8

6. Synthesis of gold nanoparticles.

Gold Nanoparticles were prepared by the citrate reduction method.¹⁸²

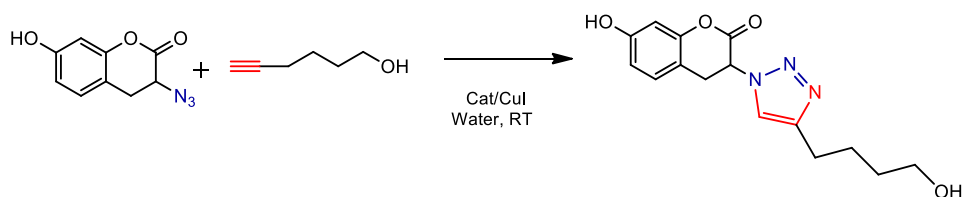
A solution of HAuCl₄ (34.3 mg) in H₂O (101 mL) was heated up to reach boiling temperature then a solution of sodium citrate (119.4 mg) in H₂O (10.1 mL) was added quickly. The solution was stirred for 10 min and then the removed from the heating source and stirred overnight at room temperature. The reddish solution was filtered and stored at 4 °C.

7. Functionalization of Gold nanoparticles with oligonucleotides.

Gold nanoparticles were incubated with oligonucleotides (Poly C sequence modified with diol groups) overnight in a 0.3M NaCl buffer. The samples were purified by centrifugation, the supernatants were removed and the particles dissolved in water. This process was repeated 3 times.

¹⁸² A. Ambrosi, M. T. Castañeda, A. J. Killard, M. R. Smyth, S. Alegret, A. Merkoçi, *Anal. Chem.* **2007**, 79, 5232–40.

8. Click reaction with Fluoreogenic reagent.



To solution of azidecumarine (0.005 μmol), in DMF 5-Hexeyn-i-ol (0.005 μmol , 1 equiv.) in DMF, NaCl (0.13M), CuI (2.5 μL of saturate solution) and a 15 μL of solution of catalyst (4 nmol/L) were catalyst is TBTA, *meta* dimer of poly C and PolyC-AuNPs, and ultrapure water for complete 200 μL were added. The reaction was maintained at room temperature for 2 hours. The course of the reaction was followed by recording the fluorescence intensity using Synergy H4 microplate reader.

Annexe 1.
DNA Synthesis.

Synthetic DNA

Nowadays, most of the molecular biology's techniques require chemically synthesized DNA or RNA. This includes primers for the polymerase chain reaction (PCR) and real time PCR, different molecular probes and regulatory nucleic acids (siRNAs and microRNAs). However, each oligonucleotide is tailored according to the specific needs of individual research.

The current automated process is based on the research carried out by Professor H. Gobind Khorana, a biochemist at the University of Wisconsin. Inspired by the chemical synthesis of peptides he evaluated dicyclohexylcarbodiimide (DCC), as coupling reagent, using various solid supports and protecting groups on both ribonucleotides and deoxyribonucleotides. With these studies, achievement decipher the genetic code. That led him to receive Nobel Prize in Physiology or Medicine in 1968.

In this strategy three protecting groups were employed. The nucleobases were protected with benzoyl or isobutyryl groups, the 3'-hydroxyl group as an acetyl group, and the 5'-hydroxyl-group as a dimethoxy trityl derivative, which was attached to a solid support (Figure 1). Thus, the synthesis takes places from 5' to 3', as in replication of DNA by polymerases.

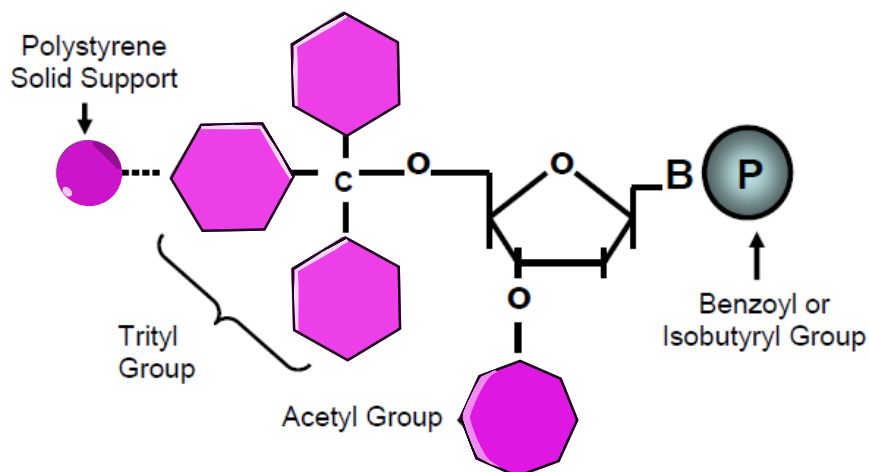


Figure 1. Starting point structure of an oligonucleotide synthesis by the Khorana group. Subsequent couplings would proceed through the 3' carbon after removal of the acetyl group. All nucleotides added from this point would have a reactive hydroxyl in place of the trityl group but would retain the other two protecting groups.

This method proved to be complicated and afforded oligonucleotides in moderate yields, however it was key in two major scientific advances. First, Khorana and his group were able to synthesize oligonucleotides that were used to confirm the genetic code. Second, in 1967, Khorana announced its intention to use this chemical process to synthesize a gene. This idea was motivated by the discovery of DNA ligases that year. They planned to ligase multiple units of oligonucleotides duplexes using these enzymes and in 1970 they published the first fully synthetic gene, the

yeast tRNA Ala 77bp.¹⁸³ In the article, they mentioned, "unpublished experiments by two of us have been encouraging the use of DNA polymerase gene replication in the presence of suitable primers."¹ Interestingly, some have speculated that this statement may have been the beginning of the invention of PCR.

Despite the different modifications on the synthesis the efficiency of the process was low till 1983, when a new process made possible the preparation of longer oligonucleotides and more efficient. In this case the synthesis was based on the use of phosphoramidite monomers as building blocks and use of tetrazole as a coupling catalysis.¹⁸⁴

In this case, the preparation of the phosphoramidite monomer required in the oligonucleotide synthesis was simpler than in the previous method. In this case, the nitrogens of nucleobases are protected as bezylesters and the 5'-hydroxyl group as dimethoxytrityl group, as previously, but in this case the DMT is not bonded to the solid support. In addition, the 3'-hydroxyl group is protected as phosphoramidate, which in the presence of imidazole is activated and the amino group on the phosphorous atom can be replaced by nucleophilic oxygens from alcohols. (Figure 2). Thus, in this case the synthesis proceeds from the 3' towards the 5' rather than 5' to 3', as reported by Khorana.

¹⁸³ K. L. Agarwal, H. Büchi, M. H. Caruthers, N. Gupta, H. G. Khorana, K. Kleppe, A. Kumar, E. Ohtsuka, U. L. Rajbhandary, J. H. Van de Sande, V. Sgaramella, H. Weber, T. Yamada, *Nature*, **1970**, 227, 5253, 27-34.

¹⁸⁴ L.J. McBride, M. H. Caruthers, *Tetrahedron Letters*, **1983**, 24, 3, 245-248.

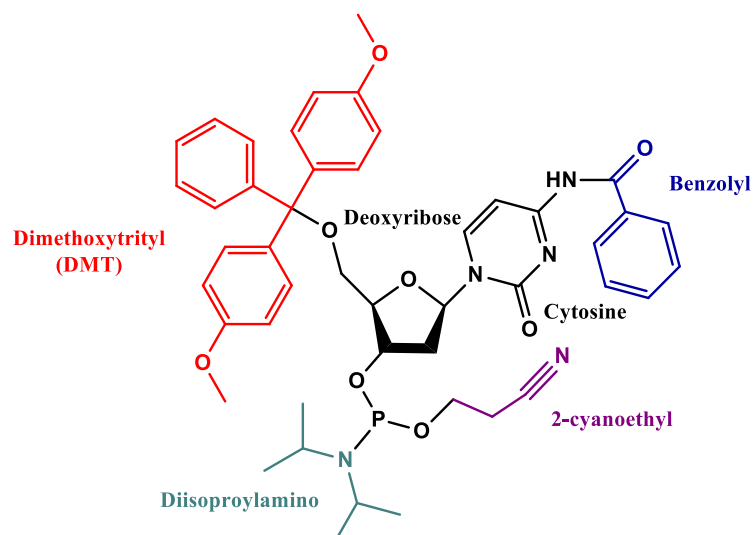


Figure 2. Protection groups

This approach implies four chemical steps that are repeated each time a new nucleotide is inserted. (Figure 3). These steps are deprotection, coupling, capping and oxidation.

1. Deprotection

In the classic deprotection step, the trityl group, which is attached to the 5' carbon of the pentose sugar of the recipient nucleotide, is removed by trichloroacetic acid (TCA) leaving a reactive hydroxyl group to which the next base is added.

2. Coupling

It is here that the advent of tetrazole activation replaces the use of condensing agents like DCC. Berner et al. showed that tetrazole, a weak acid, attacks the coupling phosphoramidite nucleoside forming a tetrazolyl phosphoramidite intermediate.¹⁸⁵ This structure then reacts with the hydroxyl group of the nucleoside attached to the CPG bead and the 5' to 3' linkage is formed. The use of tetrazole increased coupling efficiency up to 99% which has allowed the preparation of longer oligonucleotides.

3. Capping

While the increased efficiency afforded by the advent of tetrazole phosphoramidite-intermediate coupling was a major advance in oligonucleotide synthesis, it was still a chemical process and so had a finite failure rate. A coupling failure results when an oligonucleotide retains a reactive hydroxyl group on its 5'-most end. If this were to remain freely reactive, it would be able to couple in the next round and would result in a missing base in the synthesis. Thus, coupling failures must be removed from further participation in the synthesis. This is accomplished by adding an acetylating reagent composed of acetic anhydride and N-methyl imidazole. This mixture reacts only with free hydroxyl groups to irreversibly cap the oligonucleotides in which coupling failed.

¹⁸⁵ S. Berner, K. Mühlegger, H. Seliger, *Nucleic Acids Research*, **1989**, 17, 3, 853-864.

4. Oxidation

Once the capping step is accomplished, the last step in the cycle is oxidation which stabilizes the phosphate linkage between the growing oligonucleotide chain and the most recently added base. The phosphate linkage between the first and second base must be stabilized by making the phosphate group pentavalent. This is achieved by adding iodine and water which leads to the oxidation of the phosphite into phosphate leaving the phospho-triester bond stabilized.

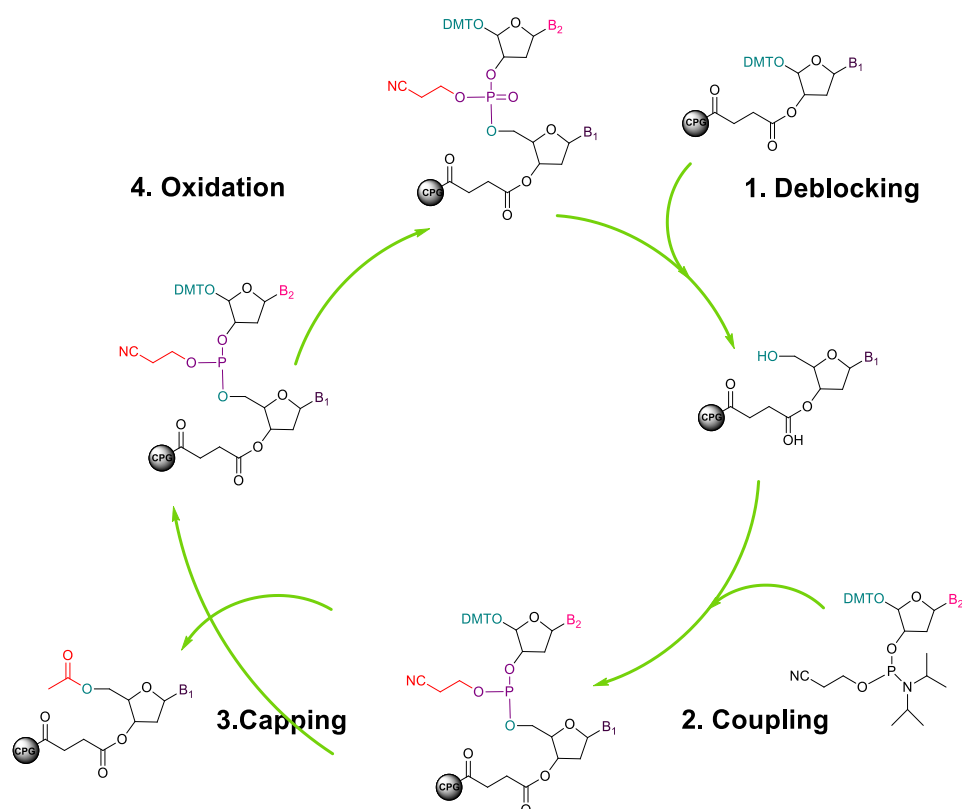


Figure 3. Scheme of cycle of synthesis of oligonucleotides based in phosphoramidite synthesis.

Nowadays, this process has been optimized and it is possible to obtain sequences of DNA and RNA up to 60 with a high yield.

Annexe 2.
Publications and Congress Presentation.

Publicaciones:

DNA Stabilized Silver nanocluster as Biosensors

Alfonso Latorre, Romina Lorca and Álvaro Somoza, *Journal of Chemistry* 2013, ID 631421.

Enhanced Fluorescence of silver nanoclusters stabilized with branched oligonucleotides

Alfonso Latorre, Romina Lorca, Félix Zamora and Álvaro Somoza, *Chem. Commun.*, 2013, 49, 4950-4952.

Antibacterial Activity of Silver Nanoclusters Tuned by Oligonucleotide Sequence

Nanoscale, ID is: NR-ART-09-2015-006629 (artículo en revisión).